GCN2 EIF2 KINASE IS CRITICAL FOR KERATINOCYTE COLLECTIVE MIGRATION AND WOUND HEALING

Rebecca Ruth Miles

Submitted to the faculty of the University Graduate School
in partial fulfillment of the requirements
for the degree
Doctor of Philosophy
in the Department of Biochemistry and Molecular Biology,
Indiana University

December 2021

Accepted by the Graduate Faculty of Indiana University, in partial fulfillment of the requirements for the degree of Doctor of Philosophy.

Doctoral Committee

_____
Ronald C. Wek, Ph.D., Chair

October 29, 2021

_____
Dan F. Spandau, Ph.D.

_____
Mark H. Kaplan, Ph.D.

_____
Matthew J. Turner, M.D., Ph.D.

_____
Josef G. Heuer, Ph.D.

DEDICATION

This dissertation is dedicated to my family and friends who encouraged and supported me along this journey, and to my niece Lauren who inspired me to understand more about molecular pathways in the skin. I am humbled and privileged to explore the vastness and intricacies of the cellular universe. After 30 years of research, the words of Ralph Waldo Emerson ring true to me, “All that I have seen teaches me to trust the creator for all I have not seen.”

ACKNOWLEDGEMENT

I would like to acknowledge members of the Wek and Spandau labs for technical assistance and collaborative data generation. This includes Sheree Wek and David Southern, Jagannath Misra for assistance with polysome profiling and tRNA charging assays, Parth Amin for assistance with RNAseq data analysis, Miguel Barriera Diaz for graphical interpretation of the GCN2 model and Michael Knierman for help with amino acid profiling. I would also like to thank Sashwati Roy, Amitava Das, Nandini Ghosh, and Tanner Guith for execution of the in vivo wound healing study.

I would also like to thank my committee members for their time and helpful suggestions along the course of this research project. I would also like to thank the Lilly Graduate Advanced Degree (LGRAD) committee for their support and vision to create opportunities for individuals to pursue graduate degrees at non-traditional time points in their professional journey.

Rebecca Ruth Miles

GCN2 EIF2 KINASE IS CRITICAL FOR KERATINOCYTE COLLECTIVE MIGRATION AND WOUND HEALING

A critical factor in the healing of a cutaneous wound is the closure of the wound bed that is accomplished by collectively migrating keratinocytes. Wounds that fail to heal appropriately are a significant burden on patient well-being as well as healthcare systems. Further understanding of the molecular pathways involved in wound healing is needed to find new treatments to accelerate healing and reduce treatment costs. Previously, we demonstrated that the integrated stress response (ISR) is critical for keratinocyte response to multiple stresses. Because wounding and repair mechanisms can induce stresses in the skin, we hypothesized that the ISR plays a central role in wound healing. The ISR features a family of stress-activated protein kinases phosphorylate the translation factor eIF2 (eIF2α-P), resulting in diminished global protein synthesis coincident with preferential translation of gene transcripts that lead to the remedy of the stress. Wounding of immortalized NTERT human keratinocyte monolayers led to rapid activation of the eIF2 kinase GCN2, and subsequent eIF2α-P and translational control. Deletion of GCN2 in wounding assays diminished eIF2α-P and translational control during wound healing. Global transcriptome analysis of wounded keratinocytes revealed that deletion of GCN2 induced a compensatory unfolded protein response and dysregulation of mRNAs important for cellular migration. Pathway analysis suggested that GCN2 is necessary for proper

activation of key signaling networks and subsequent coordination of RAC-GTP driven reactive oxygen species (ROS) generation following wounding. Additionally, amino acid control of cysteine is regulated by GCN2. We therefore investigated ROS levels following wounding and observed that GCN2 was required for proper ROS induction and actin reorganization in leading edge keratinocytes and that these changes were coincident with reduced RAC and RHO activation and cysteine depletion. The loss of leading-edge ROS in GCN2-deleted cells can be phenocopied with NOX inhibition. Lastly, mice deleted for GCN2 exhibited delayed wound healing compared to WT controls in an excisional wound healing model. These results indicate that GCN2 is required for the induction of collective cell migration and plays a critical role in coordinating the re-epithelialization of cutaneous wounds. We propose the ISR is a potential therapeutic target in chronic wounds.

Ronald C. Wek, Ph.D., Chair

Dan F Spandau, Ph.D.

Mark H. Kaplan, Ph.D.

Matthew J. Turner, M.D., Ph. D.

Josef G. Heuer, Ph. D.

TABLE OF CONTENTS

LIST OF TABLES

LIST OF FIGURES

LIST OF ABBREVIATIONS

ALOX	Arachidonate 5-Lipoxygenase
ARHGEF	Rho Guanine Nucleotide Exchange Factor
ATF	Activating transcription factor
bp	Base pair
CA	Calcium
CDS	Coding sequence
CD	Cluster of differentiation, cell surface marker
CEBP	CCAAT-enhancer-binding proteins
CHAC1	Glutathione Specific Gamma-Glutamylcyclotransferase 1
COL4A1	Collagen Type Four Alpha 1 Chain
COL18A1	Collagen Type Eighteen Alpha 1 Chain
CReP	Constitutive repressor of eIF2α phosphorylation
CRISPR	Clustered regularly interspaced short palindromic repeats
CAS9	CRISPR-associated endonuclease
crRNA	Short CRISPR ribonucleic acid
Cys	Cysteine
CE	Capillary electrophoresis
DAPI	4′,6-diamidino-2-phenylindole
DE	Differential expression
ECM	Extracellular matrix
eIF	Eukaryotic initiation factor
EIF2AK	Eukaryotic initiation factor two alpha kinase

eIF2α-P	Phosphorylated eukaryotic initiation factor two alpha
F-actin	Filamentous actin
FBS	Fetal bovine serum
FITC	Fluorescein isothiocyanate
GADD	Growth arrest and DNA damage-inducible protein
GCN	General control nonderepressible
GDP	Guanosine diphosphate
GEF	Guanine nucleotide exchange factor
GEO	Gene expression omnibus
GTP	Guanosine triphosphate
HDW	High density wounding
HMOX1	Heme oxygenase
HPLC	High performance liquid chromatography
HRI	Heme-regulated inhibitor
IL1B	Interleukin one
IL6	Interleukin six
ISR	Integrated stress response
IVL	Involucrin
IPA	Ingenuity Pathway Analysis
ITG	Integrin
KCCM	Keratinocyte collective cell migration
KO	Knock out
MMP	Matrix metalloproteinase

MS	Mass spectrometer
NADPH	Nicotinamide adenine dinucleotide phosphate
NCBI	National center for biotechnology information
NFKB	Nuclear factor kappa B
NHK	Normal human keratinocyte
NOX	NADPH oxidase
NQO1	NAD(P)H dehydrogenase (quinone)
NRF2	Nuclear factor erythroid 2–related factor 2
PBS	Phosphate buffered saline
PDGF	Platelet derived growth factor
PERK	Protein kinase R (PKR)-like endoplasmic reticulum kinase
Phe	Phenylalanine
PKR	Protein kinase R
PLXND1	Plexin D1
RAC	Ras-related C3 botulinum toxin substrate 1, Rac Family Small GTPase 1
RELA	v-rel, reticuloendotheliosis viral oncogene homolog A, p65
RHO	Rho family GTPases
ROS	Reactive oxygen species
RNA-seq	Ribonucleic acid sequencing
RPM	Reads per million mapped reads
RWD	RING finger and WD repeat containing proteins and DEAD-like helicases

SEMA4A	Semaphorin 4A
sgRNA	Single-guide ribonucleic acid
SLC7A11	Solute carrier family 7 member 11
SLC3A2	Solute carrier family 3 member 2
STAT3	Signal Transducer and Activator Of Transcription 3
TGF	Transforming growth factor
THPS	Thapsigargin
TIAM	T-lymphoma invasion and metastasis-inducing protein 1, RAC associated GEF
tRNA	transfer ribonucleic acid
tracrRNA	Trans-activating CRISPR ribonucleic acid
UPR	Unfolded protein response
UV	Ultraviolet
WT	Wild-type
xCT	Cystine transporter

CHAPTER 1. INTRODUCTION

Normal healing of cutaneous wounds requires the collective migration of epithelial keratinocytes to seal the wound bed from the environment. This introduction section will explain the medical importance of cutaneous chronic wounds and the contextual and mechanistic background to wound healing, which will be followed by a description of the integrated stress response and the biological systems contributing to cell migration during wound healing. Together, this introductory information provides a foundation for the thesis research questions that test the hypothesis that GCN2 and the integrated stress response is involved in managing the processes underlying wound repair.

1.1 The treatment of chronic wounds is an unmet medical need

An often-overlooked epidemic that is co-morbid with diabetes, aging and poor nutrition are chronic wounds. A Medicare study revealed that 8.2 million people experienced a significant wound in 2018 [1]. Although healthy individuals heal without complication, there are a profound number of patient wounds that do not resolve and require long-term medical care. Wound care has become its own specialty in the US treating more than 6 million patients annually at an estimated expense of 25-50 billion dollars [2, 3]. Typical wound care regimens involve removal of nonviable tissue, controlling infection, removing pressure on the skin, and keeping the wound bed moist with dressings. These interventions can assist wound closure but often fail due to the inability of the wound care to address the underlying pathophysiology. Chronic non-healing wounds lead to extended

periods of disability and pain, hospitalization, reduced quality of life, amputation and even death [4]. Therefore, it is important to determine the key mechanistic features of the wound healing processes, with an eye to more effective therapies.

1.2 Keratinocyte differentiation and the stages of normal wound healing

The function of the skin is to protect the entire body from the stress of the environment. As such, it is not surprising that it is the largest organ system of the body. The skin is composed of several layers: the epidermis, dermis, and hypodermis. The main cell type in the epidermis is the keratinocyte and several stratified layers form a resilient epithelial barrier. This stratification is achieved by a process of differentiation where expression of a set of molecular markers (including specific keratins, involucrin, filaggrin and loricrin) drive the layers to sequentially transform from a basal layer to an upper cornified layer. Keratinocytes remain attached to each by desmosome junctions (Figure1A). This process of differentiation and renewal is constant and the epidermis is estimated to renew a thousand times during a lifetime. [5]

In a healthy individual, a series of coordinated cellular and molecular events lead to cutaneous wound healing. These events occur in sequence via several overlapping phases. Hemostasis occurs immediately after a wound occurs and a clot is formed (Figure 1B). During the inflammation phase, neutrophils and monocytes infiltrate the wound to fight infection and degrade necrotic tissue (Figure 1C). Release of cytokines by immune cells facilitates activation of the next phase by signaling cell proliferation and epithelial cell migration [6, 7]. Epithelial

keratinocytes around the edge of the wound then proliferate and migrate across the wound bed – a process called re-epithelialization. Angiogenesis is initiated to vascularize the new tissue, followed by fibroblast infiltration and collagen deposition to form a granulation tissue (Figure 1D). Finally, the wound enters a prolonged maturation phase (Figure 1E) where the new tissue is remodeled for restored strength and flexibility [8]. If these wounding events are dysregulated and do not occur in an orderly fashion, a wound will not properly heal. Wounds are classified as chronic if they have not healed within 3 months. Wounds are most often arrested in the inflammation phase, stalling keratinocyte migration and subsequent closure of the wound bed [9]. Because re-epithelialization is impaired in all categories of chronic wounds, and a wound cannot be considered healed without an intact epithelial covering, further research is warranted to find novel therapeutic strategies to restore and enhance epithelial barrier formation [10].

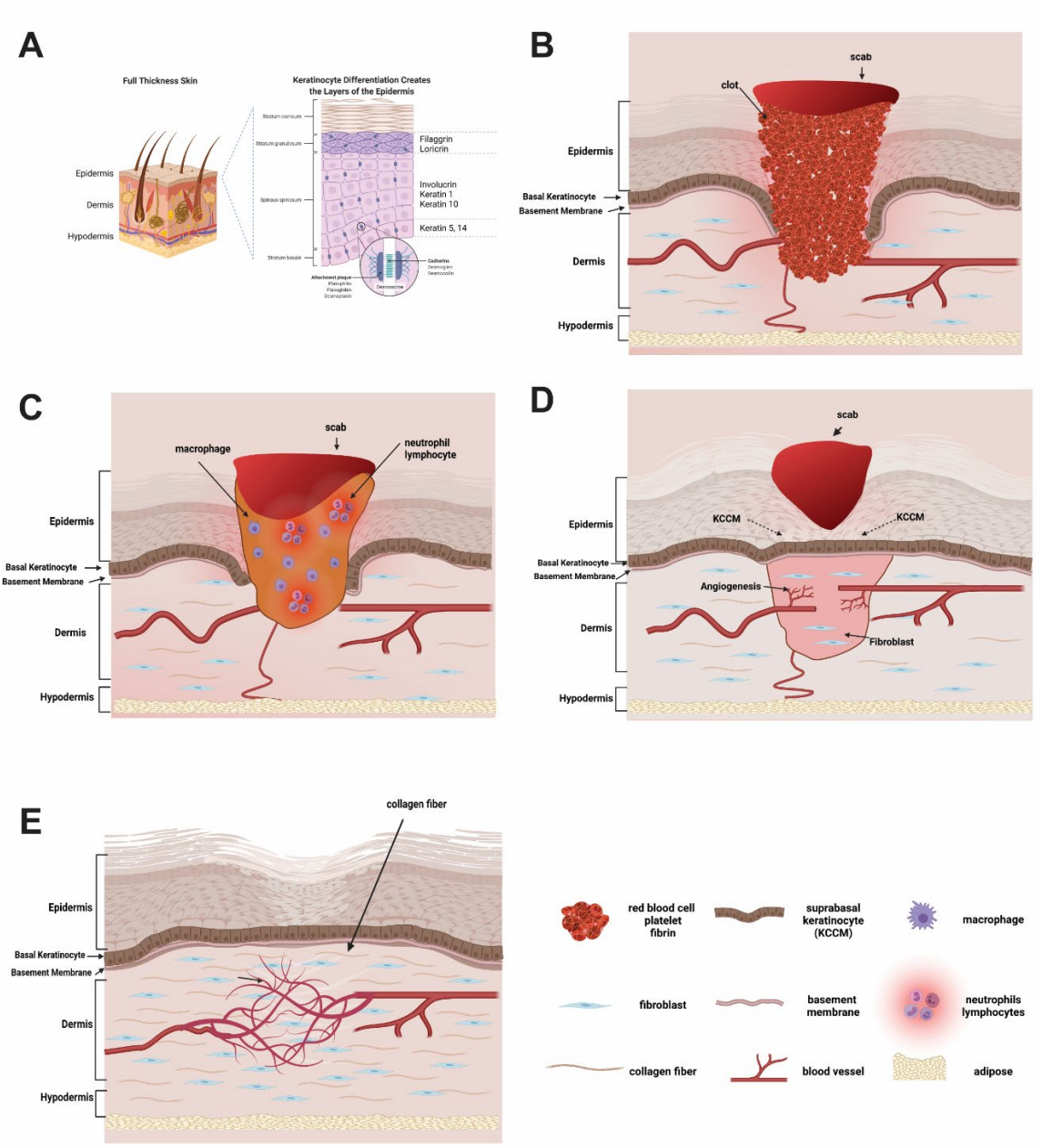

Figure 1. Normal keratinocyte differentiation and the stages of normal wound healing. (A) The skin is composed of three layers: the epidermis, dermis, and hypodermis. The epidermis is formed by 4 layers of differentiating keratinocytes undergoing a transformation from a basal to cornified layer. (B) Hemostasis begins the wound healing begins process, where activated platelets trigger fibrin clot formation that controls blood loss. (C) Inflammation occurs with the recruitment of

immune cells to remove debris and bacteria. Neutrophils are recruited to the wound first by histamine release from mast cells. Monocytes appear next and differentiate into macrophages to clear the wound bed. (D) In the proliferative phase, basal keratinocytes adjacent to the wound gap divide while those at the wound edge collectively migrate (KCCM) to close the wound gap. Angiogenesis ensues to revascularize the tissue, and fibroblasts migrate into the wound to transform the fibrin clot into (E) granulation tissue. The newly formed granulation tissue is remodeled over time to restore the underlying tissue.

1.3 Collective cell migration and re-epithelization in wound healing

Individual cell migration is a well-characterized process [11]. However, during cutaneous wound healing there is another important and arguably more complex mode of cell movement that directs keratinocytes to remain connected and migrate in unison over the wound bed. This process of coordinated cell movement in a unified direction has been termed collective cell migration (CCM) and can be observed during development, blood vessel formation and cancer. Although there may be commonly shared processes governing single cell and collective migration, there is growing evidence that the mechanisms directing each are unique and regulated differently [12].

To study wound healing, keratinocyte CCM (KCCM) is modeled in vitro by “scratching” or lifting sections of confluent sheets of differentiated keratinocytes (Figure 2B) [13-15]. In order for KCCM to occur and close the resulting wound, cells must have physical connections that remain intact during migration. To achieve the connections, keratinocytes reorganize their cytoskeleton structure to provide a direction to their unified movement. Furthermore, keratinocytes prepare their extracellular matrix to create a substrate upon which the collective sheet can effectively migrate [14]. These distinct and complex tasks have been assigned to two types of epithelial cells that are referred to as leader and follower cells (Figure 2A) [16, 17]. Leader cells appear at the wounded edge of the epithelial sheet and are identified by the emergence of lamellipodia and are often described as having a “ruffled” border” (Figure 2B). Leader cells monitor the immediate environment of the wound to establish direction to the migrating sheet. Leader cells then

communicate with follower cells to ensure alignment to the direction of movement. The function of follower cells is to maintain connections with neighboring cells and modify the extracellular matrix by secreting matrix metalloproteases [18]. Follower keratinocytes adjacent to the wound can proliferate during re-epithelialization in order to renew cells lost during injury [19].

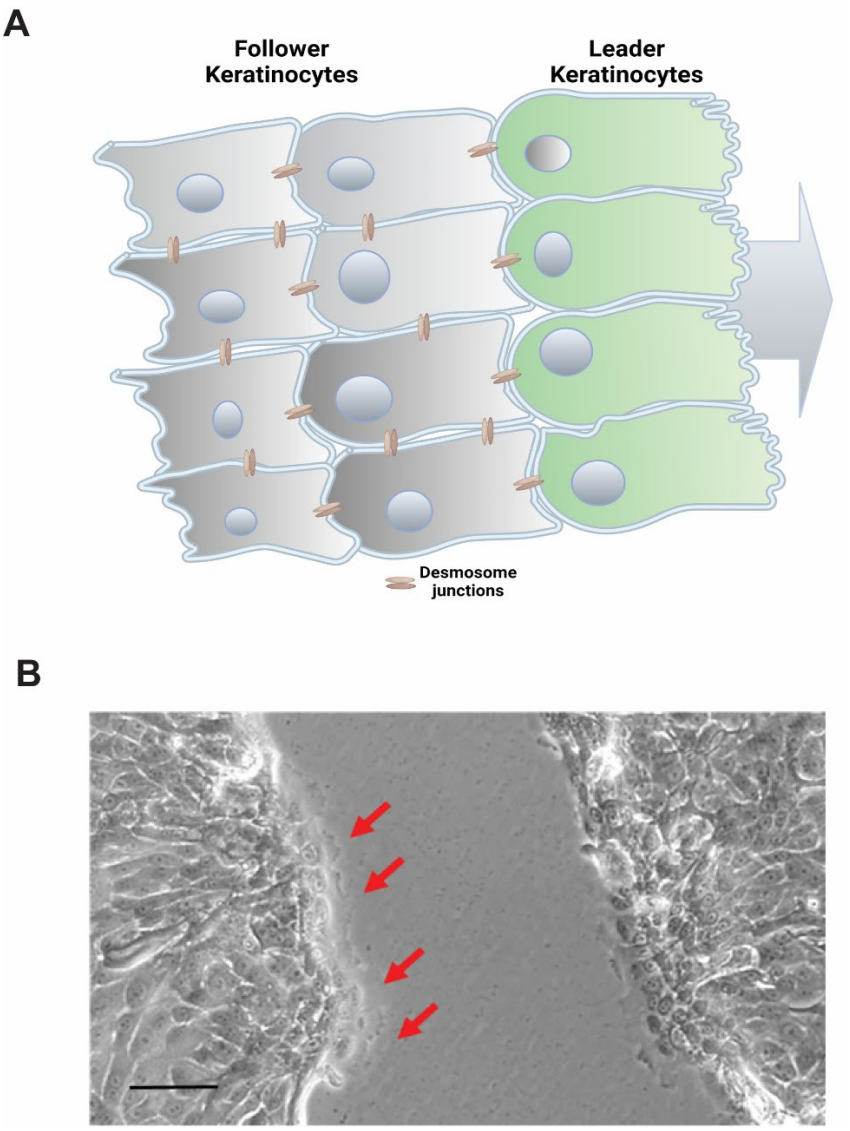

Figure 2. Keratinocyte collective cell migration and re-epithelization. (A) Upon wounding, cells positioned at the leading edge transform their cytoskeletal architecture to enable directional migration. The keratinocytes remain attached to each other through cell-to-cell contacts (desmosomes) and the cells behind the leading edge follow the direction of migration set by the leader cells. (B) Phase contrast image of NTERT cells six hours after wounding. The arrows indicate expansion of the leading edge membrane into lamellipodia. Scale bar is 100 μm.

1.4 The Integrated Stress Response

Cellular adaptation to stress is critical for survival and is achieved by mechanisms that globally slow translation initiation (Figure 3). Two major mechanisms regulating initiation of protein synthesis involve phosphorylation of 4E-BPs by mTORC1 and phosphorylation of eIF2 by stress-specific kinases [20]. The 4E-BP1 binds to the cap-binding protein eIF4E and prevents its appropriate binding to the bridge protein eIF4G, thus preventing loading of ribosomes to the 5'-cap of mRNAs [21-23]. This thesis will focus on phosphorylation of the α subunit of eIF2 (eIF2α-P), which is a conserved mechanism in all eukaryotes and occurs in response to a range of internal or external cellular insults, including nutrient and oxidative stress and perturbations to organelles such as the endoplasmic reticulum and mitochondria [24-26]. Because eIF2α-P and translational control is induced in response to range of cellular stresses, the pathway is referred to as the integrated stress response (ISR) [27-29].

A family of different eIF2 alpha kinases (EIF2AK) is expressed in mammals and each is activated by a unique stress via distinct regulatory processes (Figure 4). HRI (EIF2AK1) is activated by heme deprivation, mitochondrial stress, and during enhanced ROS conditions [30-35]. PKR (EIF2AK2) functions in an antiviral defense mechanism that is enhanced by interferon and activated by double-stranded RNA by different viruses [36-40]. The eIF2α kinase PERK (EIF2AK3) is activated by perturbations in the endoplasmic reticulum, including accumulation of misfolded proteins and disruptions of the membrane structure of this organelle [41, 42]. Finally, GCN2 (EIF2AK4) is activated by reduced amino acid levels, along

with UV irradiation [24, 43-50] (Figure 4). In response to each of these stress conditions, the ensuing induction of eIF2α-P competes with the interaction of eIF2 for its GTP-GDP exchange factor eIF2B [51], Recent structural studies of the eIF2B-eIF2 complex revealed details of this mechanism of action. The unphosphorylated and phosphorylated forms of eIF2 bind uniquely to eIF2B creating productive (nucleotide exchange-active) and unproductive (nucleotide exchange-inactive) states [52, 53]. When eIF2B-and eIF2α-P interact in an unproductive manner, creating a nucleotide exchange-inactive state, it therefore reduces the amount of active eIF2 ternary complex (TC) (eIF2-GTP-tRNAi) that is available for translation initiation. This subsequently reduces the formation and delivery of the 43S pre-initiation complex to the AUG start codon [54] and results in sharply reduced protein synthesis. Lower rates of protein synthesis in turn reduces nutrient consumption, conserving energy for the demanding task of reprogramming of gene expression to alleviate stress damage (Figure 4).

Accompanying the global reduction in protein synthesis, eIF2α-P also directs preferential translation of key genes by leveraging mechanisms of delayed translation initiation through upstream ORFs (uORFs) situated in the 5'-leader sequence of the target mRNA transcript which can alter the efficiency of translation of the gene coding sequence [55]. For example, stress-induced eIF2α-P sharply enhances ATF4 expression is via translational control mechanism involving two uORFs located in the 5′-leader of the *ATF4* mRNA transcript. In non-stressed cells when eIF2–GTP is available, ribosomes re-initiate at inhibitory uORF2 and block *ATF4* expression. When eIF2 is phosphorylated and eIF2–GTP levels drop,

re-initiation of translation is delayed and ribosomes can scan through the inhibitory uORF2, and instead re-initiate at the ATF*4*-coding region [56]. Increased *ATF4* expression in the ISR drives the transcriptional expression of genes involved in amino acid transport, amino acid synthesis, autophagy, glutathione biosynthesis, and the antioxidative stress response resulting in a program to restore the cell to homeostasis [29, 57]. Translational repression is relieved by type 1 protein phosphatase combined with one of two associated proteins that target dephosphorylation of eIF2α: CReP (PPP1R15B) or GADD34 (PPP1R15A). Expression of GADD34 is itself controlled by stress-induced signals creating a unique negative feedback loop whereby GADD34 is increased both by transcriptional activation and translational control. The resulting dephosphorylation of eIF2α-P allows translational initiation to resume once the ISR-directed transcriptome is implemented [58] (Figure 4). Expression of CReP is thought to be largely constitutively, which ensures that basal eIF2α-P is low during non-stressed conditions.

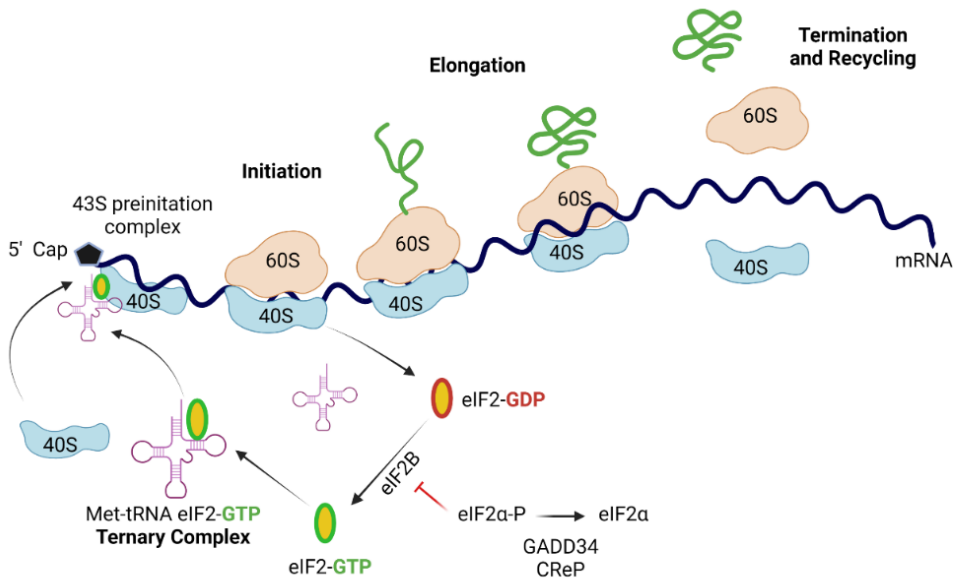

Figure 3. The stages of translation. Protein synthesis can be divided into four stages: initiation, elongation, termination, and recycling. The initiation phase is critical to control the global rate of translation and features the formation of the 43S ribosome preinitiation complex at the 5' cap of the mRNA. The 43S preinitiation complex is composed of the 40S ribosomal subunit and selected translation initiation factors, including the ternary complex (TC) containing eIF2 bound to GTP and initiating methionyl tRNA. Upon binding onto the mRNA, the 43S complex scans 5' to 3' in search for the optimal initiation codon, typically an AUG. Formation of eIF2-GTP is a rate limiting step to initiate global translation and is controlled by the GTP exchange factor (GEF) eIF2B. Phosphorylation of eIF2 on its alpha subunit (eIF2α-P) blocks this GEF and impairs eIF2-GTP formation; thus, the level of eIF2α-P can fine tune the initiation of global translation. In addition, hydrolysis of the eIF2-GTP to eIF2-GDP is a key step in AUG selection and subsequent joining of the 40S and 60S subunits into the translating 80S ribosomal subunit.

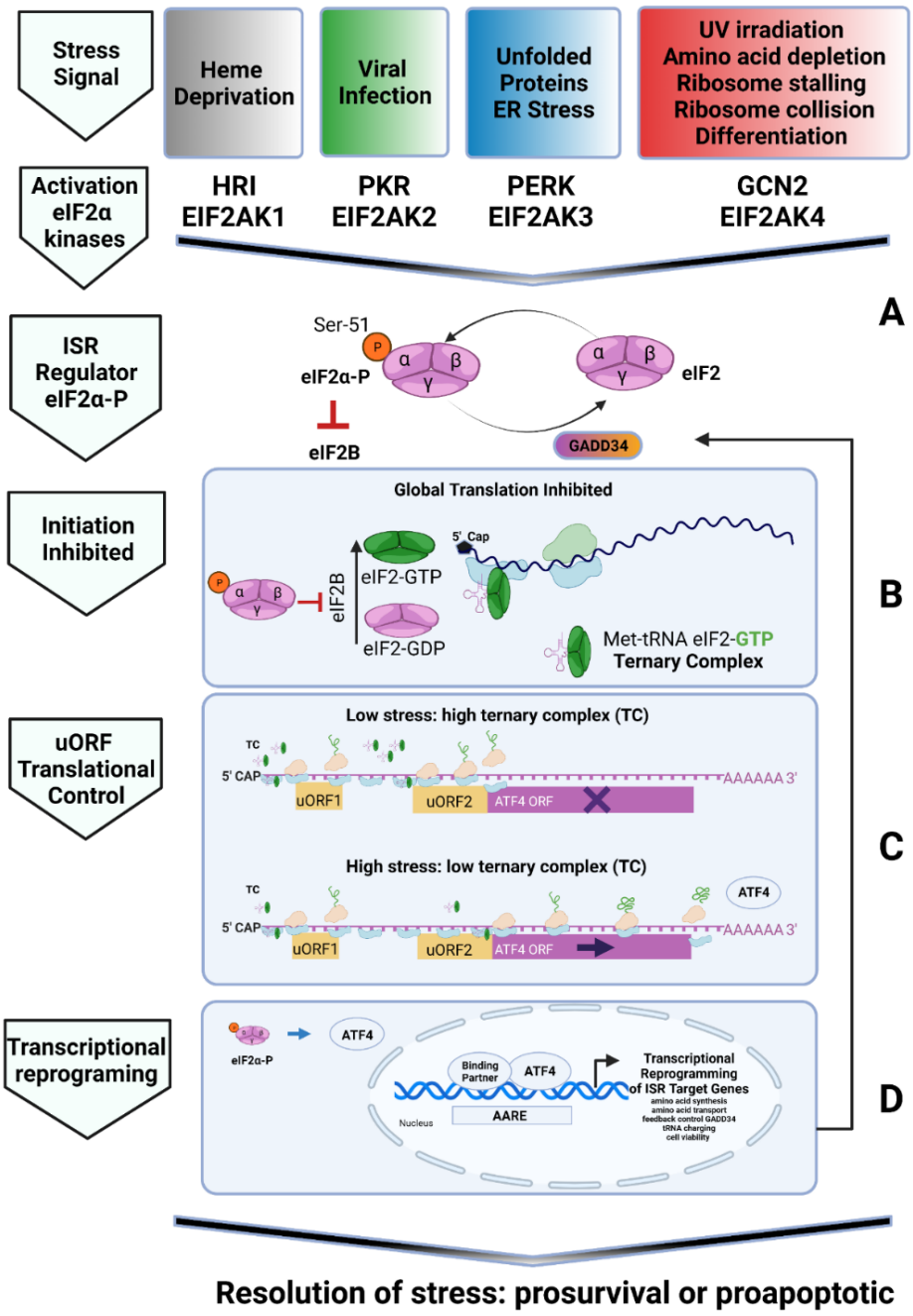

Figure 4. The Integrated Stress Response. (A) A variety of cellular stresses activate four different EIF2A kinases (HRI, PKR, PERK and GCN2) that each phosphorylate the serine-51 residue of the α subunit of eIF2. Because the stresses converge on induction of eIF2α-P and expression of ATF4, this signaling pathway

has been called the Integrated Stress Response (ISR)[26, 59]. The levels of eIF2α-P are the key regulator of the ISR and lead to three outcomes. (B) Global inhibition of translation initiation by limiting eIF2-GTP, thus reducing availability of ternary complex formation for initiation of protein synthesis. (C) Changes in levels of translation initiation allows for differential AUG codon selection in upstream 5'-uORFs and leads to preferential translation of specific mRNAs, such as *ATF4*. (D) Increased amounts of ATF4, a transcription factor that dimerizes with a binding partner, drives transcriptional reprogramming of ISR genes involved in adaptive responses to resolve cellular stress.

1.5 GCN2 directed translation control

Human GCN2 is 1649 amino acid residues in length and includes 5 domains: An N-terminal RWD (RING-finger proteins, WD repeat-containing proteins and the yeast DEAD-like helicases) domain, a pseudokinase region, a catalytically active kinase domain, a region homologous to histidyl-tRNA synthetases (HisRS), and a C-terminal domain (or CTD) (Figure 5). A central model for direct activation of GCN2 involves direct binding of uncharged tRNAs that accumulate during amino acid limitation and bind to the HisRS-related domain of GCN2, causing a conformational change in GCN2 and activation of the adjacent protein kinase domain [60, 61]. More recent studies suggest other activating factors for GCN2 that may be independent of uncharged tRNA status. For example, colliding ribosomes on damaged mRNAs can activate GCN2 during UV irradiation [62]. Furthermore, GCN2 can be associated with ribosomes and the ribosomal P-stalk alone is suggested to activate GCN2 [63-65]. Lastly, it has been suggested that there is a connection between the actin cytoskeleton and protein synthesis whereby GCN2 is activated upon disruption of F-actin and this eIF2α kinase function as an important sensor of the state of the actin cytoskeleton [66]. Modulation of GCN2 activity can also occur through associations with other proteins. For example, interaction of the GCN1/GCN20 complex with the amino-terminal RWD domain of GCN2 is proposed to enhance its access to uncharged tRNA and the protein IMPACT can in turn bind GCN1 and reduce GCN2 activation [67-69] . A recent structure of GCN1 bound to colliding ribosomes suggests that GCN1 may also be involved with activation of GCN2 during different stresses [70]

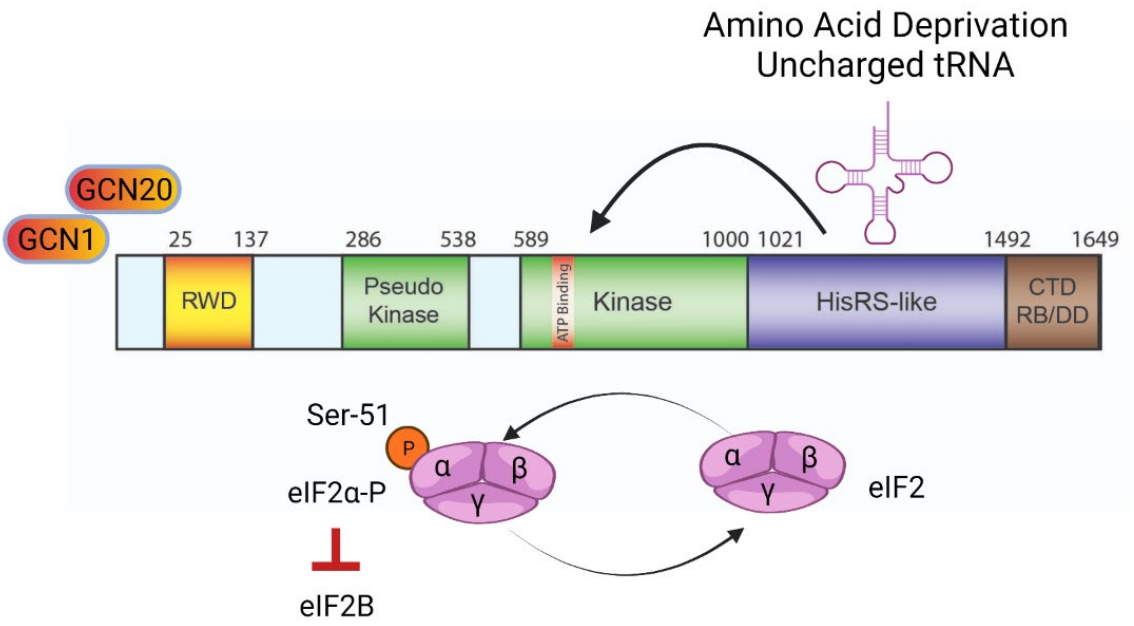

Figure 5. GCN2 directed translation control. Human GCN2 is 1649 amino acid residues in length and contains 5 domains. The N-terminus of GCN2 features a RWD (RING-finger proteins, WD repeat-containing proteins and the yeast DEAD-like helicases) domain, followed by a pseudokinase domain, a catalytically active kinase domain, a histidyl-tRNA synthetase HisRS) domain, and a C-terminal domain (or CTD). Activation of GCN2 is triggered by uncharged tRNAs accumulating during amino acid limitation that bind to the HisRS-like domain of GCN2, causing a conformational change in GCN2 and activation of the adjacent protein kinase domain. Additional mechanisms involving GCN2 association with ribosomes is also important for regulation of this eIF2α kinase.

1.6 GCN2 as amino acid sensor

GCN2 is the primary sensor detecting deficiencies in amino acid levels and coordinates the upregulation of genes that function to replenish amino acid stores through a process that some have called the amino acid response (AAR) [71, 72]. Although the AAR is made up of several signaling pathways, ATF4 has been extensively characterized and shown to have a prominent role in the AAR [72]. It is important to emphasize that while ATF4 is central for implementation of gene expression in the ISR in response to many stresses, there are certain stresses, such as UV irradiation in keratinocytes [50, 73], where the adaptive functions of the ISR occurs independent of ATF4 and through other target genes. Likewise, it is interesting that although both GCN2 and PERK activation lead to the induction of ATF4 transcriptional programs, there are unique differences in the gene signatures dependent on stress [74]. This suggests that there are other regulatory factors besides ATF4 that can bring specificity to the stress response. ATF4 is a basic leucine zipper (bZIP) transcription factor that recognizes and binds a specific DNA sequence referred to as an amino acid response element (AARE). The AARE is composed of two half sites, one of which is very conserved (ATF) and the other can be divergent (C/EBP), allowing for a diversity of binding partners forming the activating dimer complex. AAREs can be found in a host of genes involved in amino acid synthesis, transport and metabolism [29]. ATF4 has been shown to have multiple related bZIP transcription factor binding partners including different c/EBP isoforms, ATF2, ATF3, ATF5 and CHOP [71], all of which can themselves be regulated by ATF4 [75-77]. Additional interactions between members of the

ATF, C/EBP and FOS/JUN transcription factor families can contribute to the coordination of the cellular response to amino acid deficiency. Lastly, during times of amino acid starvation, ATF4 has been shown to direct a transcriptional program coordinating the process of autophagy [78]. Autophagy is a mechanism by which the cell can recycle proteins and organelles in lysosomal compartments, renewing intracellular nutrients and amino acids for maintenance of protein synthesis and essential metabolic processes. The importance of GCN2 as the key orchestrator of amino acid control is highlighted in Gcn2 -/- mice, where the absence of GCN2 shifts the gut away from a state of homeostasis to dysregulated autophagy that subsequently results in increased gut inflammation [79].

1.7 GCN2 as regulator of redox balance

Restoration of amino acid levels for protein synthesis is not the only beneficial outcome of GCN2 activation. Amino acids serve as metabolic intermediates and contribute to the formation of glutathione (GSH) that manages oxidative stress (ROS). GSH is formed by synthesis of a tripeptide of L-cysteine, L-glutamic acid and glycine. Because cysteine is the rate limiting step in GSH production, maintaining an adequate supply of intracellular cysteine is key to mitigate oxidative stress [80, 81]. Cysteine is obtained from both the diet and by endogenous production via the reverse transsulfuration pathway. It has been described as a semi-essential or conditional essential amino acid because cysteine availability can be limiting in times of stress (sickness, injury or healing). The transsulfuration pathway directs the metabolic convergence of methionine and

serine into cysteine and is utilized when the demand for glutathione is high or when cystine transport across the membrane is diminished [82]. Cysteine is delivered to tissues in its oxidized form as cystine, and then is transported into cells by the cystine glutamate antiporter system x_c^-[83]. The x_c^- system is composed of a light chain, xCT (SLC7A11), and a heavy chain of cell surface antigen 4F2hc (CD98/SLC3A2)[84]. Upon induction of the ISR with amino acid deprivation, ATF4 has been shown to play a key role in activating transcription of the cystine transporter [29, 85]. In addition, growth signals, such as insulin, stimulate the mTORC1 pathway, which can activate ATF4 independently of the ISR and lead to increased expression of *SLC7A11* and *SLC3A2* [86]. Increased expression of these SLC genes ensures appropriate uptake of cystine to support an anabolic tissue response [86].

1.8 Role of reactive oxygen species in normal and chronic wound healing

Reactive oxygen species (ROS) are important second messenger signals and can be produced in many cellular locations by a variety of sources, including mitochondrial enzymes, NADPH oxidases (NOX), nitric oxide synthase, cyclooxygenases, cytochrome P450 enzymes and lipoxygenases [87]. Proper temporal and spatial production of ROS is required to coordinate all phases of the normal wound healing response [88]. For example, ROS are produced by activated platelets upon wounding and facilitate hemostasis by inducing vasoconstriction and thrombus formation [89]. During the inflammation phase of wound healing, ROS is a chemotactic signal to phagocytic neutrophils and macrophages to

migrate into the wound site. Subsequent engulfment of bacteria triggers NAPDH oxidase (NOX) activation in the phagosome to produce and concentrate a lethal level of ROS. These cells also secrete hydrogen peroxide into the surrounding wound to neutralize bacteria growth [90, 91]. ROS production can play a role in the proliferative and remodeling phases of wound healing by activating proliferative responses in endothelial and fibroblast cell types [92, 93].

It is suggested that ROS is also important for directional cell migration [94, 95]. Activation of cell surface receptors in response to mechanical shearing or cytokine signaling can activate RAC1-GTP which is necessary to drive the formation of NADPH Peroxidase (NOX1) holoenzyme and generate endogenous ROS in the form of hydrogen peroxide at the cellular membrane [96]. A gradient of ROS at the site of shearing or receptor activation can then direct signaling pathways to coordinate directional migration [97, 98]. There are many characteristics of non-healing wounds (Figure 6), including elevated protease degradation of the extracellular matrix (MMP), dysregulated growth factors, and reduced cellular proliferation and neovascularization; however, chronic inflammation and excessive ROS are hallmarks of non-healing wounds [99]. Low levels of appropriately modulated ROS play a critical role in normal wound healing, but excessive or sustained ROS can accelerate tissue damage and have a negative impact on wound closure rates. The resulting open wound bed allows excessive bacterial growth, further fueling the chronic inflammatory response and further delaying wound repair (Figure 6) [100]. Restoring a proper balance of ROS remains a primary focus for antioxidant therapies for wound healing [101].

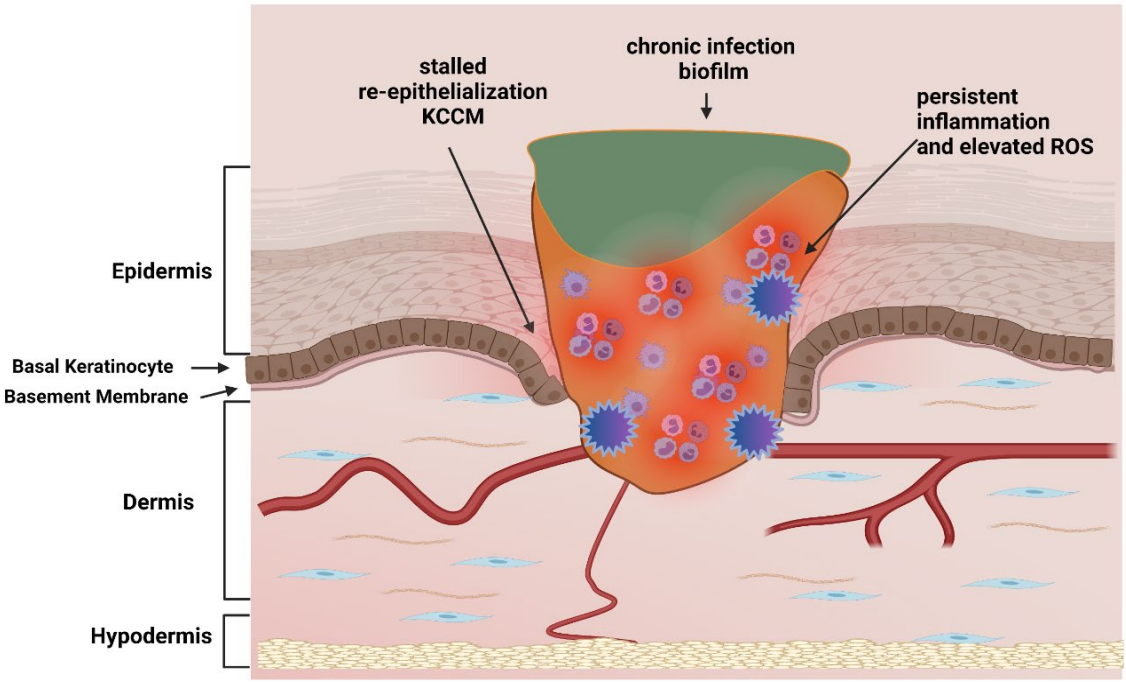

Figure 6. Characteristics of a chronic non-healing wound. A normal wound will progress through the four phases of wound healing within three weeks. However, chronic wounds take longer than three months to heal and are characterized by infection, persistent inflammation, and reactive oxygen species (ROS) production. Re-epithelialization is stalled due to ineffective keratinocyte collective migration (KCCM). Additional problems arise such as fibroblast senescence, impaired angiogenesis and elevated levels of matrix metalloproteinases (MMP).

1.9 Role of Rho GTPases in cytoskeleton remodeling

The Rho GTPases, RHO, RAC and CDC42, are well-characterized molecular players in cytoskeletal rearrangements that are necessary for cell movement and migration. The functional characterization of this family of proteins was carried out by microinjecting fibroblasts with each of the active Rho GTPases and monitoring formation of specific cytoskeletal structures. RHOA-GTP induced stress fiber and adhesion formation, RAC1-GTP induced expansion of leading edge membrane into lamellipodial protrusions and CDC42-GTP induced filopodia (Figure 7A) [102-108]. It is suggested that RAC1-driven actin expansion at the leading edge is the primary protrusive force in the cell, whereas RHOA stress fiber and focal adhesion formation is the driver for retraction in migrating cells [109]. However, recent studies in various cell types reveal a more complex co-regulation of RAC1 and RHOA in regions of the cell that transform the cytoskeleton to coordinate protrusion, retraction, and membrane ruffling (Figure 7B) [110, 111].

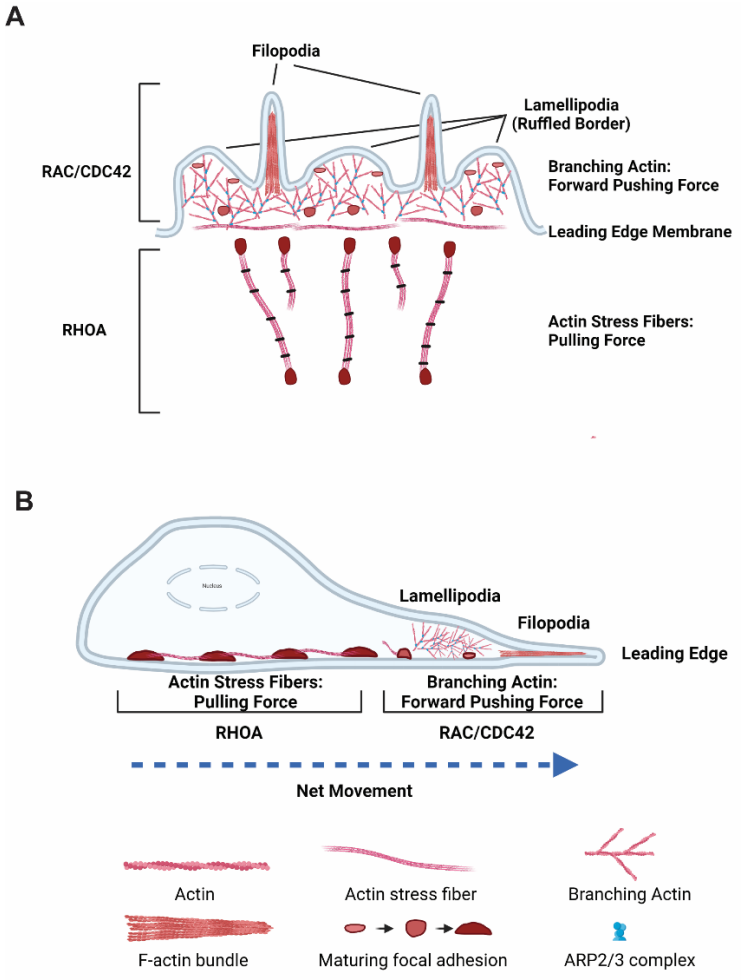

Figure 7. Rho GTPases in actin cytoskeleton remodeling and coordination of cell migration. (A) Top view of migrating cell structures necessary to generate movement. RAC is responsible for formation of branching actin at the leading edge lamellipodia and CDC42 signals are required for F-actin bunding in filopodia. Together, RAC/CDC42 facilitate forward pushing force for the migrating keratinocyte. RHOA coordinates the maturation and formation of focal adhesions that generate stress fibers that can contract and pull the cell forward. (B) Side view of the same migrating cell structures generating a net forward movement to the cell.

1.10 Interplay of Rho GTPases and ROS in coordinated migration

Directional migration requires proper temporal and spatial production of signaling molecules. Rho GTPases and ROS are an example of such interplay of signaling molecules at the leading edge of a migrating cell [112]. As mentioned above, mechanical shearing and activated cell surface receptors signal the conversion of RAC1-GDP to RAC1-GTP. Once activated, RAC1-GTP is critical to bring together the membrane associated NADPH Peroxidase holoenzyme (NOX) [96] and generate ROS. A gradient of ROS at the site of shearing then directs signaling pathways that assist SRC and PYK2 redox-sensitive activation at focal complexes. These events facilitate turnover of focal adhesion complexes and lamellipodia formation to coordinate directional migration (Figure 8) [97, 98, 113].

Another example of the interplay of Rho GTPases and ROS in coordinating migration is the finding that RHOA can be directly activated by ROS in cells [95, 114]. RHOA directly senses ROS through a redox-sensitive motif containing two cysteine residues within the phosphoryl binding loop and allows for guanine nucleotide dissociation [114], triggering formation and biochemical coordination of migrating cytoskeletal structures in leader and follower cells that are necessary for collective cell migration (Figure 9). Activation of RHOA enables contractility and creates cytoskeletal tension through the Rho kinase, ROCK which maintains myosin phosphorylation.

In a chronic wound, unmitigated ROS at the wound edge may interfere with the generation of a proper temporal and spatial production of ROS at the wound edge and impair directional KCCM. Sustained infiltration of immune cells with

concomitant release of pro-inflammatory cytokines generates excessive ROS in the chronic wound. Interestingly, diabetic wounds have been reported to trigger elevated levels of ROS and have reduced cysteine and glutathione at the wound edge [115].

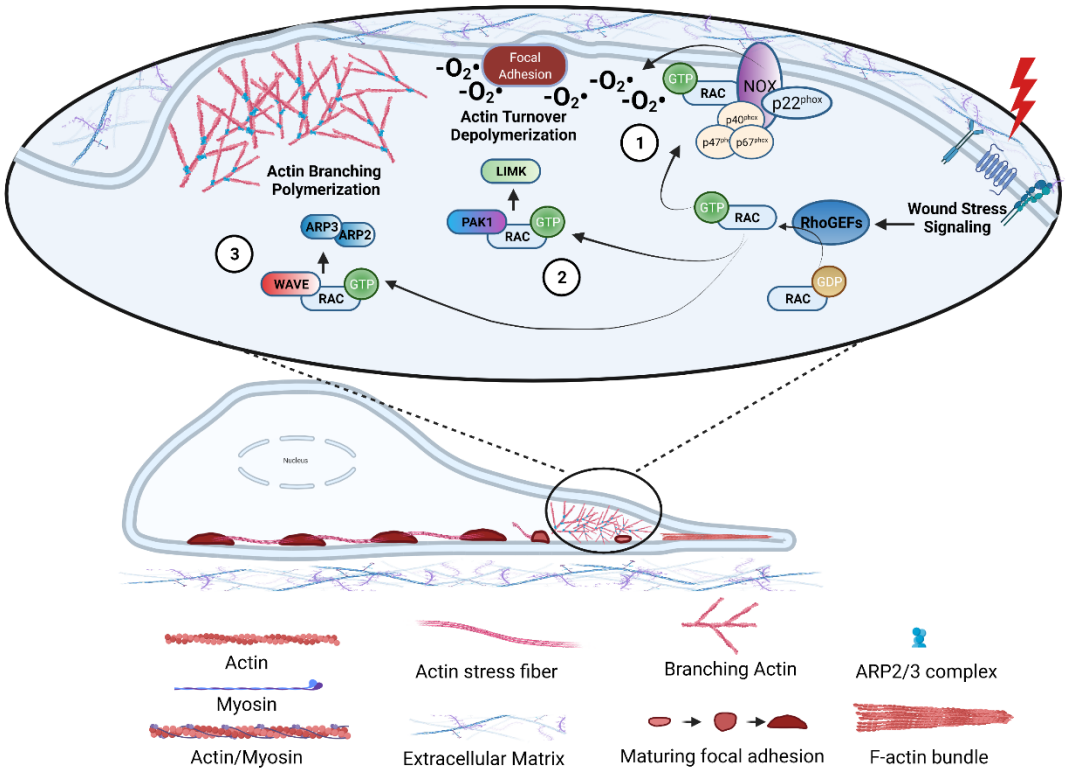

Figure 8. Activation of RAC is necessary for migration. Signaling induced by wounding leads to Rho GEF activation of RAC-GTP that triggers three key events. First, RAC-GTP is critical to localize the NOX holoenzyme to the membrane for ROS production. A ROS gradient is then implemented, which sets a direction for migration and helps facilitate focal adhesion formation and turnover through redox sensitive activation of RHOA. Second, RAC-GTP binds PAK1 and activates LIMK to control actin turnover for remodeling of the actin cytoskeleton. Third, RAC-GTP acts in concert with WAVE to activate ARP2/3 complex formation, which is necessary to drive formation of branching actin into the leading membrane.

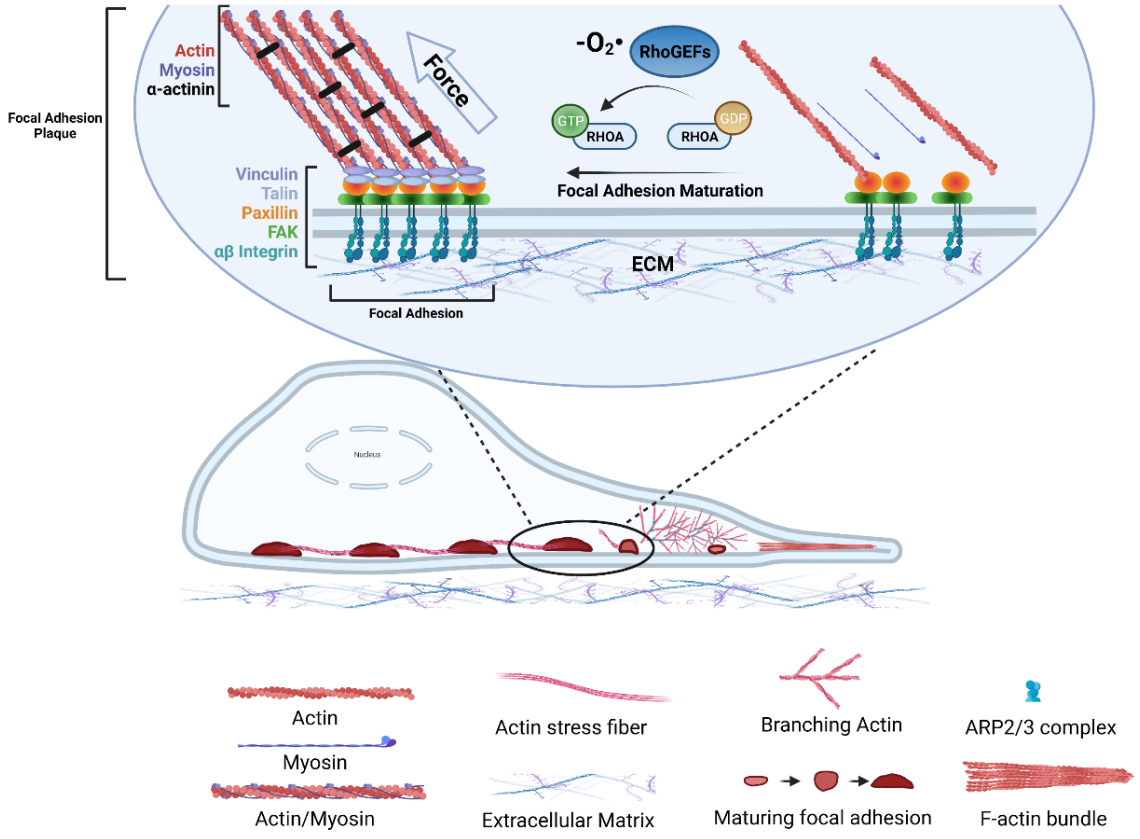

Figure 9. Activation of RHOA is important for focal adhesion maturation. RHOA can be activated by ROS or GEFs. Once activated, RHOA-GTP is required to help assemble the necessary subunits of the focal adhesion plaque and to activate the contraction of the actin/mysosin stress fibers to generate the pulling force for migration.

1.11 The role of the integrated stress response in keratinocytes

Recently, it was shown that activation of the ISR is important for keratinocytes to manage the stresses of UV irradiation and renewal of the epidermis by constant proliferation and differentiation [50, 116]. The eIF2α-P is triggered by GCN2 in response to UV irradiation, resulting in preferential translational of *CDKN1A*, which allows for appropriate checkpoint control that facilitates DNA repair [49, 73]. Furthermore, GCN2 is suggested to enhance the expression of select genes (e.g., involucrin and keratin-1) that are important for keratinocyte differentiation [117, 118]. Depletion of GCN2 in human keratinocytes used in a three-dimensional (3D) *in vitro* organotypic model resulted in improper formation and organization of the epidermis [116].

Given the important roles for GCN2 in skin homeostasis and the roles of eIF2α-P in managing environmental stress, in this thesis I addressed the roles that GCN2 and the ISR play in KCCM during re-epithelization of cutaneous wounds. Using a combination of biochemical, genetic, and cellular approaches in cell culture and mouse model systems, I describe the role that GCN2 and its attendant gene expression plays in appropriately managing amino acid levels, ROS generation, lamellipodia formation, and focal adhesion dynamics that are central to KCCM and optimal wound closure.

CHAPTER 2. EXPERIMENTAL PROCEDURES

2.1 Cell culture

Experiments were either performed using NTERT, an immortalized human keratinocyte cell line that has been shown to have normal keratinocyte differentiation properties [119] or normal human keratinocytes (NHK) that were isolated from foreskin tissue as previously described [120] and with methods approved by the Indiana University School of Medicine Institutional Review Board. Both NTERT and NHK cell were maintained and passaged in low calcium EpiLife Complete media (ThermoFisher Scientific) supplemented with human keratinocyte growth supplement (HKGS; ThermoFisher Scientific) and 1000U Penicillin-Streptomycin (PS) (Gibco Laboratories). Human keratinocytes are maintained in a basal undifferentiated state by controlling the amount of calcium and in a serum-free media. If calcium and fetal bovine serum (FBS) concentrations are increased to 2 mM and 2% respectively, the NTERT cells respond by inducing an appropriate program of differentiation [121]. It has been previously reported that loss of GCN2 can inhibit keratinocyte differentiation [116].

Keratinocytes were treated with different stress agents, as indicated, in complete EpiLife HKGS supplemented media either during differentiation into a monolayer and/or during the wounding process. Media supplements are listed in Table 1 and include 1 μM guanabenz acetate (R and D Systems), 5 μM GCN2iB (MedChemExpress), 1 μM cystine (Sigma), 50 mM NSC23766 (Tocris), 5 μM VAS2870 (Tocris), 300 nM DPI (Tocris) and 1 μM puromycin (Calbiochem).

Chemicals, Peptides, and Recombinant Proteins		
Reagent or Resource	**Source**	**Identifier**
Guanabenz acetate	R and D Systems	0885
GCN2iB	MedChemExpress	2183470-12-2
L-cystine	Sigma	C7602
VAS 2870	Tocris	6654
NSC23766	Tocris	2161
Diphenyleneiodonium chloride	Tocris	0504
puromycin	Calbiochem	58-58-2
Alt-R® S.p. HiFi Cas9 Nuclease V3	IDT	1081060
Alt-R Cas9 Electroporation Enhancer	IDT	1081058
CellRox Green	Thermo Fisher	C10444
Phalloidin	Sigma-Aldrich	P5282
DAPI	Sigma-Aldrich	P5282

Table 1. Resources for chemicals, peptides and recombinant proteins. A table summarizing the sources and catalog numbers for various chemicals, peptides and recombinant proteins used in keratinocyte experiments.

2.2 CRISPR gene editing

To create a heterogeneous population or “pool” of keratinocytes lacking GCN2, CRISPR-Cas9 was used to edit the GCN2 locus in both NTERT and normal human keratinocytes. Alt-R CRISPR-Cas9 crRNAs were designed with the Integrated DNA Technologies Custom Alt-R® CRISPR-Cas9 guide RNA design tool to target the kinase domain of GCN2 either in exon 2 AltR1/UUGUACCCUCAAGGCCUAACGUUUUAGAGCUAUGCU/AltR2 or in exon 12 AltR1/UUGUACCCUCAAGGCCUAACGUUUUAGAGCUAUGCU/AltR2. To knock out *ATF4*, two guides were designed by Parth Amin and used in combination to target and flank an 808 base pair sequence in exon four. The *ATF4* guide sequences were AltR1/GGAUUUGAAGGAGUUCGACUGUUUUAGAGCUAUGCU/AltR2 and AltR1/GCUCCUGACUAUCCUCAACUGUUUUAGAGCUAUGCU/AltR2. The crRNA and Alt-R CRISPR-Cas9 tracrRNA were prepared in equimolar concentrations to a final sgRNA duplex concentration of 100 μM and annealed by heating at 95C for 5 min and allowing to cool to RT. RNP complexes were formed by incubating the above sgRNA duplex with Alt-R S.p and HiFi Cas9 Nuclease at RT for 20 minutes. Complexes with exon 2 or exon 12 targeted guide RNAs were transfected by nucleofection using into 1 million keratinocytes using the AMAXA Nucleofector II device (Lonza) with the Amaxa Human Keratinocyte Nucleofector kit (VPD-1002, program T-018) and Alt-R Cas9 Electroporation Enhancer. Successful gene editing was assessed first by using the Surveyor Mutation Detection kit (Integrated DNA Technologies 706020) and then protein knockdown

was confirmed by immunoblot analysis of GCN2 and ATF4. Immunoblot procedures and antibodies for GCN2 and ATF4 are described below. Resources and for the cell lines, oligonucleotides, and equipment used to create these knock out cell lines are listed in Table 2 and Table 4.

Cell Line, Devices, Reagents	Source	Reference or Identifier
NTERT		*Dickson, M.A. Mol Cell Biol* **20**, 1436-1447
Normal human epidermal keratinocyte		*Int J Cancer* **80**, 431-438
IncuCyte Cell Migration Kit and plates	Essen Bioscience	Catalog: 4493; 4379
Human Keratinocyte Nucleofector Kit	Amaxa	Catalog: VPD-1002

Table 2. Resources for experimental cell models and devices. A table summarizing the sources, catalog numbers and references for the cell lines and instruments used for the development of the in vitro wound healing model.

2.3 IncuCyte kinetic wound assay

Two methods were developed to evaluate KCCM during the re-epithelialization process of wounding healing. First, a kinetic and automated 96-well cell wound assay from IncuCyte (model number) was utilized. This system was comprised of a 96-well WoundMaker Tool (4563), a software module (9600-0012), and ImageLock Plates (4679). The 96 pinheads of the WoundMaker were used to create a single, uniform, 700-800 micron wounds in a differentiated keratinocyte monolayer grown on ImageLock 96-well microplates. On day one, 40,000 keratinocytes per well were plated in ImageLock 96-well plates in normal EpiLife media supplemented with HKGS and allowed to recover overnight and reach confluence. The next day, the keratinocytes were treated with media supplemented with 2% FBS and 2 mM calcium chloride to induce differentiation [121]. Keratinocytes begin an early differentiation process (36h) that transforms the individual cells into a monolayer expressing involucrin and creates cell-cell attachments. At 36 h post treatment with FBS and calcium, the media was removed the cells and replaced with HBSS. The ImageLock plate was then transferred to the WoundMaker Tool and subjected to a uniform wound. Any debris and loose cells were washed away with HBSS containing Ca^{2+} and Mg^{2+}. The growth media was then restored and imaged for CCM at select time intervals using the IncuCyte Zoom imager.

2.4 High density wound assay

The second method that was developed to evaluate KCCM and wound healing maximized the proportion of wounded leading-edge keratinocytes to enhance measurements of the biochemical and molecular changes that drive collective cell migration. On the first day, one million keratinocytes were plated in a 6 well plate and allowed to recover overnight and reach confluence. The next day, the keratinocytes were differentiated by culturing in EpiLife media supplemented with 2% FBS and 2 mM calcium chloride. At 36 h post treatment, multiple uniform wounds were created in the plate wells with 7 multichannel pipet tips that were 1 mM wide and spaced 5 mM apart. The pipet tips were drawn across the width of the 6 well plate and then turned 90 degrees and wounded again the same way to create a high-density wounded (HDW) monolayer (Figure 10). After a designated period of CCM, the media was removed from the plate and the cells were washed in cold PBS and lysed for mRNA or protein analyses.

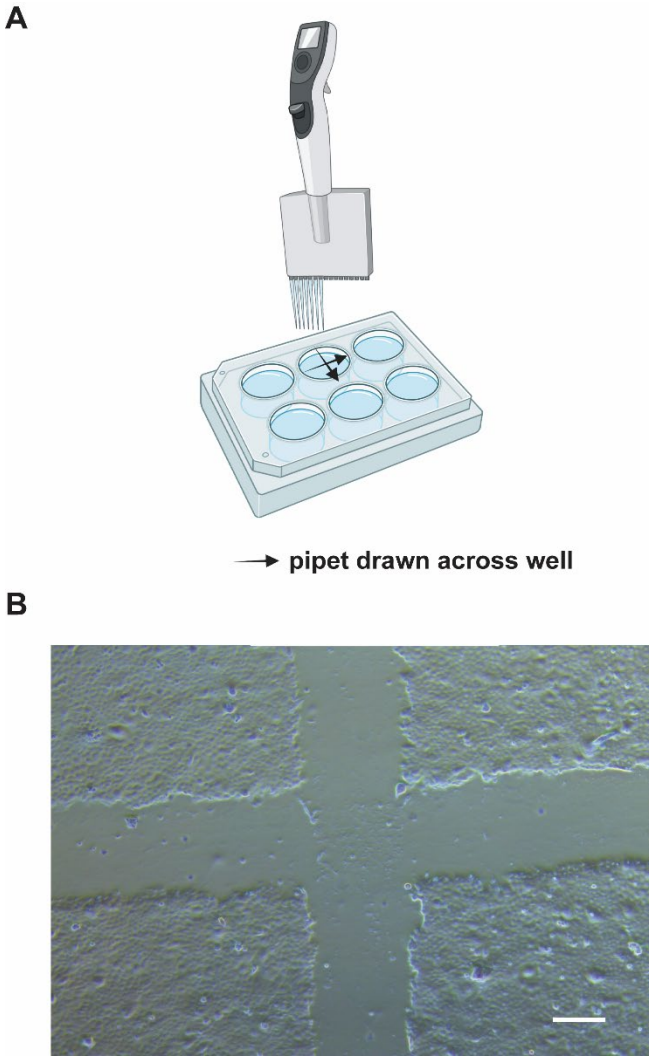

Figure 10. High density wounding model. To prepare cell lysates enriched for wound signaling mRNA and proteins, multiple uniform wounds were created in the plate wells with 7 multichannel pipet tips that were 1 mM wide and spaced 5 mM apart. The pipet tips were drawn across the width of the 6 well plate and then turned 90 degrees and wounded again the same way to create a high-density wounded (HDW) monolayer. The white scale bar is 200 μm.

2.5 Immunoblot analyses

Cell lysates were prepared by removing the growth media and washing the cells in culture in cold PBS and aspirating. Cells were either lysed directly in a breaking solution containing 1% SDS and 1X HALT protease and phosphatase inhibitor (Pierce 78429) or in a lysis solution provided in Active RHO and RAC detection kits (Active RAC detection kit, CST8815; Active RHO detection kit, CST8820). Lysates were sonicated for 5 s and heated at 95 C for 5 min, followed by a brief clearance by centrifugation at 10,000 x g. Protein concentrations were determined by the BCA assay (Pierce). Equal amounts of the protein preparations (ranging from 5 to 20 μg of lysate depending on targeted protein and applied antibody) were prepared with 6X Tris-HCL loading dye (Boston Bioproducts) and 10X denaturing solution (Invitrogen) for a total of 30 μl. Samples were heated at 95 C for 5 min and separated electrophoresis in BioRad 4-20% Tris-HCL gels with 1x Tris-Glycine/SDS running buffer (BioRad 161-0732). Protein MW ladders used in the gel electrophoresis were prepared by mixing equal volumes of SeeBlue Plus2 prestained protein ladder (Invitrogen LC5925) and Magic Mark XP (Invitrogen LC5602). Electrophoresis was carried out at 50 V for 15 minutes, then at 125V until the bromophenol blue dye front reached the bottom of the gel. Gels were first rinsed in 25% ethanol for 2-5 minutes before being transfer to nitrocellulose (BioRad 170-4159) with the BioRad turbo blotting unit (BioRad 170-4155). Protein bound blots were then blocked in an immunoblot solution containing TBS, 5% milk, and 0.1% tween-20 for 60 min at room temperature with gentle rocking. Blots were probed with the indicated primary antibodies diluted at 1:1000

overnight with rocking in immunoblot solution. The primary antibodies used include: ATF4 Cell Signaling Technology (CST), 11815, clone D4B8; GAPDH CST 2118, clone 14C10; Actin, CST 4970, clone13E5; IVL, Abcam Ab181980, EPR13054; eIF2α, CST 5324; eIF2α-P, CST3398; puromycin EMDMillipore, MABE343; CD98, Abcam Ab108300, EPR3548(2); xCT (SLC7A11), Abcam Ab175186, EPR8290(2); GCN2, Abcam Ab134053, EPR5970(2); P-GCN2, Abcam Ab75836, EPR2320Y; GADD34, Proteintech 10449-1-AP; CReP, Proteintech 14634-1-AP; ARHGEF2, CST 4076, clone 55B6; and RAC1, CST 2465. To remove unbound antibodies, blots were washed 4 times for 10-15 min each at room temperature in TBS solution containing 0.1% tween-20, followed by incubation with the respective HRP-conjugated secondary antibodies for 1 hour at room temperature. Blots were further washed 4 times for 10-15 min each at room temperature in a TBS solution supplement 0.1% tween 20 and the targeted proteins were visualized with Pierce SuperSignal West Femto (34095) and imaged on a LAS4010 Luminescent Analyzer. At least 3 biological replicates were carried out for each immunoblot measurement**.** A summary of all the antibodies used in immunoblot or pull-down experiments are listed in Table 3.

Antibodies		
Reagent or Resource	**Source**	**Identifier**
ATF4	Cell Signaling Technology (CST)	11815; clone D4B8
GAPDH	CST	2118; clone 14C10
Actin	CST	4970; clone13E5
IVL	Abcam	Ab181980; EPR13054
eIF2α	CST	5324
eIF2α-P	CST	3398
puromycin	EMDMillipore	MABE343
CD98	Abcam	Ab108300; EPR3548(2)
xCT	Abcam	Ab175186: EPR8290(2)
GCN2	Abcam	Ab134053; EPR5970(2)
GCN2-P	Abcam	Ab 75836; EPR2320Y
GADD34	Proteintech	10449-1-AP
CReP	Proteintech	14634-1-AP
ARHGEF2	CST	4076; clone 55B6
RAC1	CST	2465
Active RAC detection kit	CST	8815
Active RHO detection kit	CST	8820

Table 3. Reagent resources for experimental procedures using antibodies. A table summarizing the sources, catalog numbers for the antibodies used for protein detection by immunoblot analysis.

2.6 Measurements of protein synthesis

Protein synthesis was measured by the amount of puromycin incorporated into total cellular protein as described [122]. Culture plates with early differentiated (36h) keratinocyte monolayers were wounded and then incubated at 37 C for 4h. Cells were treated with 1 μM puromycin (Calbiochem) for the last 30 min. Media was removed and cells were washed with cold PBS solution before lysing for immunoblot analysis as described above. An anti-puromycin antibody (EMD Millipore clone 12D10) was used to detect incorporated puromycin into 10 μg of cellular lysate that was separated by SDS-PAGE and subsequently transferred to filters for western analysis.

2.7 RNA isolation and measurement by real-time PCR

Total RNA was isolated using RNeasy Plus kit according to the manufacturer's instructions (Qiagen). Keratinocytes were washed with PBS and lysed directly in the plate with RLT buffer. RNA was measured with a Nanodrop, and 260/280 ratios determined. FAST Advanced RT and TaqMan Fast Advanced Master Mix (ThermoFisher) were used to prepare cDNA using 1 μg of total RNA in a 20 μL reaction. Gene targets were amplified with FAM-labeled gene expression assays from ThermoFisher (ATF4 Hs00909569_g1 ThermoFisher 4331182; GCN2 Hs01010957_m1, ThermoFisher 4331182; GAPDH Hs02786624_g, ThermoFisher 4331182. Real-time PCR reactions were performed on a QuantStudio™ 7 Flex Real-Time PCR System (ThermoFisher Scientific) using FAST Advanced QPCR defined incubation temperatures and times for 40 cycles.

The delta-delta CT method was used to calculate relative changes in expression values between a reference housekeeping gene (GAPDH) and genes of interest.

2.8 Total RNA sequencing

Human keratinocyte WT and GCN2KO NTERT cells were plated and left unwounded or subjected to HDW in replicates of five. Post 6 hours wounding, total RNA was extracted from unwounded and HDW WT and GCN2 KO NTERTs cells using RNA easy plus kit (Qiagen) according to the manufacturer's instructions. Total RNA was submitted to GENEWIZ (South Plainfield, NJ) where they performed library preparation and sequencing. Total of 20 samples were submitted to GENEWIZ which included 5 replicates each for WT NTERTs unwounded and HDW and GCN2 KO NTERTs unwounded and HDW. Illumina HiSeq platform was used for sequencing with 150 bp paired-end reads. GENEWIZ performed differential expression (DE) analysis from raw RNA sequencing data with their standard pipeline and provided us with differentially expressed genes (DEG) list among different groups. The analysis pipeline is detailed below. After the quality check, the raw sequencing reads were trimmed for possible adapter sequences and nucleotides with poor quality using Trimmomatic v.0.36 [123]. The trimmed sequencing reads were aligned to human reference genome GRCh38 available on ENSEMBL using a STAR aligner v.2.5.2b [124]. Out of total 686,088,882 read pairs, 610,544,244 mapped uniquely to the human genome (89%). The number of uniquely mapped reads to the exons of different genes were counted using a program called featureCounts from the Subread package v.1.5.2 [125]. Lastly, the

package DESeq2 was used to determine differentially expressed genes among different groups [126]. First, I compared WT unwounded samples and GCN2 KO unwounded samples for DE analysis. The second group comparison for DE analysis was between WT HDW samples and GCN2 KO HDW samples. For the third and fourth group DE analysis, WT unwounded and GCN2 KO unwounded were compared to WT wounded and GCN2 KO wounded, respectively. The genes with log2fold change of ≥ ±1 and p-adjusted value of ≤ 0.05 were considered significant for further analyses. These genes were used for performing pathway enrichment analysis using IPA (Qiagen). RNA-seq datasets from this study are available in the NCBI GEO database (accession # GSE171666).

Oligonucleotides for PCR and CRISPR Experimental Procedures		
GCN2 exon 2 AltR1/UUGUACCCUCAAGG CCUAACGUUUUAGAGCUAUGCU/AltR2	IDT	Custom
GCN2 exon 12 AltR1/GAAGCGCA UCCCCA UCAACCGUUUUAGAGCUAUGCU/AltR2	IDT	Custom
ATF4 exon 4 AltR1/GGAUUUGAAGGAGUUCGACUGUUU UAGAGCUAUGCU/AltR2	IDT	Custom
ATF4 exon 4 AltR1/GCUCCUGACUAUCCUCAACUGUUU UAGAGCUAUGCU/AltR2	IDT	Custom
ATF4 Hs00909569_g1	ThermoFisher	4331182
GCN2 Hs01010957_m1	ThermoFisher	4331182
GAPDH Hs02786624_g1	ThermoFisher	4331182
Alt-R® CRISPR-Cas9 tracrRNA-ATT0550	IDT	1075927
Alt-R® CRISPR-Cas9 Negative Control crRNA #1	IDT	1072544

Table 4. Resources for PCR and CRISPR experimental procedures. A table summarizing the nucleotide sequences, sources, and catalog numbers for the oligonucleotides used either for CRISPR gene editing or real time PCR.

2.9 Bioinformatic Analysis

To determine which biological pathways were significantly regulated in HDW datasets of differentially regulated transcripts, DE gene datasets were submitted for IPA core analysis (Ingenuity Pathway Analysis version 60467501, Qiagen). For each biological function assigned by IPA, a statistical quantity called the activation z-score is calculated. The score is used to predict the probability of a biological function being in an active state. To identify differences in regulated biological pathways between treatment groups, the core analysis was followed by a comparison analysis in IPA. Finally, the Upstream Regulator tool was used to determine the biological impact of upstream molecules according to the genes they regulate. The Upstream Regulator tool assigned an activation z-score for that gene network [127]. Bioinformatic analyses were performed in collaboration with Parth Amin.

2.10 ZipChip capillary electrophoresis mass spectrometry

The ZipChip CE ion source from 908 Devices (Boston, MA) was interfaced with a Thermo Fisher LTQ velos Orbitrap MS (Thermo, San Jose, CA). Microfluidic chips with a 10 cm separation channel (HS, 908 Devices Inc.) and the Metabolite Assay Kit (908 Devices Inc.) were used for measurement of intracellular free amino acids. The amino acid measurements were carried out in collaboration with Michael Knierman. An injection volume of 4 nL was used and the separation was run at a field strength of 1000 V/cm. A calibration curve was prepared using a sample containing all 20 amino acids (Promega L4461). The amino acid standard

was diluted 1:100 to make 10 μM standard in BGE metabolite diluent provided in the 908 device kit. A 4-point calibration curve was made by diluting the 10 μM standard 1:2. The mass spectrometer was run in positive, profile mode scanning from 70-500 m/z in the LTQ orbitrap. The runtime for the experiment was 4 minutes. The exact M+H was calculated for each amino acid to construct a configuration file. MZMine2 software [128] was then used to calculate the area under the curve for each amino acid peak. Each area was normalized to another amino acid within the same sample lysate/run. Cell lysates for CE/MS were prepared from 2 million keratinocytes. Monolayers were trypsinized and harvested by centrifugation, washed in 1X cold PBS, carefully aspirated to remove residual liquid. Cells were lysed in 50 μl water containing 20% HPLC grade methanol and 0.1 % methylmercaptoethanol as an antioxidant. The lysate was clarified by centrifugation at 12,000g, 4^{o}C for 15 min, and the supernatant was transferred to a new tube. Lysates were prepared and analyzed immediately to avoid changes in cysteine or tryptophan due to oxidation or light exposure. Next, 10 μl of lysate was diluted 1:10 in 908 devices provided metabolite diluent and 10 μl of diluted lysate was loaded onto the ZipChip for separation via capillary electrophoresis. The sample separates based on size and charge through the ZipChip, and the sample was electrosprayed from the ZipChip into the MS. If the peaks were of out of scale, the sample was diluted 1:10 again to get into the linear range of the amino acid standards.

2.11 tRNA charging assay

Cellular charged tRNA levels were measured in collaboration with Jagannath Misra as previously described [129]. Briefly, RNA was extracted from cells using TRIzol (Life Technologies, 15596018). RNA was then treated with either 12.5 mM NaIO4 (oxidized) or 12.5 mM NaCl (nonoxidized control) in sodium acetate buffer (pH=4.5) in dark at room temperature for 20 min, followed by quenching with 0.3 M glucose. Samples were spiked with 7.3 ng yeast $tRNA^{Phe}$ (R4018, Sigma) and then subjected to desalination using a MicroSpin G-50 column (27533001, GE Healthcare). Next, RNA was deacetylated (tRNA discharging) in 50 mM Tris-HCl (pH=9.0) solution at 37°C for 45 min. Following deacylation, 5'-adenylated adaptor (5′-/5rApp/TGGAATTCTCGGGTGCCAAGG/3ddC/-3′) DNA oligomer was ligated to the tRNA using T4 RNA ligase2 truncated KQ (M0351L, New England BioLabs). An oligomer (5'-GCCTTGGCACCCGAGAATTCCA-3'), complementary to the adaptor sequence, was used for cDNA synthesis using SuperScript IV RT kit (Invitrogen, 18090050). cDNA was used for qPCR-based detection of tRNA with the following primers: yeast phenylalanine fw-5'-GCGGAYTTAGCTCAGTTGGGAGAG-3', rev-5'-GAGAATTCCATGGTGCGAAYTCTGT GG-3'; human cysteine fw-5'-GGGGGTATAGCTCA-3', rev-5'-GAGAATTCCATGGAGGG GGCACC-3'; human tryptophan, fw-5'-GACCTCGTGGCGCA-3', rev-5'-GAGAATTCCATG GTGACCCCGACGTGA-3'. Results were first normalized to yeast phenylalanine; uncharged tRNA fractions were calculated by subtracting the charged fraction (NaIO4 treated) from total (NaCl treated).

2.12 Phase contrast, fluorescent and confocal microscopy

A Leica microscope with Intensilight epifluorescence and QImaging camera were used for phase and fluorescent imaging purposes. Images were taken using a 20X objective lens at 25 C. QImaging and Nikon Elements software were used for data acquisition. CellROX® Green Reagent is a fluorescent dye (ThermoFisher) for detecting oxidative stress in living cells. The dye is cell permeable and does not fluoresce in a reducing environment. When ROS is present, the oxidized dye emits bright green fluorescence and binds DNA, with absorption/emission at 485/520 nm. Wounded monolayers were prepared as described above and allowed to begin preparing for collective migration for 6 h. The CellROX® reagent was added to the culture media at a final concentration of 5 µM and incubated with the cells for 30 minutes at 37°C. Media was removed and cells were washed 3 times with PBS solution before imaging at 488 nM wavelength with 20X water objective using the PerkinElmer Opera Phenix High Content Screening System. Images were analyzed using the Harmony analysis software. To visualize actin architecture, confluent monolayers of WT or GCN2KO NTERT cells were wounded and then fixed in 4 percent paraformaldehyde and permeabilized with 0.1% Triton™ X-100 (Sigma T8532). Cells were then stained with 1 μg/mL DAPI (4’,6-diamido-2-phenylindole dihydrochloride, Sigma-Aldrich D9542) and fluorescein isothiocyanate labeled Phalloidin (Sigma-Aldrich P5282).

2.13 In vivo wound healing model

WT C57BL/6J and *Gcn2*$^{-/-}$ C57BL/6J (*Eif2ak4*$^{tm1.2Dron}$) mice were reported [130] and were used for assessment of wound healing using the splinted excisional wound model to deter contraction of the wound edge and mimic the human mode of wound healing that involves re-epithelization and formation of granulation tissue instead of wound margin contracture used by rodents [131]. The in vivo wound healing experiment was performed in collaboration with Amitava Das, Nandini Ghosh, Tanner Guith, and Sashwati Roy; located at the Department of Surgery and the Indiana Center for Regenerative Medicine and Engineering, Indiana University School of Medicine. Mice were anesthetized, and fur removed to use punch biopsy tools that create regular 8 mM wounds, and the opening was held in place with a silicone splint. This prevented the rodent from contracting the muscle around the skin and closing the wound in a manner not connected to re-epithelialization. Wound closure was documented by imaging beginning on day 0, day 5, and day 10. Microscopic wound re-epithelialization was calculated using ZenBlue (Zeiss, Germany) software by measuring the original width of the wound (W) and then measuring the portions of the wound that had re-epithelialized (E). Percent-re-epithelialized was calculated as: (E/W) × 100 as previously described [132]. All animal experiments were approved by the Indiana University Institutional Animal Care and Use Committee, which ensures compliance with the guide for the care and use of laboratory animals published by the NIH. [133]

2.14 Statistical analyses

GraphPad Prism v9.0.1 was used to generate all graphs and perform relevant statistical tests. Statistical comparisons were performed as appropriate for the experimental design using two-tailed t-tests, one-way or two-way ANOVA, as indicated. When significance was measured in the ANOVA, multiple comparisons between groups were made using Dunnett's or Tukey's post hoc analysis. A significance level (α) was defined as $\alpha = 0.05$. Individual values were shown in all bar graphs while data variability as the standard deviation (SD) from the mean or standard error of measure (SEM) were shown in error bars for bar graphs or scatter plot line graphs, as indicated. Significance was drawn on graphs and bar charts and defined with asterisks using the following format: *p<0.05. **p<0.01, ***p<0.001, ****p<0.0001. Numbers of biological replicates are designated as (n) in each figure legend.

2.15 Illustrations

Illustrations for the figures were prepared using BioRender.com software. The model presented in Figure 20 was rendered in collaboration with Miguel Barriera Diaz.

CHAPTER 3. RESULTS

3.1 Role for GCN2 in keratinocyte collective cell migration in wounding

NTERT human keratinocytes are a well-established model to study skin biology and KCCM [50, 73, 116, 134, 135]. KCCM during wound healing was measured using an IncuCyte Zoom instrument. Upon uniform scratch wounding of the NTERT cells with a WoundMaker tool, sequential time-lapse images were taken at regular intervals to show that the differentiated keratinocytes move forward into the wounded space as a sheet of cells (Figure 1A-B). These results confirm that our model recapitulates KCCM [136]. Given that complete closure of the wound can occur within 9 hours, this result indicates that KCCM was a primary result of migration and not proliferation since NTERT keratinocytes have a doubling time of 24-30 hours in vitro [137].

I addressed the role of GCN2 in KCCM by using CRISPR/CAS9 and sgRNAs for targeted deletion of exon 2, which encodes the N-terminal RWD domain, or exon 12, a region encoding the critical lysine reside in the kinase domain (Figure 11C). The resulting sgRNAs edited the *GCN2* (*EIF2AK4*) loci, creating a pool of knockout (KO) keratinocytes effectively lacking GCN2 protein expression (GCN2KO) (Figure 11D). Early passage GCN2KO cells were used in all experiments. Using wound healing assays, a marked reduction in wound closure was observed in the GCN2KO cells compared to the WT NTERT controls (Figure 11F). These results were confirmed using two different primary normal human epidermal keratinocytes (NHK) that were isolated from foreskin tissue from separate donors [120]. The sgRNA targeting exon 12 was used to delete *GCN2* in

NHKs derived from two separate individuals (Figure 11E) and analysis of wound closure in both donor GCN2KO cells showed delayed closure (Figure 1G). These results indicate that GCN2 facilitates KCCM in during wounding.

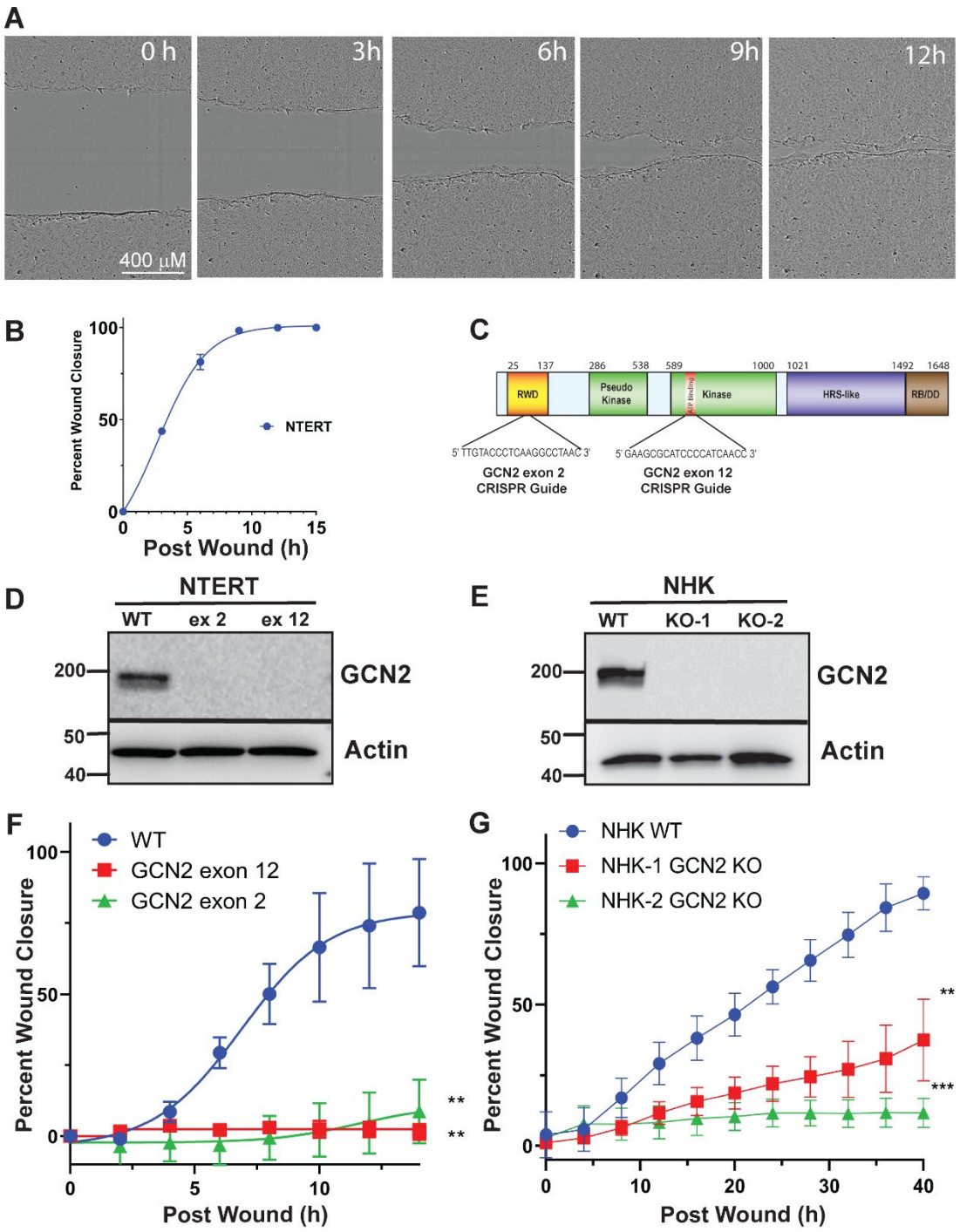

Figure 11. GCN2 facilitates collective cell migration in cultured human keratinocytes during wounding. (A) NTERT human keratinocytes were subjected to wounding and wound closure was monitored by an IncuCyte ZOOM

Live-Cell Analysis System. Images show closure of the wound for up to 12 h post wounding. (B) Percent wound closure of NTERT cells over time. (C) CRISPR/CAS9 guide design for targeting *GCN2* exon 2, which corresponds to the N-terminal RWD region, or exon 12 that encodes the ATP binding site in the kinase domain of GCN2. Efficiency of CRISPR/CAS9 GCN2KO was assessed by immunoblot measurements of GCN2 protein in (D) pooled NTERT cells edited with exon 2 or exon 12 sgRNA and (E) two independent pools of normal human keratinocytes (NHK) cells edited with the RNA guide targeting exon 12. Wild-type (WT) NTERT and NHK indicates cells with control sgRNA. Representative of three independent immunoblots. (F-G) Wound closure over time in control sgRNA WT and GCN2KO NTERT (n=4) and normal human keratinocytes NHEK cells (n=6). WT vs KO One-way ANOVA Tukey's multiple comparisons test. Error bars are SD and ** represents $p<0.01$ and *** $p<0.001$ represents.

3.2 Wounding activates GCN2 and the eIF2α kinase is required to sustain the integrated stress response

To determine the molecular consequences of depleting GCN2 in the initiation of KCCM following wounding, I developed a technique called high-density wounding (HDW) (Figure 10). This method enhances the numbers of keratinocytes in proximity to the scratch wound using tips attached to a multichannel pipettor to make parallel scratch wounds on tissue culture plates. Using constant pressure, the tips were drawn across the well once in both horizontal and vertical directions. The HDW method created a regularly spaced wound grid, enriching the number of leader cells to organize the initiation of KCCM. Given that measurable progression of the leading front can be detected between 2-4 h post wounding, I collected cell lysates at intervals from 5 minutes to 4 hours post wounding to capture the initiation, amplitude, and duration of the ISR. Control WT and GCN2KO NTERT cells were differentiated into epithelial sheets for 48 h before being subjected to HDW. Immunoblot analyses of WT NTERT lysates revealed that wounding leads to activation of GCN2, as measured by GCN2 phosphorylation, within 30 min to 1 h post injury (Figure 12A). Of importance, the WT NTERT cells showed enhanced eIF2α-P in the unwounded cells compared to GCN2KO and these levels were sustained in the WT cells throughout the wounding time course (Figure 12B). By comparison, eIF2α-P was reduced in the unwounded GCN2KO cells and was sharply depleted after 1 h of wounding. These results indicate that activated GCN2 during wounding is necessary to sustain eIF2α-P levels and is critical for KCCM.

ATF4 has a prominent role in the implementation of the ISR during many environmental insults. ATF4 expression was increased following wounding; however, elevated ATF4 protein levels occurred independent of the functional status of GCN2 (Figure 12B). While eIF2α-P is typically important for translation induction of *ATF4*, there are other reported mechanisms involving changes in *ATF4* mRNA synthesis and turnover and ATF4 protein stability, which significantly contribute to enhanced ATF4 protein levels, and some of these processes involve ancillary pathways [138-144]. The role of ATF4 in the wound closure will be further addressed below. ISR-directed translation is controlled in part by negative feedback through induced expression of GADD34 and CReP. The increase in GADD34 and CReP expression following wounding was similar in both WT and GCN2KO keratinocytes. These results suggest that loss of GCN2 combined with increased GADD34 and CReP levels, contributes to reduced eIF2α-P in wounded GCN2KO cells.

Translational control in WT and GCN2KO NTERT cells subjected to HDW was measured using puromycin labeling. There was about a 2-fold increase in protein synthesis in unwounded GCN2KO cells compared to control WT (Figure 12C-D). Upon wounding, there was a 3-fold average increase in global translation in GCN2KO keratinocytes compared to control WT. These results support the model that GCN2 and associated eIF2α-P contribute to lowered global protein synthesis following wounding.

Small molecule inhibitors are frequently used as modulators of the ISR. For example, GCN2iB is a potent inhibitor of GCN2 [145] and guanabenz interferes

with GADD34-directed dephosphorylation of eIF2α-P resulting in ISR activation [146]. WT and GCN2KO NTERT cells were measured in the wound healing assay and treated with vehicle, GCN2iB, or guanabenz prior to and during the wounding assay. GCN2iB impaired wound closure of WT NTERT cells whereas guanabenz compensated for the loss of GCN2 and restored KCCM in GCN2KO cells. Treatment of WT NTERT cells with guanabenz did not alter wound closure kinetics. Similarly, treatment of GCN2KO cells with GCN2iB did not change KCCM following wounding (Figure 12E). These results further support the model that eIF2α-P by GCN2 is critical for wound closure.

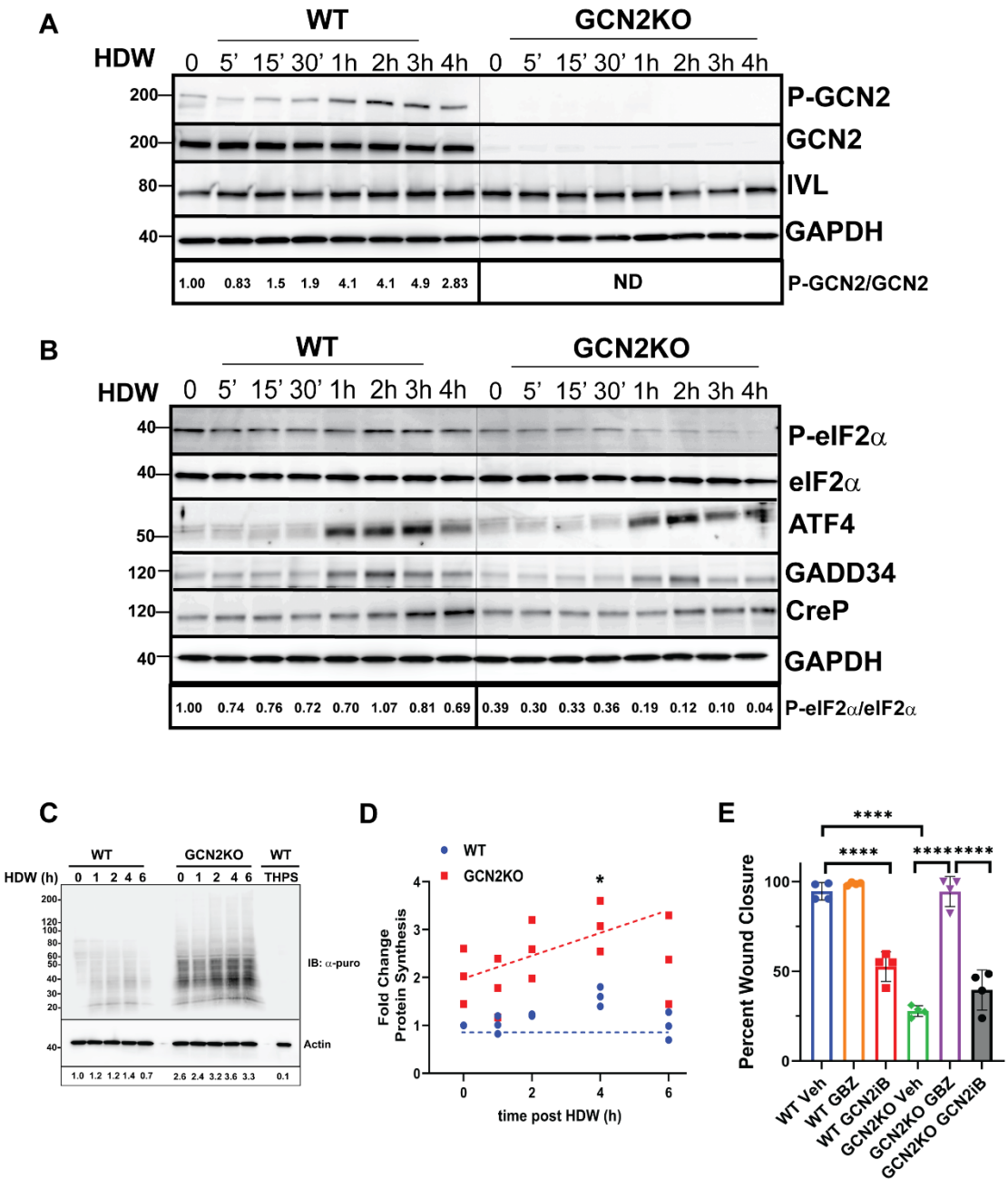

Figure 12. High-density wounding induces GCN2-P and sustains eIF2α-P during keratinocyte collective cell migration. (A-B) WT and GCN2KO cells were subjected to HDW, and lysates were collected at specified times after wounding for immunoblot analyses. Immunoblot analyses using antibodies specific to the indicated proteins. Immunoblot panels for WT and GCNKO cells for each

protein were carried out in one experiment to allow for direct comparisons. (A) Fold change for phospho-GCN2 is indicated at the bottom of the immunoblot panels. "ND" indicates that total and phosphorylated GCN2 was no detectable in the GCN2KO in the immunoblot analyses. (B) Fold change for phospho-eIF2α is indicated at the bottom of the figure panels. (C) WT and GCN2KO NTERT cells were collected at 6 h following wounding. Thirty minutes prior to harvest, 1 μM puromycin was added to the cultures to label nascent polypeptides. Lysates were prepared, subjected to SDS-PAGE, and puromycin-labeled nascent polypeptides were identified on immunoblots using antibodies specific to puromycin. As a control, the WT or GCN2KO cells were treated with 1 μM thapsigargin (THPS) for 4 h in the absence of HDW. The bottom panel shows an immunoblot measurement of GAPDH to illustrate that equal amount of protein were analyzed for each lysate preparation. D) The average fold change in puromycin tagged proteins in three experiments are shown relative to WT cells not subjected to HDW. One-way ANOVA Dunnett's multiple comparisons test (n=3); Error bars are SD and * represents $p<0.05$. (E) WT NTERT and GCN2KO cells were treated with 5 μM GCN2iB or 1 μM guanabenz at the time of wounding and percent wound closure was measured at 16 h. One-way ANOVA Tukey's multiple comparisons test (n=4); Error bars are SD and **** represents $p<0.0001$.

3.3 Loss of ATF4 does not disrupt keratinocyte collective cell migration

It is curious that wounding induced ATF4 expression in both WT and GCN2KO NTERT cells as previously it was demonstrated that UVB-induced activation of GCN2 in NTERT keratinocytes does not lead to increased ATF4 expression [50, 73]. I used CRISPR/CAS9 to delete an 800 bp region of ATF4 exon 4. As expected, ATF4 protein as measured by immunoblot was induced in WT NTERT cells upon exposure to thapsigargin, a potent ER stress agent, whereas there was minimal ATF4 in the knockout cells (Figure 13A). Given this functional validation of the ATF4KO cell line, WT and ATF4KO NTERT cells were then tested in the wound healing assay. There was no difference in wound closure between WT and ATF4KO cells (Figure 13B). However, treatment of the ATF4KO cells with GCN2iB delayed wound closure (Figure 13C), showing that the knockout cells still required the GCN2-directed ISR for KCCM. These results are consistent with the results that induced ATF4 expression in NTERT cells is independent of GCN2 and suggests other target(s) for GCN2-directed wound closure in keratinocytes.

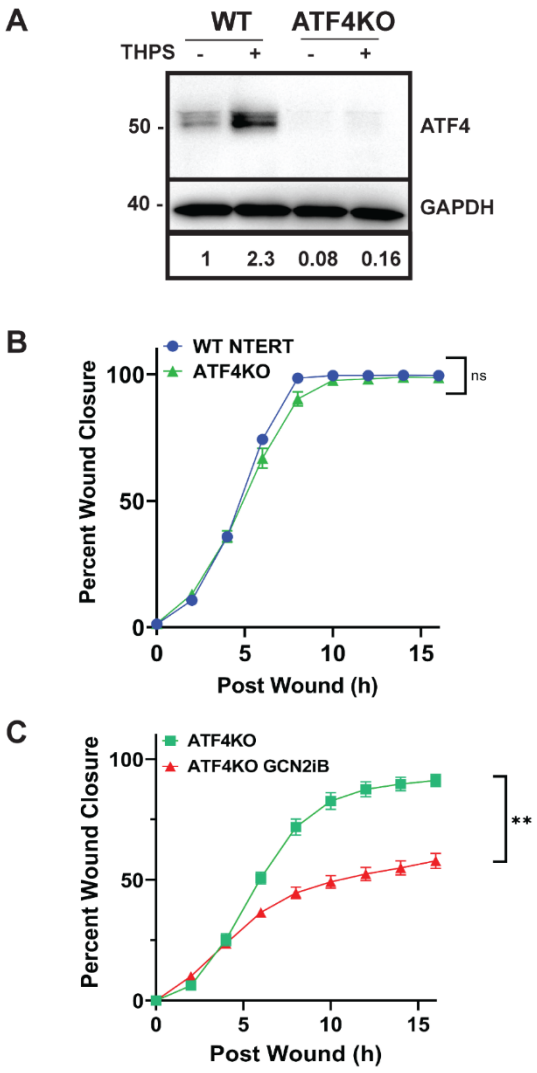

Figure 13. Depletion of ATF4 in NTERT keratinocytes does not impair KCCM. (A) WT and ATF4KO cells were treated with 1 μM thapsigargin (THPS) for 6 h and the levels of ATF4 protein were measured by immunoblot analyses. (B) WT and ATF4KO cells were analyzed for closure during wound healing. n.s. $p>0.05$ two-tailed paired T-test (n=8) (C) ATF4KO cells were treated at the time of wounding with 5 μM GCN2iB or vehicle and wound closure was measured with IncuCyte ZOOM Live-Cell Analysis System. Two-tailed paired T-test (n=11), ** $p<0.01$, error bars are SD.

3.4 Transcriptome analyses during keratinocyte collective cell migration in WT and GCN2KO cells

To delineate GCN2-dependent gene expression pathways in KCCM, I pursued an unbiased transcriptome analysis. WT and GCN2KO NTERT cells were unwounded or subjected to HDW, and RNA was isolated and analyzed by RNA-seq. DESeq2 was used to determine differentially expressed (DE) genes among different groups [126]. Genes with log2fold change of ≥ ±1 and p-adjusted value of ≤ 0.05 were considered significant for further analyses. Expression of 1263 genes were significantly enhanced, and 1222 genes were significantly lowered upon deletion of GCN2 in NTERTs compared to unwounded WT NTERTs cells (Figure 14A). With HDW, 1070 gene transcripts showed a significant increase, while 1209 were reduced in GCN2KO compared to WT (Figure 14B). In WT NTERT cells, 400 gene transcripts showed a significant increase upon HDW, while 230 were lowered (Figure 14C). By comparison, in GCN2KO subjected to HDW cells only 73 gene transcripts showed a significant increase while 23 were significantly decreased, indicating that loss of GCN2 sharply diminishes the plasticity of mRNA expression upon wounding (Figure 14D). These results show that wounding triggers significant changes in the transcriptome in WT keratinocytes and that loss of GCN2 significantly altered mRNA expression in both unwounded and wounded cells.

To distinguish which biological networks were affected by GCN2, I conducted pathway enrichment analysis using Ingenuity Pathway Analysis (IPA) software from Qiagen. HDW in the WT keratinocytes induced gene expression in

wounding, cellular migration, cytoskeletal reorganization, and inflammation (Figure 15A). By comparison, there were negative activation scores for these biological functions in wounded GCN2KO cells. Of importance, HDW in the GCN2KO cells enhanced genes involved in generation of ROS. Next, I used the IPA Upstream Regulator Analysis tool to predict which transcriptional regulators were disrupted with deletion of GCN2 (Figure 15B). This tool uses a statistical approach by defining a quantity (z-score) that determines whether an upstream transcription regulator has significantly more “activated” predictions than “inhibited” predictions of changes in target gene expression. The positive or negative sign of the calculated z-score will reflect the predicted activation state of the regulator; for example, if the score is less than zero, it is predicted to be inhibited, whereas a score greater than zero is predicted to be activated. There were positive activation scores for genes regulated by the ATF transcription factor family (ATF2, ATF3, and ATF4) and negative activation scores for genes regulated by the CEBP transcription factor family (CEBPA, CEBPB, and CEBPD). Genes associated with wound-associated cytokine signaling (PDGFBB, TGFB1, and IL1B) and inflammatory pathways (RELA, NFKB complex, IL6, and STAT3) also had negative activation scores in the GCN2KO cells. It is also noteworthy that genes associated with *RAC1* and hydrogen peroxide formation had significant negative activation in GCN2KO cells (Figure 15D). These results suggest that GCN2 is critical for appropriate programming of multiple transcription networks affecting diverse cell functions, including stress responses, inflammation, and ROS generation.

I next addressed the differences in gene expression in unwounded WT and GCN2KO keratinocytes that could alter the capacity for wound healing prior to any wound induced stress. In the unwounded GCN2KO cells, there was significant increased expression of genes involved the unfolded protein response (UPR) compared to unwounded WT cells (Figure 15C). This result may reflect the demand placed upon the ER in GCN2KO cells to synthesize and correctly fold proteins in a cellular state with reduced eIF2α-P and translational control. Analysis of amino acid transporters in the unwounded state revealed upregulation of cystine co-transporter genes, *SLC7A11* (*xCT*) and *SLC3A2,* in the GCN2KO cells versus WT (Figure 14I). *CHAC1*, an enzyme that converts cytosolic glutathione into free cysteine, was also sharply enhanced in the GCN2-deficient keratinocytes. Import of cystine and maintenance of free cellular cysteine is critical for glutathione production and ROS management [147].

I also assessed changes in HDW upon loss of GCN2 for gene transcripts involved in KCCM, including ECM, cytoskeletal dynamics, and ROS (Figure 15D). In a comparison between HDW GCN2KO vs WT keratinocytes, there were significant reductions in the levels of gene transcripts encoding key basement membrane proteins, *COL4A1*, *COL18A1*, laminin alpha chains, as well as many matrix metalloproteinases (MMPs). Expression of key integrins *ITGA4*, *ITGB5,* and interacting transmembrane genes *SEMA4A* and *PLXND1* were also sharply lowered with deletion of GCN2, as were expression of genes involved in RAC1 signaling. RAC1 coordinates ROS production, which is required for actin cytoskeletal rearrangements necessary for formation of leading edge lamellipodia.

Among genes involved in ROS management in the GCN2KO cells, expression of NRF2 target genes, *HMOX1*, *ATF3, and NQO1* were significantly increased, suggesting an adaptive response against active oxidative stress is occurring. However, other genes known to contribute to ROS generation, such *ALOX5* and *CEBPD*, were down regulated in GCN2KO cells. These results underscore that GCN2 is critical for appropriate management of multiple critical transcriptome networks involved in KCCM. These networks are suggested to be implemented by GCN2, ensuring the ability of these cells to implement key phases in wound healing.

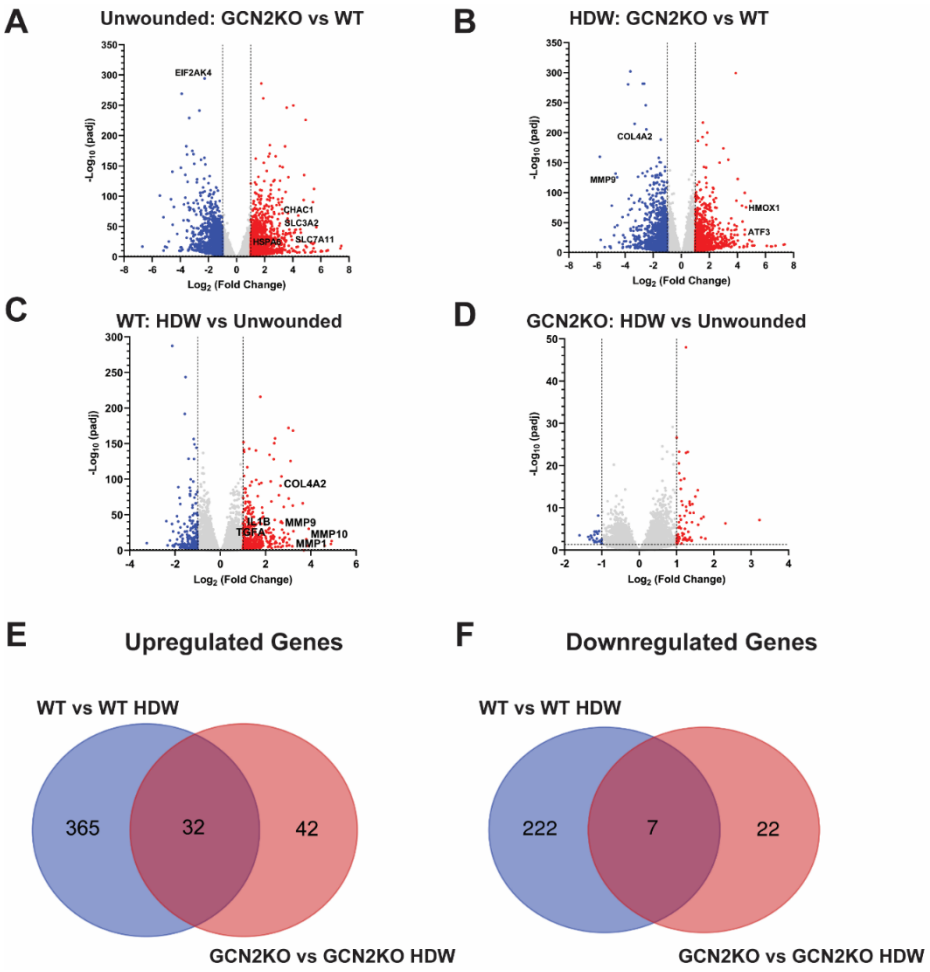

Figure 14. Transcriptome profiling of wounded keratinocytes. (A-D) Volcano plots illustrating log2 fold change with p-adjusted value (-log base 10) between unwounded GCN2 KO versus WT (A), wounded GCN2 KO versus WT (B), WT wounded vs unwounded (C) and GCN2 KO wounded vs unwounded (D). Venn diagrams showing the number of genes upregulated (E) or downregulated (F) with wounding in WT and GCN2KO keratinocytes. The number of genes commonly regulated with wounding are shown in the intersection.

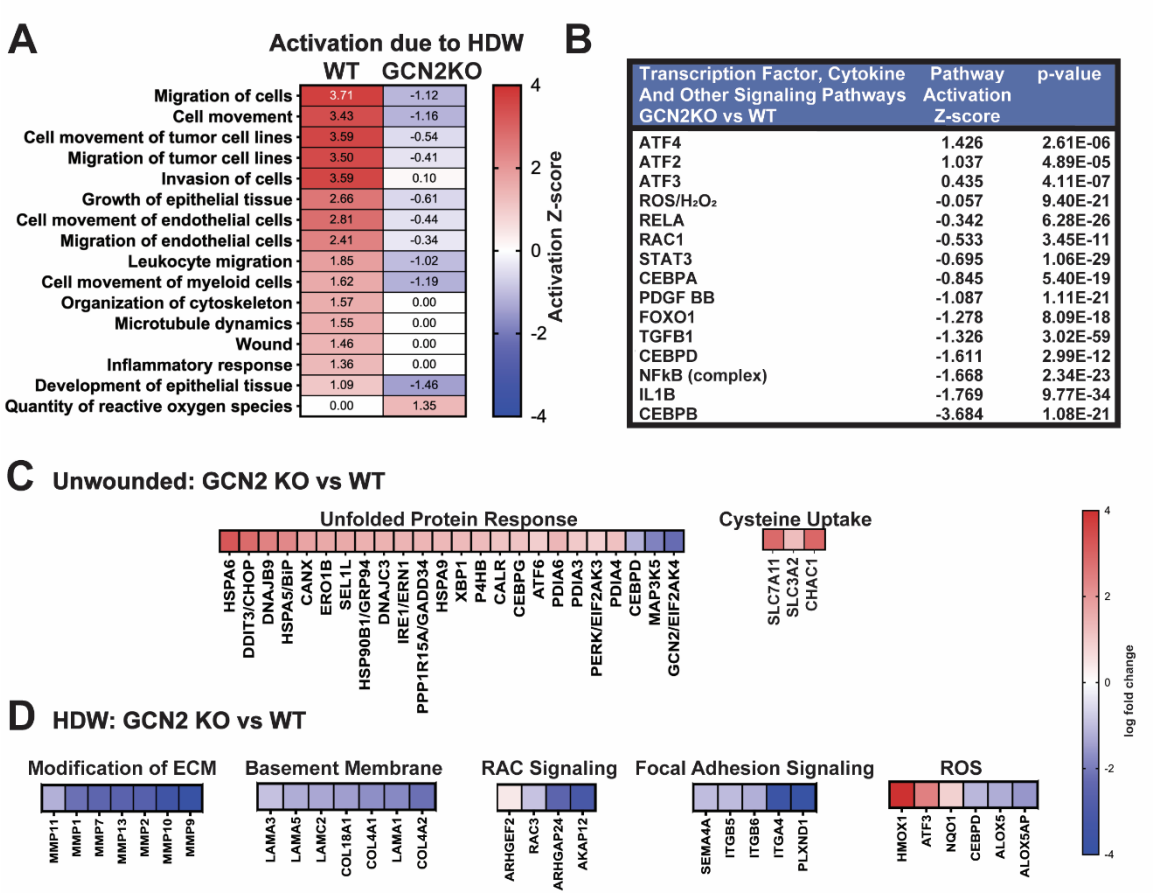

Figure 15. Pathway analysis of global transcriptome changes in wounded keratinocytes indicates altered expression of genes involved in cellular migration and the unfolded protein response. (A) Heat map of activated molecular functions comparison between WT HDW-unwounded and GCN2 KO HDW-unwounded made using comparison tool of IPA. Heat map shows activation Z-scores with the scale showing highest z scores in red and lowest in blue. (B) Table of upstream regulators of DEG in HDW GCN2 KO versus HDW WT group predicted using Upstream Regulator Effects Analysis tool of IPA. (C) Heat map of differentially expressed UPR genes and genes regulating cystine uptake identified in unwounded GCN2 KO NTERT cells. Data is depicted as log2fold change of genes in GCN2 KO unwounded versus WT unwounded group. The scale shows

the highest log2fold change is denoted as red and the lowest is denoted as blue. (D) Heat maps illustrating a group of differentially expressed genes in wounded GCN2 KO NTERT cells. The genes are categorized based on distinct roles in different stages of cell migration. Data is represented as log2fold change of genes in GCN2 KO HDW versus WT HDW group. The scale to the right of the panels shows the highest log2fold change as denoted as red and the lowest represented as blue.

3.5 GCN2 and cysteine maintenance during keratinocyte collective cell migration and wound closure

Given the canonical role for GCN2 as a monitor of amino acid availability via uncharged tRNAs [27], it was important to explore whether amino acid deprivation coincided with activation of GCN2 following wounding. Using capillary electrophoresis mass spectrometry to profile amino acid levels during HDW, free cysteine levels in cells were determined to be decreased with wounding and were further reduced in GCN2KO cells when translation is not appropriately regulated (Figure 16 and 17A).

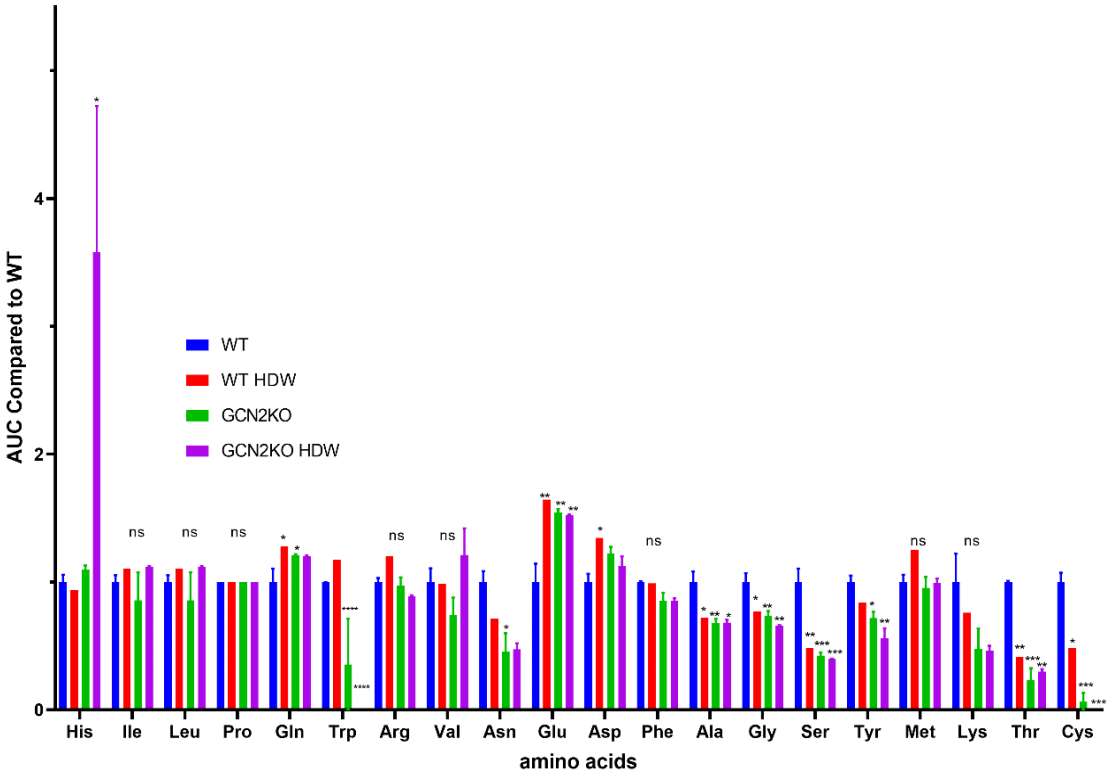

Figure 16. Measurements of free amino acids in unwounded and wounded WT and GCN2KO cells. Measurements of free amino acids in unwounded WT and GCN2KO cells and 4 h after wounding**.** The bar graph shows the area under the curve (AUC) values for the indicated amino acids in unwounded and wounded WT and GCN2KO cells relative to WT cells not subject to wounding. One-way ANOVA Dunnett's multiple comparisons to WT. Each measurement is derived from 3 biological replicates. The error bars represent the standard error (SEM) from the mean.

Reduced cysteine upon wounding was also corroborated by the analysis of aminoacylated $tRNA^{Cys}$ in WT and GCN2KO cells following wounding. There were increased levels of uncharged $tRNA^{Cys}$ in WT cells subjected to wounding, with elevated levels in both unwounded and wounded GCN2KO cells (Figure 17B-C). These results suggest that wounding can enhance levels of uncharged tRNAs that can activate GCN2.

I next addressed the roles that GCN2 plays in ensuring appropriate cysteine levels in wounded keratinocytes. First as noted above, there was elevated protein synthesis in GCN2KO that was exacerbated upon wounding, suggesting that loss of appropriate translation dampening upon eIF2α-P can lead to increased demand for free amino acids (Figure 12C). Furthermore, as noted in the transcriptome analyses (Figure 15C), expression of *SLC3A2* and *SLC7A11* mRNAs, encoding subunits of a cystine/glutamate antiporter system, were increased in WT NTERT cells upon wounding and in GCN2KO cells independent of wounding (Figure 17D). However, levels of SLC3A2 protein were lowered in GCN2KO cells independent of wounding and SLC7A11 was partly reduced in wounded in the knockout cells (Figure 17E). These results suggest that GCN2 serves to enhance synthesis of SLC3A2 and SLC7A11 proteins, which would ensure appropriate uptake of cystine. Deletion of GCN2 would reduce the levels of these transporter protein despite elevated gene transcript levels.

Given that free cysteine is severely limiting in GCN2KO cells, it was important to determine whether the addition of additional amounts of cystine, the oxidized dimer form of cysteine, to the medium prior to and during wounding would

rescue the KCCM defect that was observed in the GCN2-deficient keratinocytes. Analysis of wound closure with cystine supplementation showed that additional cystine in the culture medium significantly improved wound closure in the GCN2KO cells (Figure 17F). Finally, eIF2α–P levels of WT keratinocytes supplemented with cystine during HDW showed reduced levels of eIF2α-P (Figure 17G), indicating relief of the amino acid stress and consequently lowered activation of GCN2.

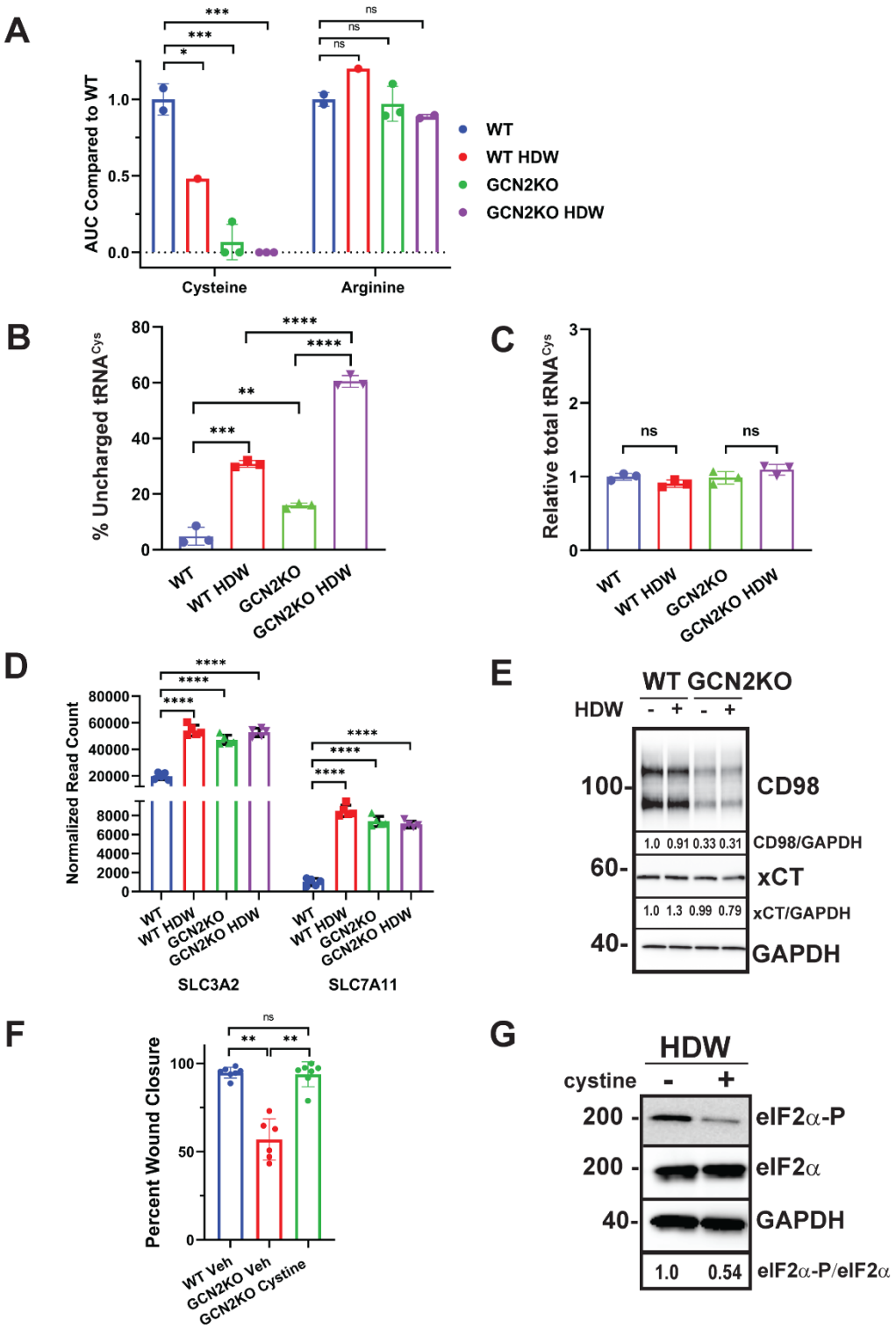

Figure 17. GCN2 is required for maintenance of free cysteine levels in keratinocytes. (A) Quantitative CE-MS measurement of free cysteine and

arginine levels in WT and GCN2KO cells harvested at 4 h post-wounding. Area under the curve (AUC) values are shown relative to WT cells not subject to wounding. One-way ANOVA Tukey's multiple comparisons. * $p < 0.05$, n.s. $p > 0.05$. (B) Levels of uncharged $tRNA^{Cys}$ and (C) total $tRNA^{Cys}$ were measured in WT and GCN2KO NTERT cells subjected to wounding. Two-tailed t-test, * $p < 0.05$, ** $p < 0.01$, *** $p < 0.001$, **** $p < 0.0001$ (n=3). Error bars are SD. (D) *SLC3A2* and *SLC7A11* gene transcripts were measured in unwounded WT and GCN2KO keratinocytes or 6 h post-wounding. Values are shown as normalized read counts. One-way ANOVA Tukey's multiple comparisons **** $p < 0.0001$ (n=5). (E) Immunoblot measurement of CD98 transporter protein levels (SLC3A2 and SLC7A11) in 6h HDW WT and GCN2KO cell lysates. Fold change in the expression of each protein for this blot is shown, following normalization to GAPDH expression. Representative of 3 biological replicates. (F) WT and GCN2KO cells were subjected to wounding and the percent wound closure determined after 16 hours. Wounded GCN2KO cells were cultured in media supplemented 6 h prior to wounding with 1 μM cystine or vehicle, as indicated. Tukey's multiple comparisons ** $p < 0.01$, *** $p < 0.001$ (n=6). (G) Levels of phosphorylated and total eIF2α, along with GAPDH, were measured by immunoblot analyses in WT NTERT cells that were subjected to HDW. Media of the wounded cells were supplemented with 1 μM cystine (+) or no additional amino acids (-). Relative levels of eIF2α-P/ total eIF2α for this blot are shown at the bottom of panel G. Representative of three independent blots.

3.6 GCN2, generation of ROS and cytoskeletal dynamics

Keratinocytes proximal to the wound undergo a transformation of the actin cytoskeleton that expands into the leading edge membrane, creating a directional force to propel the keratinocytes forward. Lamellipodia and filopodia are specialized F-actin-containing structures visible on the leading edge keratinocytes in a scratch wound. Lamellipodia have been described as a ruffled border [148], which is clearly visible extending from KCCM of the WT cells (Figure 18A, black arrows). By comparison, no ruffled border was visible at the front of KCCM in GCN2KO cells. When the keratinocytes were stained with phalloidin-FITC to visualize F-actin bundles, WT keratinocytes displayed numerous fine F-actin-containing filopodia (yellow arrows) and lamellipodia (white arrows) in the leading edge keratinocytes of WT (Figure 18A). Once again, these F-actin structures were largely absent in GCN2KO cells.

Given that balanced production of ROS at the leading edge is a key event in the cytoskeletal reorganization in KCCM [113, 149, 150] and GCN2KO altered expression of genes involved in ROS production (Figure 15A and D), I next stained WT and GCN2KO keratinocytes with CellROX green which emits fluorescence in the presence of oxidative conditions [151]. CellROX green staining revealed organized ROS accumulation predominantly localized to cells within the leading edge of WT wounded cells (Figure 18B). However, ROS staining in the GCN2KO cells was not appropriately situated in cells at the leading edge of the wound but instead there was disorganized fluorescence in cells scattered throughout the keratinocyte monolayer. Furthermore, pharmacological inhibition of GCN2 using

GCN2iB in WT cells subject to wounding showed a KCCM with impaired localized ROS production (Figure 18B).

RAC activation of NOX at the leading edge of wounded cells has been shown to be critical for localized ROS production (Ushio-Fukai, 2006) and our RNA-seq analysis suggested that RAC signaling was disrupted in GCN2KO keratinocytes (Figure 17E and H). To directly determine whether inhibition of RAC activation or direct inhibition of NOX disrupts ROS production at the leading edge and the potential contribution of GCN2 in this signaling process, wounded keratinocyte monolayers were treated with small molecule inhibitors targeting RAC activation (NSC23766) or NOX (VAS2870, DPI) and stained with CellROX green. Application of each of these inhibitors impaired the coordinated production of ROS at the leading edge (Figure 18B), similar to what was seen in GCN2KO cells. Furthermore, the pharmacological inhibition of RAC and NOX reduced the wound closure rate of WT NTERT cells to levels observed with loss of GCN2 (Figure 18C).

Cellular activators of RAC-GTP include the GTP exchange factors (GEFs) ARHGEF2, ARHGEF6*,* ARHGEF18*,* TIAM1 *and* TIAM2. Expression of *ARHGEF2* mRNA as judged by RPM reads in our RNA-seq analysis was highest among these GEFs and was further enhanced upon knockout of GCN2 (Figure 18D). By comparison, *TIAM1* and *TIAM2* transcripts levels were modestly, but significantly decreased in GCN2KO cells. No change in *ARHGEF6* or *ARHGEF18* expression was detected between WT and GCN2KO keratinocytes. While the *ARHGEF2* mRNA levels were enhanced in GCN2KO cells, the levels of ARHGEF2 protein were lower with loss of GCN2, suggesting that GCN2 functions to enhance the

synthesis of ARHGEF2 (Figure 18E). ARHGEF2 is known to activate both RAC and RHO for lamellipodia expansion into the leading edge [152-154]. To more directly determine whether loss of GCN2 disrupts activation of RAC and RHO, I used an affinity purification system that bound active GTP forms of both proteins. Immunoblot analyses of active RHO or active RAC from equal input lysates from WT or GCN2KO cells showed that GCN2 is required to maintain their fully active forms in an unwounded monolayer of keratinocytes and during wounding (Figure 18F). RAC-GTP was reduced in unwounded GCN2KO, with further diminishment upon wounding. RHO-GTP levels were lowered about 2-fold in GCN2KO independent of wounding. Taken together, these results suggest an important role for GCN2 in induction of ROS at the leading edge via RAC activation of NOX or RHO activation to drive the subsequent expansion of the leading edge actin structures to facilitate KCCM.

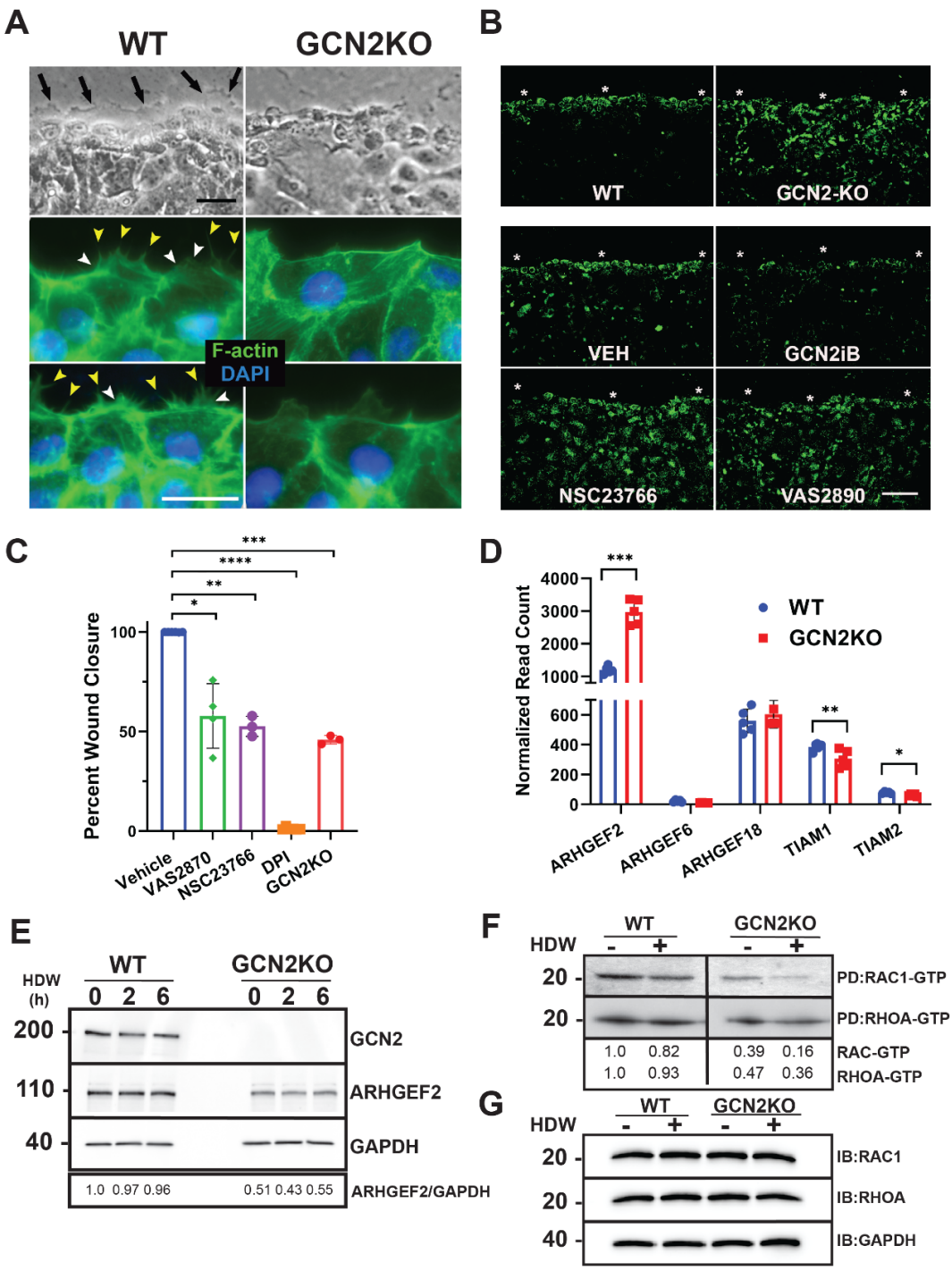

Figure 18. Loss of reactive oxygen species at the leading edge of wounded GCN2KO keratinocytes is coincident with reduced RAC-GTP and branching F-actin. (A) Leading edge of migrating keratinocytes at 6 hours post-wounding in both WT and GCN2KO cells. Top two panels demonstrate ruffled edge (black

arrows) of WT keratinocytes that are absent in GCN2KO keratinocytes (phase contrast, black bar = 20μm). Bottom four panels stained with phalloidin-FITC (F-actin, green) and DAPI (nuclei, blue). Filopodia (yellow arrows) and lamellipodia (white arrows) are seen on the leading edge keratinocytes of WT but not GCN2KO cells (white bar = 10μm). In the lower four panels, WT NTERT were treated with vehicle (DMSO), 5 μM GCN2iB, 5 μM NOX inhibitor VAS2870, or 50 μM RAC-GTP inhibitor NSC23766, as indicated, and cells and were stained for ROS with CellRox Green 6h after wounding. Cells were imaged with an Opera Phenix confocal microscope (100 μm scale bar). (C) WT NTERT cells were treated with NOX inhibitors 5 μM VAS2870 or 300 nM DPI, or RAC-GTP inhibitor 50 μM NSC23766 as indicated, at the time of wounding. As a control, GCN2KO cells were wounded without treatment. Percent wound closure was measured at 16 h post wounding. One-way ANOVA Dunnett's multiple comparisons, (n=3). (D) Levels of RAC-GTP exchange factors *ARHGEF2*, *ARHGEF6, ARHGEF18, TIAM1 and TIAM2* mRNAs in WT vs GCN2KO cells. Values are presented as normalized read counts from our RNA-seq analyses. Multiple unpaired t-tests, (n=5). (E) WT and GCNKO NTERT cells were subjected to wounding for up to 6 h and ARHGEF2, GCN2, and GAPDH levels were measured by immunoblot analyses. (F) Measurements of RHO-GTP and RAC-GTP by affinity purification assays. GST-Rhotekin or GST-PAK1-PBD fusion protein was used to bind the activated form of GTP-bound RHO or RAC1, respectively, in equivalent amounts of lysates prepared from WT and GCN2KO NTERT cells subjected to HDW (+) or no wounding (-). Levels of bound activated RHOA and RAC1 were collected using glutathione beads then measured

by immunoblot using an antibody specific to total RAC1 or RHOA proteins. GAPDH levels were measured in the starting lysates to show that equal amounts of proteins were used in the binding assays. The measurements for each of the protein measurements (RAC-GTP, RHOA-GTP, and GAPDH) in the WT and GCN2KO cells were carried out in the same in same immunoblot experiment and therefore a directly comparable. Error bars are SD. * $p<0.05$, ** $p<0.01$, *** $p<0.001$, and **** represents $p<0.0001$.

3.7 Role for GCN2 in an in vivo model of wound healing

While a wealth of information can be obtained from studies using two-dimensional cell culture, it is important to validate the key results using three-dimensional skin in vivo. Therefore, it was important to compare the wound healing capabilities of murine skin using C57BL/6J mice and C57BL/6J mice containing a homogeneous deletion of GCN2 (GCN2KO; *Eif2ak4*$^{tm1.2Dron}$/J). A splinted excisional wound model was used to deter muscle contraction of the wound edge. This approach is necessary to mimic the human mode of wound healing that involves re-epithelization and formation of granulation tissue instead of the wound margin contracture used by rodents [131]. Quantification of the wound size at both day 5 and 10 post wounding showed that wound closure was significantly impaired in GCN2KO animals compared to the WT (Figure 19A-B). Furthermore, at day 10 the wounded skin was removed, and the gap was determined in the cryosections spanning the wound bed that were stained with an antibody to KRT14 and with DAPI to identify cellular nuclei and visualized by microscopy (Figure 19C-D). These experiments also showed that there was significant reduction in wound closure in the GCN2KO skin compared to WT. These results support an essential role for GCN2 to facilitate wound closure in the context of full thickness skin.

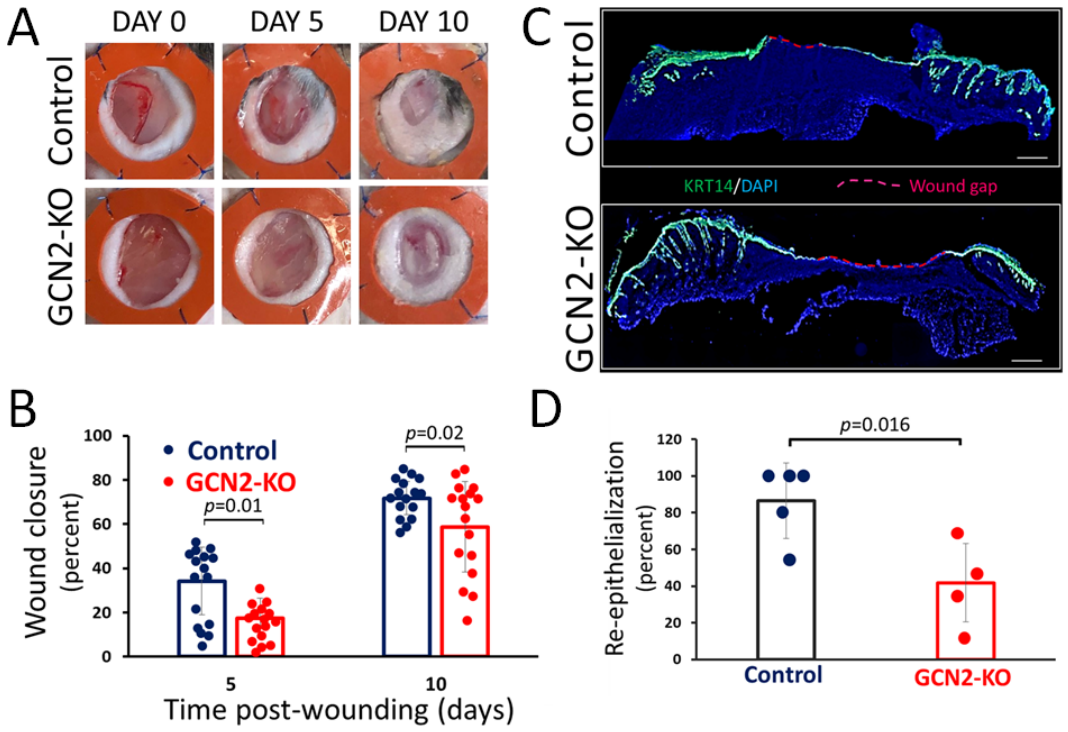

Figure 19. In vivo wound healing is impaired in the absence of GCN2. Circular excisional wounds (8 mm) were created on each flank of WT (blue dots) and GCN2KO (red dots) C57BL/6J mice. Silicone splint donuts were placed over the opening of each wound to ensure wound closure occurred due to epithelial sheet migration. (A) The size of the wound opening was determined from standardized photographs taken on Day 0, Day 5, and Day 10 post-wounding. Representative images for the experiment are provided (B) The percent wound closure at Day 5 and Day 10 was determined following comparison to the wound opening at Day 0. Each dot on the graph represents an individual measurement; the solid bars indicate the mean, and the dotted boxes represent the SD for each set. Indicated *p*-values were determined by two-tailed student t-test. (C) At Day 10, the splints were removed, the wounded skin harvested, and cryosections spanning the wound

bed were created. To identify the location of migrating sheets of epidermis, the cryosections were stained with an antibody to KRT14 (green) and with DAPI (blue) to identify cellular nuclei as visualized by microscopy. The remaining wound gap (red) was determined by measuring the total wound distance and subtracting the distance the epithelial sheets had migrated. (D) Graphical representation of percent wound closure by measuring the remaining wound gap at Day 10, as described in (C). Each dot on the graph represents an individual measurement; the solid bars indicate the mean, and the dotted boxes represent the SD for each set. Indicated *p*-values were determined by two-tailed student t-test.

CHAPTER 4. DISCUSSION

4.1 GCN2 is critical for keratinocyte collective cell migration and wound closure

Herein I present the discovery that GCN2 eIF2α kinase is critical for KCCM and wound closure. There is elevated eIF2α-P in differentiated keratinocytes and activation of GCN2 is essential for maintaining P-eIF2α upon wounding. Deletion of GCN2 led to sharply lowered levels of eIF2α-P and enhanced bulk protein synthesis by 4 hours post wounding (Fig. 12B and C). As highlighted in the model illustrated in Figure 19, GCN2 and attendant gene expression direct key processes that are critical for KCCM. For example, GCN2 provides for maintenance of cysteine levels, which are important for appropriate protein synthesis and control of ROS, both processes critical for KCCM. Maintenance of cysteine levels is also suggested to be critical for activation of GCN2 via $tRNA^{Cys}$ charging that are diminished upon wounding (Figure 17B). Furthermore, GCN2 is important for F-actin remodeling, along with the generation and localization of ROS, in the leading edge on wounded keratinocytes. While the ruffled border was readily detected in wounded WT keratinocytes, these leading edge structures were absent in GCN2KO cells (Figure 18A). The F-actin bundles extending in the migrating sheet of keratinocytes were largely absent in the GCN2-deficient cells. Appropriate ROS production is critical for cytoskeletal reorganization in the KCCM, and while WT cells showed ROS situated at the leading edge the genetic or pharmacological disruption of GCN2 led to diminished and disorganized ROS (Figure 18B). Finally, the importance of GCN2 in wounding healing was confirmed using splinted

excisional wound model in mice. Mice deleted for GCN2 showed a significant impaired in the closure of wound (Figure 19) Together, these results indicate that GCN2 contributes to KCCM by multiple processes and the loss of GCN2 in keratinocytes impairs many key processes that are critical for implementing wound healing (Figure 20**).**

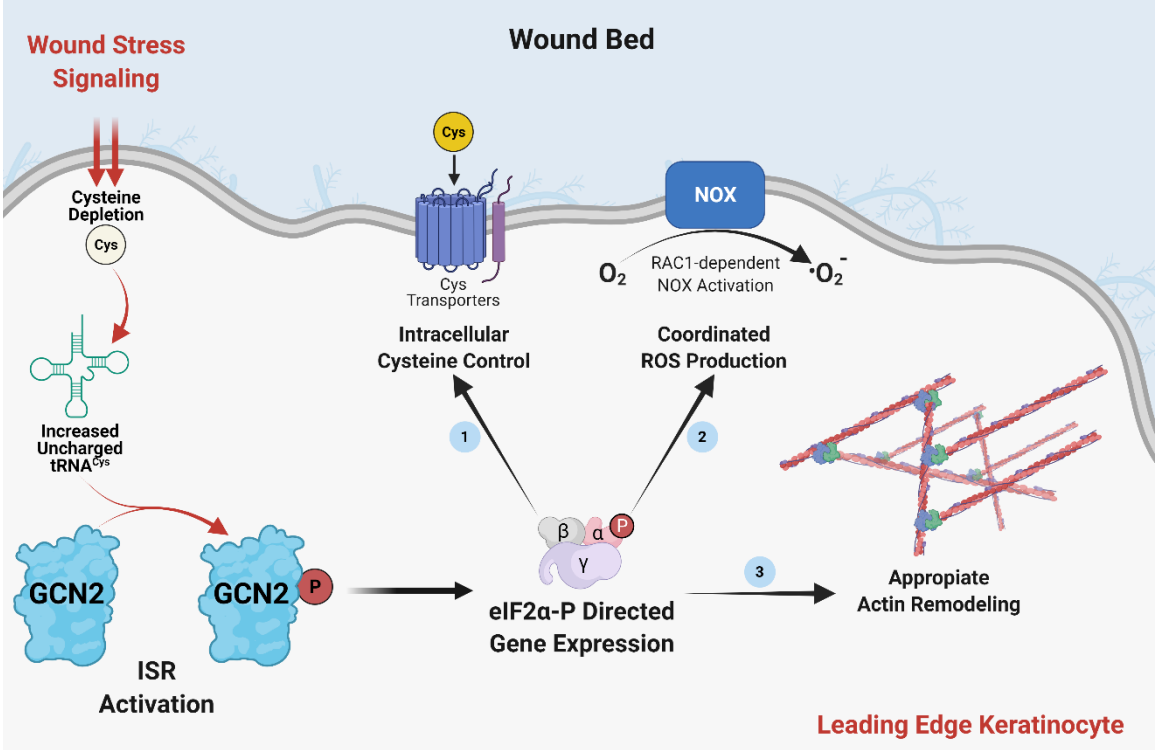

Figure 20. Model of the activation and function of GCN2 in KCCM and wound healing. The wound bed is illustrated, along with the leading edge of keratinocytes. GCN2 is activated in response to wounding, which is indicated by its phosphorylation. Free cysteine levels are depleted in the wounded keratinocytes, which is suggested to be a direct activator of GCN2. Induced GCN2 facilitates KCCM during wounding by multiple mechanisms. (1) Enhanced synthesis of cysteine transporters, including SLC7A11 and SLC3A2, serves to maintain availability of intracellular cysteine which is important for glutathione production and management of ROS. (2) RAC-dependent NOX1 activation and coordinated ROS generation and localization at the leading edge; and (3) Appropriate remodeling of the cytoskeleton and formation of leading edge structures necessary for collective cell migration.

4.2 GCN2 directs an ISR that dispenses ATF4 function for keratinocyte collective cell migration and wound closure

It was surprising that while there was induced expression of ATF4 protein in response to wound healing, this process occurred independent of GCN2 (Figure 12B). Furthermore, ATF4 is dispensable for the GCN2-directed KCCM and wound healing (Figure 13). These results suggest that the ISR in wound healing involves other ISR target genes that contribute to critical structural and metabolic processes in the KCCM. Previously it was reported that the ISR functioned independent of ATF4 through other target genes in response to UV irradiation and differentiation in keratinocytes [50, 73, 116]. For wound healing, the RNA-seq and biochemical analyses suggested that GCN2 contributes to activation of RAC and RHO through a process that involved regulation of ARHGEF2 expression (Figure 18D-F). While *ARHGEF2* mRNA was significantly enhanced in GCN2KO cells, ARHGEF2 protein was diminished (Figure 18E). These results suggest that GCN2 is required for the proper translation of *ARHGEF2.* Increased ARHGEF2 protein would enhance the GDP to GTP exchange for RAC and RHO and ensure that these critical Rho-GTPases are available at sufficient levels for the actin remodeling required for KCCM (Figure 18A). Furthermore, GCN2 enhanced the expression of cystine transporters, SLC3A2 and SLC7A11, supporting the idea that the eIF2α kinase has a critical function in maintaining cysteine levels in keratinocytes. It is noteworthy that despite the reductions in protein levels, that *ARHGEF2*, *SLC3A2*, and *SLC7A11* transcript levels are each elevated in GCN2KO cells (Figures 15A and 18D). These results suggest that eIF2α-P by GCN2 likely plays a critical role

in their enhanced mRNA translation. Other mechanisms independent of the ISR are suggested to contribute to increased transcript levels for these genes, but without GCN2 these transcriptome changes are insufficient to transmit to enhanced ARHGEF2, SLC3A2, and SLC7A11 protein levels.

4.3 Role of nutrition, aging and diabetes in KCCM

Chronic wounds are associated with diabetes, aging, and poor nutrition [3, 4, 155], necessitating complex and long-term care. Given the central role for GCN2 in amino acid sensing and maintaining intracellular availability, it is important to note that nutrition is also a central component in managing wound care [156]. Arginine is a well-studied amino acid in wound healing that can be conditionally essential during increased demand [157]. Arginine has a variety of roles in the multiple cell types involved in wound healing. For example, arginine is a precursor to nitric oxide, which is utilized by immune cells during the inflammation stage of wound healing and by fibroblasts to stimulate collagen production during the maturation phase. During re-epithelialization, keratinocytes at the wound edge demonstrate a dependency on nitric oxide to trigger proliferation during wound repair [158-162]. Glutamine is another amino acid that can become conditionally essential during times of metabolic stress and can play important roles in wound healing [163-165]. For example, immune cells involved in tissue repair have high demand for glutamine, and supplementation following injury, surgery, infection, or severe burns can be beneficial. Glutamine may enhance wound healing, in part, because it is a precursor to arginine and citrulline, thereby enhancing nitric oxide

synthesis. In addition, the cyclization of glutamate produces proline, an amino acid important for synthesis of collagen and connective tissue during wound healing. Lastly, glutamine is a component of the antioxidant glutathione and is important for the appropriate mediation of oxidative stress. [164, 166-168].

Amino acid profiling in GCN2KO NTERT cells did not reveal a dependency on GCN2 to maintain intracellular levels of arginine or glutamine (Figure 16). However, GCN2 is critical for maintenance of cysteine levels in keratinocytes and further investigation of the impact of cysteine limitation or supplementation on wound closure rates in the in vivo wounding model is warranted. The amino acids used for endogenous production of cysteine are the sulfur containing amino acids methionine and serine. Recent studies have shown that dietary sulfur amino acid restriction (SAAR) improves some aspects of metabolic homeostasis by activating the integrated stress response (ISR); however, this can occur in a GCN2 independent manner. In Gcn2 -/- mice subjected to SAAR, PERK activation corresponded with induction of the ISR and the nuclear respiratory factor 2 (NRF2) antioxidant program but not ER stress. Cysteine supplementation reversed the activation of PERK and eIF2α-P, suggesting a novel glutathione-sensing mechanism in the liver that functions independently of GCN2 [169, 170]. Given the gene expression data (Figure 15C) indicating an induction of the UPR in GCN2KO keratinocytes and that cysteine supplementation reduced eIF2α-P (Figure 17G), the role of PERK activation to compensate for cysteine depletion GCN2KO keratinocytes should be investigated. Similar to our results in KCCM, ATF4 is dispensable in SAAR while being important for endogenous hydrogen sulfide

production. This result may indicate a role for GCN2 in cysteine synthesis and hydrogen sulfide production and could be investigated in this model of KCCM [171, 172].

The role of GCN2 in aging skin and wound repair is interesting given our findings. Although GCN2 has been shown to extend the life span of *C. elegans,* its contribution to aging process in mammals has yet to be fully elucidated. However, it is known that amino acid restriction via caloric restriction extends lifespan and may be related to beneficial metabolic control offered by GCN2 as it regulates autophagy, inflammation, and redox balance. These same processes affect aging as well as wound healing. Therefore GCN2 may affect the ability of aged skin to heal appropriately [173]. This hypothesis could be tested in aged WT and GCN2KO mice.

Glucose is a major source of energy for cells, and they rely on glucose transporters (GLUT) to fuel the conversion of glucose to energy. Amino acids also provide fuel to the tricarboxylic acid (TCA) cycle after being converted to acetyl-CoA or α-keto acid intermediates like pyruvate, oxaloacetate, and succinyl-CoA. Because of this important intersection of glucose and amino acid transport and catabolism to maintain energy demands for keratinocytes, cross talk between the mTOR pathway and GCN2 is another area deserving of attention in wound healing. [174].

4.4 Therapeutic implications of the ISR in keratinocyte collective cell migration and wound healing

The ISR is typically associated resolution with acute stresses. However, with chronic environmental and physiological stresses, the ISR can be altered from its adaptive functions to one that signals significant tissue damage [59, 175, 176]. Given the important functions of GCN2 in KCCM and wound healing, it is inviting to suggest that aberrant regulation of the ISR are contributors to the transitions to chronic wounds. Many of the underlying contributors to chronic wounds potently modify the ISR. For example, hyperglycemia and poor nutrition invoke eIF2α-P and translational control. In these conditions, the multiple stresses may shift the ISR from its functioning adaptive window to one that is hyperactivated and maladaptive. Furthermore, deficiencies in GCN2 functions due to genetic alterations and aging may impair appropriate ISR and deter the KCCM. Therefore, the ISR and translational control may be a critical therapeutic target to improve wound healing outcomes. There are several small molecules reported that contribute to enhancement or inhibition of the eIF2α-P and translational control (Figure 21) [145, 175, 177, 178], and future studies should investigate the utility of these and related drugs for treatment of chronic wounds.

A

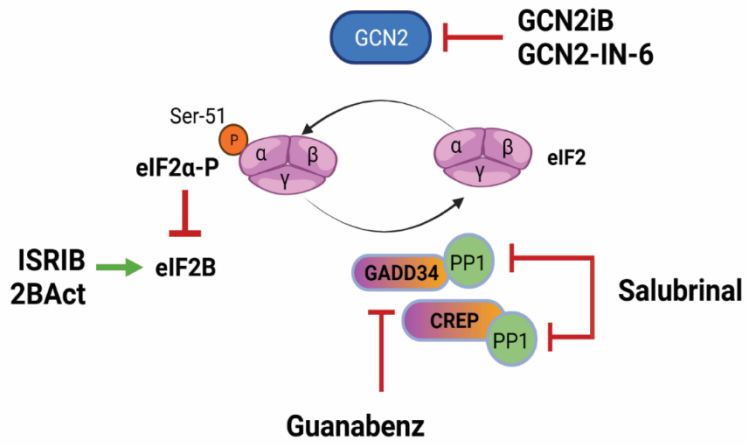

B

Modulator	Target ISR Protein	eIF2α-P changes	ISR Regulation
Guanabenz	GADD34 inhibition	Increase	Sustains
Salubrinal	PP1 inhibition	Increase	Sustains
GCN2iB	GCN2 kinase inhibition	Decrease	Decrease
GCN2-IN-6	GCN2 kinase inhibition	Decrease	Decrease
ISRIB	eIF2B activator	No change	Decrease
2BAct	eIF2B activator	No change	Decrease

Figure 21. Modulators of the Integrated Stress Response. (A) A schematic diagram depicting the various ISR proteins and the small molecules that can alter their activity. Guanabenz (GADD34) and salubrinal (PP1) target and inhibit the eIF2α phosphatases that relieve the ISR and restore translation initiation. The kinase activity of GCN2 can be inhibited with either GCN2iB or GCN2-IN-6 thus reducing the eIF2α-P and blocking the induction of the ISR. Activators of eIF2B have been shown to induce a more active holocomplex of eIF2B that serves to enhance protein translation independent of the presence of moderate levels of eIF2α-P. (B) A tabular summarization of the activities and interactions of these modulators on the target ISR protein, the subsequent changes in eIF2α-P levels and the resulting impact on the ISR.

Both guanabenz and salubrinal, which serve to enhance eIF2α-P, have the potential to restore the ISR in the context of wound healing. Because guanabenz has been approved by the FDA for high blood pressure and it appears to enhance KCCM in the in vitro wound closure model, prioritizing this molecule for testing in either the GCN2KO mice or in other diabetic wound healing models may help to determine if there is the potential to accelerate healing of full thickness wounds upon restoration of the ISR. Additionally, the eIF2B activating molecules, ISRIB and 2BAct, would also be of interest given their ability to provide relief from chronic or maladaptive ISR induction. Diabetic and aged patient populations at highest risk for chronic non-healing wounds may suffer from such chronic or maladaptive ISR induction and benefit greatly from treatment with these molecules.

REFERENCES

1. Nussbaum SR, Carter MJ, Fife CE, DaVanzo J, Haught R, Nusgart M and Cartwright D (2018) An Economic Evaluation of the Impact, Cost, and Medicare Policy Implications of Chronic Nonhealing Wounds. Value Health 21:27-32. doi: 10.1016/j.jval.2017.07.007

2. Sen CK, Gordillo GM, Roy S, Kirsner R, Lambert L, Hunt TK, Gottrup F, Gurtner GC and Longaker MT (2009) Human skin wounds: a major and snowballing threat to public health and the economy. Wound Repair Regen 17:763-71. doi: 10.1111/j.1524-475X.2009.00543.x

3. Han G and Ceilley R (2017) Chronic Wound Healing: A Review of Current Management and Treatments. Adv Ther 34:599-610. doi: 10.1007/s12325-017-0478-y

4. Frykberg RG and Banks J (2015) Challenges in the Treatment of Chronic Wounds. Adv Wound Care (New Rochelle) 4:560-582. doi: 10.1089/wound.2015.0635

5. Eckert RL (1989) Structure, function, and differentiation of the keratinocyte. Physiol Rev 69:1316-46. doi: 10.1152/physrev.1989.69.4.131610orDelete281

6. Eming SA, Krieg T and Davidson JM (2007) Inflammation in wound repair: molecular and cellular mechanisms. J Invest Dermatol 127:514-25. doi: 10.1038/sj.jid.5700701

7. Eming SA, Wynn TA and Martin P (2017) Inflammation and metabolism in tissue repair and regeneration. Science 356:1026-1030. doi: 10.1126/science.aam7928

8. Reinke JM and Sorg H (2012) Wound repair and regeneration. Eur Surg Res 49:35-43. doi: 10.1159/000339613

9. Rousselle P, Braye F and Dayan G (2018) Re-epithelialization of adult skin wounds: Cellular mechanisms and therapeutic strategies. Adv Drug Deliv Rev. doi: 10.1016/j.addr.2018.06.019

10. Pastar I, Stojadinovic O, Yin NC, Ramirez H, Nusbaum AG, Sawaya A, Patel SB, Khalid L, Isseroff RR and Tomic-Canic M (2014) Epithelialization in Wound Healing: A Comprehensive Review. Adv Wound Care (New Rochelle) 3:445-464. doi: 10.1089/wound.2013.0473

11. De Pascalis C and Etienne-Manneville S (2017) Single and collective cell migration: the mechanics of adhesions. Mol Biol Cell 28:1833-1846. doi: 10.1091/mbc.E17-03-0134

12. Lintz M, Munoz A and Reinhart-King CA (2017) The Mechanics of Single Cell and Collective Migration of Tumor Cells. J Biomech Eng 139. doi: 10.1115/1.4035121

13. Poujade M, Grasland-Mongrain E, Hertzog A, Jouanneau J, Chavrier P, Ladoux B, Buguin A and Silberzan P (2007) Collective migration of an epithelial

monolayer in response to a model wound. Proc Natl Acad Sci U S A 104:15988-93. doi: 10.1073/pnas.0705062104

14. Friedl P and Gilmour D (2009) Collective cell migration in morphogenesis, regeneration and cancer. Nat Rev Mol Cell Biol 10:445-57. doi: 10.1038/nrm2720

15. Ilina O and Friedl P (2009) Mechanisms of collective cell migration at a glance. J Cell Sci 122:3203-8. doi: 10.1242/jcs.036525

16. Theveneau E and Mayor R (2013) Collective cell migration of epithelial and mesenchymal cells. Cell Mol Life Sci 70:3481-92. doi: 10.1007/s00018-012-1251-7

17. Theveneau E, Steventon B, Scarpa E, Garcia S, Trepat X, Streit A and Mayor R (2013) Chase-and-run between adjacent cell populations promotes directional collective migration. Nat Cell Biol 15:763-72. doi: 10.1038/ncb2772

18. Theveneau E and Linker C (2017) Leaders in collective migration: are front cells really endowed with a particular set of skills? F1000Res 6:1899. doi: 10.12688/f1000research.11889.1

19. Wallace HA and Zito PM (2019) Wound Healing Phases. StatPearls, Treasure Island (FL)

20. Sonenberg N and Hinnebusch AG (2009) Regulation of translation initiation in eukaryotes: mechanisms and biological targets. Cell 136:731-45. doi: 10.1016/j.cell.2009.01.042

21. Gingras AC, Raught B and Sonenberg N (1999) eIF4 initiation factors: effectors of mRNA recruitment to ribosomes and regulators of translation. Annu Rev Biochem 68:913-63. doi: 10.1146/annurev.biochem.68.1.913

22. Ma XM and Blenis J (2009) Molecular mechanisms of mTOR-mediated translational control. Nat Rev Mol Cell Biol 10:307-18. doi: 10.1038/nrm2672

23. Qin X, Jiang B and Zhang Y (2016) 4E-BP1, a multifactor regulated multifunctional protein. Cell Cycle 15:781-6. doi: 10.1080/15384101.2016.1151581

24. Wek SA, Zhu S and Wek RC (1995) The histidyl-tRNA synthetase-related sequence in the eIF-2 alpha protein kinase GCN2 interacts with tRNA and is required for activation in response to starvation for different amino acids. Mol Cell Biol 15:4497-506.

25. Dever TE, Feng L, Wek RC, Cigan AM, Donahue TF and Hinnebusch AG (1992) Phosphorylation of initiation factor 2 alpha by protein kinase GCN2 mediates gene-specific translational control of GCN4 in yeast. Cell 68:585-96. doi: 10.1016/0092-8674(92)90193-g

26. Wek RC, Jiang HY and Anthony TG (2006) Coping with stress: eIF2 kinases and translational control. Biochem Soc Trans 34:7-11. doi: 10.1042/BST20060007

27. Baird TD and Wek RC (2012) Eukaryotic initiation factor 2 phosphorylation and translational control in metabolism. Adv Nutr 3:307-21. doi: 10.3945/an.112.002113

28. Sood R, Porter AC, Olsen DA, Cavener DR and Wek RC (2000) A mammalian homologue of GCN2 protein kinase important for translational control by phosphorylation of eukaryotic initiation factor-2alpha. Genetics 154:787-801.

29. Harding HP, Zhang Y, Zeng H, Novoa I, Lu PD, Calfon M, Sadri N, Yun C, Popko B, Paules R, Stojdl DF, Bell JC, Hettmann T, Leiden JM and Ron D (2003) An integrated stress response regulates amino acid metabolism and resistance to oxidative stress. Mol Cell 11:619-33. doi: 10.1016/s1097-2765(03)00105-9

30. Chen JJ (2007) Regulation of protein synthesis by the heme-regulated eIF2alpha kinase: relevance to anemias. Blood 109:2693-9. doi: 10.1182/blood-2006-08-041830

31. Han AP, Fleming MD and Chen JJ (2005) Heme-regulated eIF2alpha kinase modifies the phenotypic severity of murine models of erythropoietic protoporphyria and beta-thalassemia. J Clin Invest 115:1562-70. doi: 10.1172/JCI24141

32. Han AP, Yu C, Lu L, Fujiwara Y, Browne C, Chin G, Fleming M, Leboulch P, Orkin SH and Chen JJ (2001) Heme-regulated eIF2alpha kinase (HRI) is required for translational regulation and survival of erythroid precursors in iron deficiency. EMBO J 20:6909-18. doi: 10.1093/emboj/20.23.6909

33. Rafie-Kolpin M, Chefalo PJ, Hussain Z, Hahn J, Uma S, Matts RL and Chen JJ (2000) Two heme-binding domains of heme-regulated eukaryotic initiation

factor-2alpha kinase. N terminus and kinase insertion. J Biol Chem 275:5171-8. doi: 10.1074/jbc.275.7.5171

34. Uma S, Matts RL, Guo Y, White S and Chen JJ (2000) The N-terminal region of the heme-regulated eIF2alpha kinase is an autonomous heme binding domain. Eur J Biochem 267:498-506. doi: 10.1046/j.1432-1327.2000.01021.x

35. Chen JJ (2014) Translational control by heme-regulated eIF2alpha kinase during erythropoiesis. Curr Opin Hematol 21:172-8. doi: 10.1097/MOH.0000000000000030

36. Feng GS, Chong K, Kumar A and Williams BR (1992) Identification of double-stranded RNA-binding domains in the interferon-induced double-stranded RNA-activated p68 kinase. Proc Natl Acad Sci U S A 89:5447-51. doi: 10.1073/pnas.89.12.5447

37. Garcia MA, Meurs EF and Esteban M (2007) The dsRNA protein kinase PKR: virus and cell control. Biochimie 89:799-811. doi: 10.1016/j.biochi.2007.03.001

38. Meurs E, Chong K, Galabru J, Thomas NS, Kerr IM, Williams BR and Hovanessian AG (1990) Molecular cloning and characterization of the human double-stranded RNA-activated protein kinase induced by interferon. Cell 62:379-90. doi: 10.1016/0092-8674(90)90374-n

39. Clemens MJ, Hershey JW, Hovanessian AC, Jacobs BC, Katze MG, Kaufman RJ, Lengyel P, Samuel CE, Sen GC and Williams BR (1993) PKR:

proposed nomenclature for the RNA-dependent protein kinase induced by interferon. J Interferon Res 13:241. doi: 10.1089/jir.1993.13.241

40. Dey M, Cao C, Dar AC, Tamura T, Ozato K, Sicheri F and Dever TE (2005) Mechanistic link between PKR dimerization, autophosphorylation, and eIF2alpha substrate recognition. Cell 122:901-13. doi: 10.1016/j.cell.2005.06.041

41. Shi Y, Vattem KM, Sood R, An J, Liang J, Stramm L and Wek RC (1998) Identification and characterization of pancreatic eukaryotic initiation factor 2 alpha-subunit kinase, PEK, involved in translational control. Mol Cell Biol 18:7499-509. doi: 10.1128/MCB.18.12.7499

42. Wek RC and Cavener DR (2007) Translational control and the unfolded protein response. Antioxid Redox Signal 9:2357-71. doi: 10.1089/ars.2007.1764

43. Zhu S and Wek RC (1998) Ribosome-binding domain of eukaryotic initiation factor-2 kinase GCN2 facilitates translation control. J Biol Chem 273:1808-14.

44. Zhang P, McGrath BC, Reinert J, Olsen DS, Lei L, Gill S, Wek SA, Vattem KM, Wek RC, Kimball SR, Jefferson LS and Cavener DR (2002) The GCN2 eIF2alpha kinase is required for adaptation to amino acid deprivation in mice. Mol Cell Biol 22:6681-8.

45. Zaborske JM, Narasimhan J, Jiang L, Wek SA, Dittmar KA, Freimoser F, Pan T and Wek RC (2009) Genome-wide analysis of tRNA charging and activation of the eIF2 kinase Gcn2p. J Biol Chem 284:25254-67. doi: 10.1074/jbc.M109.000877

46. Lu W, Laszlo CF, Miao Z, Chen H and Wu S (2009) The role of nitric-oxide synthase in the regulation of UVB light-induced phosphorylation of the alpha subunit of eukaryotic initiation factor 2. J Biol Chem 284:24281-8. doi: 10.1074/jbc.M109.008821

47. Wu S, Hu Y, Wang JL, Chatterjee M, Shi Y and Kaufman RJ (2002) Ultraviolet light inhibits translation through activation of the unfolded protein response kinase PERK in the lumen of the endoplasmic reticulum. J Biol Chem 277:18077-83. doi: 10.1074/jbc.M110164200

48. Deng J, Harding HP, Raught B, Gingras AC, Berlanga JJ, Scheuner D, Kaufman RJ, Ron D and Sonenberg N (2002) Activation of GCN2 in UV-irradiated cells inhibits translation. Curr Biol 12:1279-86.

49. Jiang HY and Wek RC (2005) GCN2 phosphorylation of eIF2alpha activates NF-kappaB in response to UV irradiation. Biochem J 385:371-80. doi: 10.1042/BJ20041164

50. Collier AE, Wek RC and Spandau DF (2015) Translational Repression Protects Human Keratinocytes from UVB-Induced Apoptosis through a Discordant eIF2 Kinase Stress Response. J Invest Dermatol 135:2502-11. doi: 10.1038/jid.2015.177

51. Marintchev A and Ito T (2020) eIF2B and the Integrated Stress Response: A Structural and Mechanistic View. Biochemistry 59:1299-1308. doi: 10.1021/acs.biochem.0c00132

52. Kashiwagi K, Yokoyama T, Nishimoto M, Takahashi M, Sakamoto A, Yonemochi M, Shirouzu M and Ito T (2019) Structural basis for eIF2B inhibition in integrated stress response. Science 364:495-499. doi: 10.1126/science.aaw4104

53. Kenner LR, Anand AA, Nguyen HC, Myasnikov AG, Klose CJ, McGeever LA, Tsai JC, Miller-Vedam LE, Walter P and Frost A (2019) eIF2B-catalyzed nucleotide exchange and phosphoregulation by the integrated stress response. Science 364:491-495. doi: 10.1126/science.aaw2922

54. Gordiyenko Y, Llacer JL and Ramakrishnan V (2019) Structural basis for the inhibition of translation through eIF2alpha phosphorylation. Nat Commun 10:2640. doi: 10.1038/s41467-019-10606-1

55. Chen HH and Tarn WY (2019) uORF-mediated translational control: recently elucidated mechanisms and implications in cancer. RNA Biol 16:1327-1338. doi: 10.1080/15476286.2019.1632634

56. Vattem KM and Wek RC (2004) Reinitiation involving upstream ORFs regulates ATF4 mRNA translation in mammalian cells. Proc Natl Acad Sci U S A 101:11269-74. doi: 10.1073/pnas.0400541101

57. Fusakio ME, Willy JA, Wang Y, Mirek ET, Al Baghdadi RJ, Adams CM, Anthony TG and Wek RC (2016) Transcription factor ATF4 directs basal and stress-induced gene expression in the unfolded protein response and cholesterol metabolism in the liver. Mol Biol Cell 27:1536-51. doi: 10.1091/mbc.E16-01-0039

58. Lee YY, Cevallos RC and Jan E (2009) An upstream open reading frame regulates translation of GADD34 during cellular stresses that induce eIF2alpha phosphorylation. J Biol Chem 284:6661-73. doi: 10.1074/jbc.M806735200

59. Pakos-Zebrucka K, Koryga I, Mnich K, Ljujic M, Samali A and Gorman AM (2016) The integrated stress response. EMBO Rep 17:1374-1395. doi: 10.15252/embr.201642195

60. Dong J, Qiu H, Garcia-Barrio M, Anderson J and Hinnebusch AG (2000) Uncharged tRNA activates GCN2 by displacing the protein kinase moiety from a bipartite tRNA-binding domain. Mol Cell 6:269-79. doi: 10.1016/s1097-2765(00)00028-9

61. Wek RC, Jackson BM and Hinnebusch AG (1989) Juxtaposition of domains homologous to protein kinases and histidyl-tRNA synthetases in GCN2 protein suggests a mechanism for coupling GCN4 expression to amino acid availability. Proc Natl Acad Sci U S A 86:4579-83.

62. Wu CC, Peterson A, Zinshteyn B, Regot S and Green R (2020) Ribosome Collisions Trigger General Stress Responses to Regulate Cell Fate. Cell 182:404-416 e14. doi: 10.1016/j.cell.2020.06.006

63. Harding HP, Ordonez A, Allen F, Parts L, Inglis AJ, Williams RL and Ron D (2019) The ribosomal P-stalk couples amino acid starvation to GCN2 activation in mammalian cells. Elife 8. doi: 10.7554/eLife.50149

64. Inglis AJ, Masson GR, Shao S, Perisic O, McLaughlin SH, Hegde RS and Williams RL (2019) Activation of GCN2 by the ribosomal P-stalk. Proc Natl Acad Sci U S A 116:4946-4954. doi: 10.1073/pnas.1813352116

65. Ishimura R, Nagy G, Dotu I, Chuang JH and Ackerman SL (2016) Activation of GCN2 kinase by ribosome stalling links translation elongation with translation initiation. Elife 5. doi: 10.7554/eLife.14295

66. Silva RC, Sattlegger E and Castilho BA (2016) Perturbations in actin dynamics reconfigure protein complexes that modulate GCN2 activity and promote an eIF2 response. J Cell Sci 129:4521-4533. doi: 10.1242/jcs.194738

67. Marton MJ, Crouch D and Hinnebusch AG (1993) GCN1, a translational activator of GCN4 in Saccharomyces cerevisiae, is required for phosphorylation of eukaryotic translation initiation factor 2 by protein kinase GCN2. Mol Cell Biol 13:3541-56. doi: 10.1128/mcb.13.6.3541-3556.1993

68. Marton MJ, Vazquez de Aldana CR, Qiu H, Chakraburtty K and Hinnebusch AG (1997) Evidence that GCN1 and GCN20, translational regulators of GCN4, function on elongating ribosomes in activation of eIF2alpha kinase GCN2. Mol Cell Biol 17:4474-89. doi: 10.1128/MCB.17.8.4474

69. Pereira CM, Sattlegger E, Jiang HY, Longo BM, Jaqueta CB, Hinnebusch AG, Wek RC, Mello LE and Castilho BA (2005) IMPACT, a protein preferentially expressed in the mouse brain, binds GCN1 and inhibits GCN2 activation. J Biol Chem 280:28316-23. doi: 10.1074/jbc.M408571200

70. Pochopien AA, Beckert B, Kasvandik S, Berninghausen O, Beckmann R, Tenson T and Wilson DN (2021) Structure of Gcn1 bound to stalled and colliding 80S ribosomes. Proc Natl Acad Sci U S A 118. doi: 10.1073/pnas.2022756118

71. Kilberg MS, Balasubramanian M, Fu L and Shan J (2012) The transcription factor network associated with the amino acid response in mammalian cells. Adv Nutr 3:295-306. doi: 10.3945/an.112.001891

72. Kilberg MS, Shan J and Su N (2009) ATF4-dependent transcription mediates signaling of amino acid limitation. Trends Endocrinol Metab 20:436-43. doi: 10.1016/j.tem.2009.05.008

73. Collier AE, Spandau DF and Wek RC (2018) Translational control of a human CDKN1A mRNA splice variant regulates the fate of UVB-irradiated human keratinocytes. Mol Biol Cell 29:29-41. doi: 10.1091/mbc.E17-06-0362

74. Dang Do AN, Kimball SR, Cavener DR and Jefferson LS (2009) eIF2alpha kinases GCN2 and PERK modulate transcription and translation of distinct sets of mRNAs in mouse liver. Physiol Genomics 38:328-41. doi: 10.1152/physiolgenomics.90396.2008

75. Teske BF, Fusakio ME, Zhou D, Shan J, McClintick JN, Kilberg MS and Wek RC (2013) CHOP induces activating transcription factor 5 (ATF5) to trigger apoptosis in response to perturbations in protein homeostasis. Mol Biol Cell 24:2477-90. doi: 10.1091/mbc.E13-01-0067

76. Zhou D, Palam LR, Jiang L, Narasimhan J, Staschke KA and Wek RC (2008) Phosphorylation of eIF2 directs ATF5 translational control in response to diverse stress conditions. J Biol Chem 283:7064-73. doi: 10.1074/jbc.M708530200

77. Jiang HY, Wek SA, McGrath BC, Lu D, Hai T, Harding HP, Wang X, Ron D, Cavener DR and Wek RC (2004) Activating transcription factor 3 is integral to the eukaryotic initiation factor 2 kinase stress response. Mol Cell Biol 24:1365-77.

78. B'Chir W, Maurin AC, Carraro V, Averous J, Jousse C, Muranishi Y, Parry L, Stepien G, Fafournoux P and Bruhat A (2013) The eIF2alpha/ATF4 pathway is essential for stress-induced autophagy gene expression. Nucleic Acids Res 41:7683-99. doi: 10.1093/nar/gkt563

79. Galluzzi L and Kroemer G (2016) Amino acid deprivation promotes intestinal homeostasis through autophagy. Oncotarget 7:29877-8. doi: 10.18632/oncotarget.8841

80. Meister A (1995) Glutathione metabolism. Methods Enzymol 251:3-7. doi: 10.1016/0076-6879(95)51106-7

81. Meister A (1995) Glutathione biosynthesis and its inhibition. Methods Enzymol 252:26-30. doi: 10.1016/0076-6879(95)52005-8

82. McBean GJ (2012) The transsulfuration pathway: a source of cysteine for glutathione in astrocytes. Amino Acids 42:199-205. doi: 10.1007/s00726-011-0864-8

83. Bannai S and Tateishi N (1986) Role of membrane transport in metabolism and function of glutathione in mammals. J Membr Biol 89:1-8. doi: 10.1007/BF01870891

84. Sato H, Tamba M, Ishii T and Bannai S (1999) Cloning and expression of a plasma membrane cystine/glutamate exchange transporter composed of two distinct proteins. J Biol Chem 274:11455-8. doi: 10.1074/jbc.274.17.11455

85. Sato H, Nomura S, Maebara K, Sato K, Tamba M and Bannai S (2004) Transcriptional control of cystine/glutamate transporter gene by amino acid deprivation. Biochem Biophys Res Commun 325:109-16. doi: 10.1016/j.bbrc.2004.10.009

86. Torrence ME, MacArthur MR, Hosios AM, Valvezan AJ, Asara JM, Mitchell JR and Manning BD (2021) The mTORC1-mediated activation of ATF4 promotes protein and glutathione synthesis downstream of growth signals. Elife 10. doi: 10.7554/eLife.63326

87. Holmstrom KM and Finkel T (2014) Cellular mechanisms and physiological consequences of redox-dependent signalling. Nat Rev Mol Cell Biol 15:411-21. doi: 10.1038/nrm3801

88. Dunnill C, Patton T, Brennan J, Barrett J, Dryden M, Cooke J, Leaper D and Georgopoulos NT (2017) Reactive oxygen species (ROS) and wound healing: the functional role of ROS and emerging ROS-modulating technologies for

augmentation of the healing process. Int Wound J 14:89-96. doi: 10.1111/iwj.12557

89. Qiao J, Arthur JF, Gardiner EE, Andrews RK, Zeng L and Xu K (2018) Regulation of platelet activation and thrombus formation by reactive oxygen species. Redox Biol 14:126-130. doi: 10.1016/j.redox.2017.08.021

90. Bylund J, Bjornsdottir H, Sundqvist M, Karlsson A and Dahlgren C (2014) Measurement of respiratory burst products, released or retained, during activation of professional phagocytes. Methods Mol Biol 1124:321-38. doi: 10.1007/978-1-62703-845-4_21

91. Hyslop PA, Hinshaw DB, Scraufstatter IU, Cochrane CG, Kunz S and Vosbeck K (1995) Hydrogen peroxide as a potent bacteriostatic antibiotic: implications for host defense. Free Radic Biol Med 19:31-7. doi: 10.1016/0891-5849(95)00005-i

92. Murrell GA, Francis MJ and Bromley L (1990) Modulation of fibroblast proliferation by oxygen free radicals. Biochem J 265:659-65. doi: 10.1042/bj2650659

93. Stone JR and Collins T (2002) The role of hydrogen peroxide in endothelial proliferative responses. Endothelium 9:231-8. doi: 10.1080/10623320214733

94. Hurd TR, DeGennaro M and Lehmann R (2012) Redox regulation of cell migration and adhesion. Trends Cell Biol 22:107-15. doi: 10.1016/j.tcb.2011.11.002

95. Aghajanian A, Wittchen ES, Campbell SL and Burridge K (2009) Direct activation of RhoA by reactive oxygen species requires a redox-sensitive motif. PLoS One 4:e8045. doi: 10.1371/journal.pone.0008045

96. Bosco EE, Mulloy JC and Zheng Y (2009) Rac1 GTPase: a "Rac" of all trades. Cell Mol Life Sci 66:370-4. doi: 10.1007/s00018-008-8552-x

97. Niethammer P, Grabher C, Look AT and Mitchison TJ (2009) A tissue-scale gradient of hydrogen peroxide mediates rapid wound detection in zebrafish. Nature 459:996-9. doi: 10.1038/nature08119

98. Loo AE, Ho R and Halliwell B (2011) Mechanism of hydrogen peroxide-induced keratinocyte migration in a scratch-wound model. Free Radic Biol Med 51:884-92. doi: 10.1016/j.freeradbiomed.2011.06.001

99. Nunan R, Harding KG and Martin P (2014) Clinical challenges of chronic wounds: searching for an optimal animal model to recapitulate their complexity. Dis Model Mech 7:1205-13. doi: 10.1242/dmm.016782

100. Cano Sanchez M, Lancel S, Boulanger E and Neviere R (2018) Targeting Oxidative Stress and Mitochondrial Dysfunction in the Treatment of Impaired Wound Healing: A Systematic Review. Antioxidants (Basel) 7. doi: 10.3390/antiox7080098

101. Fitzmaurice SD, Sivamani RK and Isseroff RR (2011) Antioxidant therapies for wound healing: a clinical guide to currently commercially available products. Skin Pharmacol Physiol 24:113-26. doi: 10.1159/000322643

102. Nobes CD and Hall A (1995) Rho, rac, and cdc42 GTPases regulate the assembly of multimolecular focal complexes associated with actin stress fibers, lamellipodia, and filopodia. Cell 81:53-62. doi: 10.1016/0092-8674(95)90370-4

103. Nobes CD, Hawkins P, Stephens L and Hall A (1995) Activation of the small GTP-binding proteins rho and rac by growth factor receptors. J Cell Sci 108 (Pt 1):225-33.

104. Hall A (1992) Small GTP-binding proteins--a new family of biologic regulators. Am J Respir Cell Mol Biol 6:245-6. doi: 10.1165/ajrcmb/6.3.245

105. Hall A (1994) Small GTP-binding proteins and the regulation of the actin cytoskeleton. Annu Rev Cell Biol 10:31-54. doi: 10.1146/annurev.cb.10.110194.000335

106. Ridley AJ and Hall A (1992) The small GTP-binding protein rho regulates the assembly of focal adhesions and actin stress fibers in response to growth factors. Cell 70:389-99. doi: 10.1016/0092-8674(92)90163-7

107. Ridley AJ and Hall A (1992) Distinct patterns of actin organization regulated by the small GTP-binding proteins Rac and Rho. Cold Spring Harb Symp Quant Biol 57:661-71. doi: 10.1101/sqb.1992.057.01.072

108. Ridley AJ, Paterson HF, Johnston CL, Diekmann D and Hall A (1992) The small GTP-binding protein rac regulates growth factor-induced membrane ruffling. Cell 70:401-10. doi: 10.1016/0092-8674(92)90164-8

109. Pertz O, Hodgson L, Klemke RL and Hahn KM (2006) Spatiotemporal dynamics of RhoA activity in migrating cells. Nature 440:1069-72. doi: 10.1038/nature04665

110. Nayak RC, Chang KH, Vaitinadin NS and Cancelas JA (2013) Rho GTPases control specific cytoskeleton-dependent functions of hematopoietic stem cells. Immunol Rev 256:255-68. doi: 10.1111/imr.12119

111. Spiering D and Hodgson L (2011) Dynamics of the Rho-family small GTPases in actin regulation and motility. Cell Adh Migr 5:170-80. doi: 10.4161/cam.5.2.14403

112. Park HS, Lee SH, Park D, Lee JS, Ryu SH, Lee WJ, Rhee SG and Bae YS (2004) Sequential activation of phosphatidylinositol 3-kinase, beta Pix, Rac1, and Nox1 in growth factor-induced production of H2O2. Mol Cell Biol 24:4384-94. doi: 10.1128/MCB.24.10.4384-4394.2004

113. Ushio-Fukai M (2006) Localizing NADPH oxidase-derived ROS. Sci STKE 2006:re8. doi: 10.1126/stke.3492006re8

114. Heo J and Campbell SL (2005) Mechanism of redox-mediated guanine nucleotide exchange on redox-active Rho GTPases. J Biol Chem 280:31003-10. doi: 10.1074/jbc.M504768200

115. Mudge BP, Harris C, Gilmont RR, Adamson BS and Rees RS (2002) Role of glutathione redox dysfunction in diabetic wounds. Wound Repair Regen 10:52-8. doi: 10.1046/j.1524-475x.2002.10803.x

116. Collier AE, Wek RC and Spandau DF (2017) Human keratinocyte differentiation requires translational control by the eIF2alpha kinase GCN2. J Invest Dermatol. doi: 10.1016/j.jid.2017.04.029

117. Fuchs E and Green H (1980) Changes in keratin gene expression during terminal differentiation of the keratinocyte. Cell 19:1033-42. doi: 10.1016/0092-8674(80)90094-x

118. Watt FM (1983) Involucrin and other markers of keratinocyte terminal differentiation. J Invest Dermatol 81:100s-3s. doi: 10.1111/1523-1747.ep12540786

119. Dickson MA, Hahn WC, Ino Y, Ronfard V, Wu JY, Weinberg RA, Louis DN, Li FP and Rheinwald JG (2000) Human keratinocytes that express hTERT and also bypass a p16(INK4a)-enforced mechanism that limits life span become immortal yet retain normal growth and differentiation characteristics. Mol Cell Biol 20:1436-47.

120. Kuhn C, Hurwitz SA, Kumar MG, Cotton J and Spandau DF (1999) Activation of the insulin-like growth factor-1 receptor promotes the survival of human keratinocytes following ultraviolet B irradiation. Int J Cancer 80:431-8. doi: 10.1002/(sici)1097-0215(19990129)80:3<431::aid-ijc16>3.0.co;2-5

121. Borowiec AS, Delcourt P, Dewailly E and Bidaux G (2013) Optimal differentiation of in vitro keratinocytes requires multifactorial external control. PLoS One 8:e77507. doi: 10.1371/journal.pone.0077507

122. Deliu LP, Ghosh A and Grewal SS (2017) Investigation of protein synthesis in Drosophila larvae using puromycin labelling. Biol Open 6:1229-1234. doi: 10.1242/bio.026294

123. Bolger AM, Lohse M and Usadel B (2014) Trimmomatic: a flexible trimmer for Illumina sequence data. Bioinformatics 30:2114-20. doi: 10.1093/bioinformatics/btu170

124. Dobin A, Davis CA, Schlesinger F, Drenkow J, Zaleski C, Jha S, Batut P, Chaisson M and Gingeras TR (2013) STAR: ultrafast universal RNA-seq aligner. Bioinformatics 29:15-21. doi: 10.1093/bioinformatics/bts635

125. Liao Y, Smyth GK and Shi W (2014) featureCounts: an efficient general purpose program for assigning sequence reads to genomic features. Bioinformatics 30:923-30. doi: 10.1093/bioinformatics/btt656

126. Love MI, Huber W and Anders S (2014) Moderated estimation of fold change and dispersion for RNA-seq data with DESeq2. Genome Biol 15:550. doi: 10.1186/s13059-014-0550-8

127. Kramer A, Green J, Pollard J, Jr. and Tugendreich S (2014) Causal analysis approaches in Ingenuity Pathway Analysis. Bioinformatics 30:523-30. doi: 10.1093/bioinformatics/btt703

128. Pluskal T, Castillo S, Villar-Briones A and Oresic M (2010) MZmine 2: modular framework for processing, visualizing, and analyzing mass spectrometry-

based molecular profile data. BMC Bioinformatics 11:395. doi: 10.1186/1471-2105-11-395

129. Jiang J, Srivastava S, Seim G, Pavlova NN, King B, Zou L, Zhang C, Zhong M, Feng H, Kapur R, Wek RC, Fan J and Zhang J (2019) Promoter demethylation of the asparagine synthetase gene is required for ATF4-dependent adaptation to asparagine depletion. J Biol Chem 294:18674-18684. doi: 10.1074/jbc.RA119.010447

130. Maurin AC, Jousse C, Averous J, Parry L, Bruhat A, Cherasse Y, Zeng H, Zhang Y, Harding HP, Ron D and Fafournoux P (2005) The GCN2 kinase biases feeding behavior to maintain amino acid homeostasis in omnivores. Cell Metab 1:273-7. doi: 10.1016/j.cmet.2005.03.004

131. Chen JS, Longaker MT and Gurtner GC (2013) Murine models of human wound healing. Methods Mol Biol 1037:265-74. doi: 10.1007/978-1-62703-505-7_15

132. Roy S, Biswas S, Khanna S, Gordillo G, Bergdall V, Green J, Marsh CB, Gould LJ and Sen CK (2009) Characterization of a preclinical model of chronic ischemic wound. Physiol Genomics 37:211-24. doi: 10.1152/physiolgenomics.90362.2008

133. Committee for the Update of the Guide for the Care and Use of Laboratory Animals. Guide for the care and use of laboratory animals. National Academics Press, Washington DC

134. Lewis DA, Yi Q, Travers JB and Spandau DF (2008) UVB-induced senescence in human keratinocytes requires a functional insulin-like growth factor-1 receptor and p53. Mol Biol Cell 19:1346-53. doi: 10.1091/mbc.E07-10-1041

135. Serezani AP, Bozdogan G, Sehra S, Walsh D, Krishnamurthy P, Sierra Potchanant EA, Nalepa G, Goenka S, Turner MJ, Spandau DF and Kaplan MH (2017) IL-4 impairs wound healing potential in the skin by repressing fibronectin expression. J Allergy Clin Immunol 139:142-151 e5. doi: 10.1016/j.jaci.2016.07.012

136. Grada A, Otero-Vinas M, Prieto-Castrillo F, Obagi Z and Falanga V (2017) Research Techniques Made Simple: Analysis of Collective Cell Migration Using the Wound Healing Assay. J Invest Dermatol 137:e11-e16. doi: 10.1016/j.jid.2016.11.020

137. Papini S, Cecchetti D, Campani D, Fitzgerald W, Grivel JC, Chen S, Margolis L and Revoltella RP (2003) Isolation and clonal analysis of human epidermal keratinocyte stem cells in long-term culture. Stem Cells 21:481-94. doi: 10.1634/stemcells.21-4-481

138. Park Y, Reyna-Neyra A, Philippe L and Thoreen CC (2017) mTORC1 Balances Cellular Amino Acid Supply with Demand for Protein Synthesis through Post-transcriptional Control of ATF4. Cell Rep 19:1083-1090. doi: 10.1016/j.celrep.2017.04.042

139. Lassot I, Segeral E, Berlioz-Torrent C, Durand H, Groussin L, Hai T, Benarous R and Margottin-Goguet F (2001) ATF4 degradation relies on a phosphorylation-dependent interaction with the SCF(betaTrCP) ubiquitin ligase. Mol Cell Biol 21:2192-202. doi: 10.1128/MCB.21.6.2192-2202.2001

140. Milani M, Rzymski T, Mellor HR, Pike L, Bottini A, Generali D and Harris AL (2009) The role of ATF4 stabilization and autophagy in resistance of breast cancer cells treated with Bortezomib. Cancer Res 69:4415-23. doi: 10.1158/0008-5472.CAN-08-2839

141. Scortegagna M, Kim H, Li JL, Yao H, Brill LM, Han J, Lau E, Bowtell D, Haddad G, Kaufman RJ and Ronai ZA (2014) Fine tuning of the UPR by the ubiquitin ligases Siah1/2. PLoS Genet 10:e1004348. doi: 10.1371/journal.pgen.1004348

142. Rutkowski DT, Arnold SM, Miller CN, Wu J, Li J, Gunnison KM, Mori K, Sadighi Akha AA, Raden D and Kaufman RJ (2006) Adaptation to ER stress is mediated by differential stabilities of pro-survival and pro-apoptotic mRNAs and proteins. PLoS Biol 4:e374. doi: 10.1371/journal.pbio.0040374

143. Ait Ghezala H, Jolles B, Salhi S, Castrillo K, Carpentier W, Cagnard N, Bruhat A, Fafournoux P and Jean-Jean O (2012) Translation termination efficiency modulates ATF4 response by regulating ATF4 mRNA translation at 5' short ORFs. Nucleic Acids Res 40:9557-70. doi: 10.1093/nar/gks762

144. Gardner LB (2008) Hypoxic inhibition of nonsense-mediated RNA decay regulates gene expression and the integrated stress response. Mol Cell Biol 28:3729-41. doi: 10.1128/MCB.02284-07

145. Nakamura A, Nambu T, Ebara S, Hasegawa Y, Toyoshima K, Tsuchiya Y, Tomita D, Fujimoto J, Kurasawa O, Takahara C, Ando A, Nishigaki R, Satomi Y, Hata A and Hara T (2018) Inhibition of GCN2 sensitizes ASNS-low cancer cells to asparaginase by disrupting the amino acid response. Proc Natl Acad Sci U S A 115:E7776-E7785. doi: 10.1073/pnas.1805523115

146. Tsaytler P, Harding HP, Ron D and Bertolotti A (2011) Selective inhibition of a regulatory subunit of protein phosphatase 1 restores proteostasis. Science 332:91-4. doi: 10.1126/science.1201396

147. Koppula P, Zhang Y, Zhuang L and Gan B (2018) Amino acid transporter SLC7A11/xCT at the crossroads of regulating redox homeostasis and nutrient dependency of cancer. Cancer Commun (Lond) 38:12. doi: 10.1186/s40880-018-0288-x

148. Rousselle P, Braye F and Dayan G (2019) Re-epithelialization of adult skin wounds: Cellular mechanisms and therapeutic strategies. Adv Drug Deliv Rev 146:244-365. doi: 10.1016/j.addr.2018.06.019

149. Ridley AJ (2011) Life at the leading edge. Cell 145:1012-22. doi: 10.1016/j.cell.2011.06.010

150. Stanley A, Thompson K, Hynes A, Brakebusch C and Quondamatteo F (2014) NADPH oxidase complex-derived reactive oxygen species, the actin cytoskeleton, and Rho GTPases in cell migration. Antioxid Redox Signal 20:2026-42. doi: 10.1089/ars.2013.5713

151. Choi H, Yang Z and Weisshaar JC (2015) Single-cell, real-time detection of oxidative stress induced in Escherichia coli by the antimicrobial peptide CM15. Proc Natl Acad Sci U S A 112:E303-10. doi: 10.1073/pnas.1417703112

152. Machacek M, Hodgson L, Welch C, Elliott H, Pertz O, Nalbant P, Abell A, Johnson GL, Hahn KM and Danuser G (2009) Coordination of Rho GTPase activities during cell protrusion. Nature 461:99-103. doi: 10.1038/nature08242

153. Nalbant P, Chang YC, Birkenfeld J, Chang ZF and Bokoch GM (2009) Guanine nucleotide exchange factor-H1 regulates cell migration via localized activation of RhoA at the leading edge. Mol Biol Cell 20:4070-82. doi: 10.1091/mbc.E09-01-0041

154. Lawson CD and Ridley AJ (2018) Rho GTPase signaling complexes in cell migration and invasion. J Cell Biol 217:447-457. doi: 10.1083/jcb.201612069

155. Sen CK (2019) Human Wounds and Its Burden: An Updated Compendium of Estimates. Adv Wound Care (New Rochelle) 8:39-48. doi: 10.1089/wound.2019.0946

156. Quain AM and Khardori NM (2015) Nutrition in Wound Care Management: A Comprehensive Overview. Wounds 27:327-35.

157. Debats IB, Wolfs TG, Gotoh T, Cleutjens JP, Peutz-Kootstra CJ and van der Hulst RR (2009) Role of arginine in superficial wound healing in man. Nitric Oxide 21:175-83. doi: 10.1016/j.niox.2009.07.006

158. Schaffer MR, Tantry U, Thornton FJ and Barbul A (1999) Inhibition of nitric oxide synthesis in wounds: pharmacology and effect on accumulation of collagen in wounds in mice. Eur J Surg 165:262-7. doi: 10.1080/110241599750007153

159. Kirk SJ, Hurson M, Regan MC, Holt DR, Wasserkrug HL and Barbul A (1993) Arginine stimulates wound healing and immune function in elderly human beings. Surgery 114:155-9; discussion 160.

160. Leigh B, Desneves K, Rafferty J, Pearce L, King S, Woodward MC, Brown D, Martin R and Crowe TC (2012) The effect of different doses of an arginine-containing supplement on the healing of pressure ulcers. J Wound Care 21:150-6. doi: 10.12968/jowc.2012.21.3.150

161. Frank S, Kampfer H, Wetzler C and Pfeilschifter J (2002) Nitric oxide drives skin repair: novel functions of an established mediator. Kidney Int 61:882-8. doi: 10.1046/j.1523-1755.2002.00237.x

162. Stallmeyer B, Kampfer H, Kolb N, Pfeilschifter J and Frank S (1999) The function of nitric oxide in wound repair: inhibition of inducible nitric oxide-synthase severely impairs wound reepithelialization. J Invest Dermatol 113:1090-8. doi: 10.1046/j.1523-1747.1999.00784.x

163. Soeters PB and Grecu I (2012) Have we enough glutamine and how does it work? A clinician's view. Ann Nutr Metab 60:17-26. doi: 10.1159/000334880

164. Newsholme P (2001) Why is L-glutamine metabolism important to cells of the immune system in health, postinjury, surgery or infection? J Nutr 131:2515S-22S; discussion 2523S-4S. doi: 10.1093/jn/131.9.2515S

165. Ardawi MS (1988) Glutamine and glucose metabolism in human peripheral lymphocytes. Metabolism 37:99-103. doi: 10.1016/0026-0495(88)90036-4

166. Peng X, Yan H, You Z, Wang P and Wang S (2005) Clinical and protein metabolic efficacy of glutamine granules-supplemented enteral nutrition in severely burned patients. Burns 31:342-6. doi: 10.1016/j.burns.2004.10.027

167. Peng X, You ZY, Huang XK, Zhang CQ, He GZ, Quan ZF and Xie WG (2005) [Effects of glutamine granules on immunofunction in trauma patients: a double-blind randomized controlled, multi-center clinical trail with 120 patients]. Zhonghua Wai Ke Za Zhi 43:1123-6.

168. Blass SC, Goost H, Tolba RH, Stoffel-Wagner B, Kabir K, Burger C, Stehle P and Ellinger S (2012) Time to wound closure in trauma patients with disorders in wound healing is shortened by supplements containing antioxidant micronutrients and glutamine: a PRCT. Clin Nutr 31:469-75. doi: 10.1016/j.clnu.2012.01.002

169. Pettit AP, Jonsson WO, Bargoud AR, Mirek ET, Peelor FF, 3rd, Wang Y, Gettys TW, Kimball SR, Miller BF, Hamilton KL, Wek RC and Anthony TG (2017)

Dietary Methionine Restriction Regulates Liver Protein Synthesis and Gene Expression Independently of Eukaryotic Initiation Factor 2 Phosphorylation in Mice. J Nutr 147:1031-1040. doi: 10.3945/jn.116.246710

170. Wanders D, Stone KP, Forney LA, Cortez CC, Dille KN, Simon J, Xu M, Hotard EC, Nikonorova IA, Pettit AP, Anthony TG and Gettys TW (2016) Role of GCN2-Independent Signaling Through a Noncanonical PERK/NRF2 Pathway in the Physiological Responses to Dietary Methionine Restriction. Diabetes 65:1499-510. doi: 10.2337/db15-1324

171. Jonsson WO, Margolies NS, Mirek ET, Zhang Q, Linden MA, Hill CM, Link C, Bithi N, Zalma B, Levy JL, Pettit AP, Miller JW, Hine C, Morrison CD, Gettys TW, Miller BF, Hamilton KL, Wek RC and Anthony TG (2021) Physiologic Responses to Dietary Sulfur Amino Acid Restriction in Mice Are Influenced by Atf4 Status and Biological Sex. J Nutr 151:785-799. doi: 10.1093/jn/nxaa396

172. Longchamp A, Mirabella T, Arduini A, MacArthur MR, Das A, Trevino-Villarreal JH, Hine C, Ben-Sahra I, Knudsen NH, Brace LE, Reynolds J, Mejia P, Tao M, Sharma G, Wang R, Corpataux JM, Haefliger JA, Ahn KH, Lee CH, Manning BD, Sinclair DA, Chen CS, Ozaki CK and Mitchell JR (2018) Amino Acid Restriction Triggers Angiogenesis via GCN2/ATF4 Regulation of VEGF and H2S Production. Cell 173:117-129 e14. doi: 10.1016/j.cell.2018.03.001

173. Falcon P, Escandon M, Brito A and Matus S (2019) Nutrient Sensing and Redox Balance: GCN2 as a New Integrator in Aging. Oxid Med Cell Longev 2019:5730532. doi: 10.1155/2019/5730532

174. Cibrian D, de la Fuente H and Sanchez-Madrid F (2020) Metabolic Pathways That Control Skin Homeostasis and Inflammation. Trends Mol Med 26:975-986. doi: 10.1016/j.molmed.2020.04.004

175. Wek RC (2018) Role of eIF2alpha kinases in translational control and adaptation to cellular stress. Cold Spring Harb Perspect Biol 10:a032870. doi: 10.1101/cshperspect.a032870

176. Marciniak SJ and Ron D (2006) Endoplasmic reticulum stress signaling in disease. Physiol Rev 86:1133-49. doi: 10.1152/physrev.00015.2006

177. Wong YL, LeBon L, Basso AM, Kohlhaas KL, Nikkel AL, Robb HM, Donnelly-Roberts DL, Prakash J, Swensen AM, Rubinstein ND, Krishnan S, McAllister FE, Haste NV, O'Brien JJ, Roy M, Ireland A, Frost JM, Shi L, Riedmaier S, Martin K, Dart MJ and Sidrauski C (2019) eIF2B activator prevents neurological defects caused by a chronic integrated stress response. Elife 8:e42940. doi: 10.7554/eLife.42940

178. Fujimoto J, Kurasawa O, Takagi T, Liu X, Banno H, Kojima T, Asano Y, Nakamura A, Nambu T, Hata A, Ishii T, Sameshima T, Debori Y, Miyamoto M, Klein MG, Tjhen R, Sang BC, Levin I, Lane SW, Snell GP, Li K, Kefala G, Hoffman ID, Ding SC, Cary DR and Mizojiri R (2019) Identification of Novel, Potent, and Orally Available GCN2 Inhibitors with Type I Half Binding Mode. ACS Med Chem Lett 10:1498-1503. doi: 10.1021/acsmedchemlett.9b00400

CURRICULUM VITAE

Rebecca Ruth Miles

EDUCATION

Indiana University Purdue University Indianapolis, IN

PhD 2017-2021

College of William and Mary, Williamsburg, VA

Master of Arts in Biology May 1994

Indiana Wesleyan University, Marion, IN

Bachelor of Science in Biology and Political Science May 1990

PROFESSIONAL EXPERIENCE

Principal Research Scientist, Lilly Research Labs, Indianapolis, IN

RNA Therapeutics, Pharmacology Team Leader, RNAi chemistry and synthetic mRNA specialist: Lead a team of vitro and in vivo scientists to screen modified siRNAs for potent knockdown of target gene in cell lines, primary cells and in animals to support hepatic and extra-hepatic target validation. Provide training and coaching in RNAi methods across the company. Manage multiple cross-functional projects with therapeutic areas, ADME and chemistry. 2019 to present

Consultant Biologist, Lilly Research Labs, Indianapolis, IN

Drug Discovery Research areas: Target identification and validation of molecular mechanisms of action for bone formation, osteoporosis, uterine leiomyomas, breast cancer, osteoarthritis, insulin secretion, atherosclerosis, metabolic syndrome and kidney disease. Cell and molecular biologist highly experienced in assay design, development and validation. Screening of small molecule, peptide and antibody therapeutics for portfolio entry. Investigation of synthetic mRNA as a novel therapeutic modality. Experienced in mRNA synthesis and formulation of mRNA in nanoparticles for in vivo delivery and expression. July 1994 to October 2009, June 2011 to 2019

Research Specialist, Dow AgroSciences LLC, Indianapolis, IN

Discovery Research, Advanced Technology and Development Department. Project leader role supporting the development of gene editing strategies using zinc-finger nuclease technology in maize. Additionally, provided active research support as a molecular biologist in charge of designing and assembling gene targeting vectors for multiple projects. Member of Construct Oversight Committee and Competitive Intelligence Committee. November 2009 to June 2011

Adjunct Faculty, Indiana Wesleyan University, Marion, IN

Instructor for Human Anatomy and Physiology. Fall 2000, Spring 1997

Teaching Assistant, College of William and Mary, Williamsburg, VA

Introduction to Cell, Molecular and Developmental Biology; Introduction to Organisms, Ecology and Evolution; and Developmental Biology. August 1992 to May 1994

Research Assistant, University of Chicago, Chicago, IL

Investigated the role of estrogen and progesterone receptors in breast cancer. August 1991 to February 1992

Laboratory Technician, AAT Laboratories, Grand Rapids, MI

Analyzed hazardous wastewater and effluents for environmental contaminants. June 1990 to June 1991

PUBLICATIONS

1. Miles, R.R., Amin, P.H., Diaz, M.B., Misra J., Aukerman E., Das A., Ghosh N., Guith T., Knierman M.D., Roy S., Spandau D.F. and Wek R.C. (2021) The eIF2 kinase GCN2 directs keratinocyte collective cell migration during wound healing via coordination of reactive oxygen species and amino acids. J Biol Chem:101257. doi: 10.1016/j.jbc.2021.101257

2. Ainley, W. M., Sastry-Dent, L., Welter, M. E., Murray, M. G., Zeitler, B., Amora, R., Corbin, D. R., Miles, R. R., Arnold, N. L., Strange, T. L., Simpson, M. A., Cao, Z., Carroll, C., Pawelczak, K. S., Blue, R., West, K., Rowland, L. M., Perkins, D., Samuel, P., Dewes, C. M., Shen, L., Sriram, S., Evans, S. L., Rebar, E. J., Zhang, L., Gregory, P. D., Urnov, F. D., Webb, S. R., and Petolino, J. F. (2013) Trait stacking via targeted genome editing. Plant Biotechnol J 11, 1126-1134

3. Boguslawski, G., Hale, L. V., Yu, X. P., Miles, R. R., Onyia, J. E., Santerre, R. F., and Chandrasekhar, S. (2000) Activation of osteocalcin transcription involves interaction of protein kinase A- and protein kinase C-dependent pathways. J Biol Chem 275, 999-1006

4. Borg, M. L., Massart, J., Schonke, M., De Castro Barbosa, T., Guo, L., Wade, M., Alsina-Fernandez, J., Miles, R., Ryan, A., Bauer, S., Coskun, T., O'Farrell, E., Niemeier, E. M., Chibalin, A. V., Krook, A., Karlsson, H. K., Brozinick,

J. T., and Zierath, J. R. (2019) Modified UCN2 Peptide Acts as an Insulin Sensitizer in Skeletal Muscle of Obese Mice. Diabetes 68, 1403-1414

5. Dotzlaf, J., Carpenter, J., Luo, S., Miles, R. R., Fisher, D., Qian, Y. W., Ehsani, M., Wang, X., Lin, A., McClure, D. B., Chen, V. J., and Zuckerman, S. H. (2007) Derivation and characterization of monoclonal antibodies against human folypolyglutamate synthetase. Hybridoma (Larchmt) 26, 155-161

6. Feister, H. A., Onyia, J. E., Miles, R. R., Yang, X., Galvin, R., Hock, J. M., and Bidwell, J. P. (2000) The expression of the nuclear matrix proteins NuMA, topoisomerase II-alpha, and -beta in bone and osseous cell culture: regulation by parathyroid hormone. Bone 26, 227-234

7. Halladay, D. L., Miles, R. R., Thirunavukkarasu, K., Chandrasekhar, S., Martin, T. J., and Onyia, J. E. (2001) Identification of signal transduction pathways and promoter sequences that mediate parathyroid hormone 1-38 inhibition of osteoprotegerin gene expression. J Cell Biochem 84, 1-11

8. Helvering, L. M., Adrian, M. D., Geiser, A. G., Estrem, S. T., Wei, T., Huang, S., Chen, P., Dow, E. R., Calley, J. N., Dodge, J. A., Grese, T. A., Jones, S. A., Halladay, D. L., Miles, R. R., Onyia, J. E., Ma, Y. L., Sato, M., and Bryant, H. U. (2005) Differential effects of estrogen and raloxifene on messenger RNA and matrix metalloproteinase 2 activity in the rat uterus. Biol Reprod 72, 830-841

9. Helvering, L. M., Liu, R., Kulkarni, N. H., Wei, T., Chen, P., Huang, S., Lawrence, F., Halladay, D. L., Miles, R. R., Ambrose, E. M., Sato, M., Ma, Y. L., Frolik, C. A., Dow, E. R., Bryant, H. U., and Onyia, J. E. (2005) Expression profiling of rat femur revealed suppression of bone formation genes by treatment with alendronate and estrogen but not raloxifene. Mol Pharmacol 68, 1225-1238

10. Kulkarni, N. H., Halladay, D. L., Miles, R. R., Gilbert, L. M., Frolik, C. A., Galvin, R. J., Martin, T. J., Gillespie, M. T., and Onyia, J. E. (2005) Effects of parathyroid hormone on Wnt signaling pathway in bone. J Cell Biochem 95, 1178-1190

11. Ma, Y. L., Cain, R. L., Halladay, D. L., Yang, X., Zeng, Q., Miles, R. R., Chandrasekhar, S., Martin, T. J., and Onyia, J. E. (2001) Catabolic effects of continuous human PTH (1--38) in vivo is associated with sustained stimulation of RANKL and inhibition of osteoprotegerin and gene-associated bone formation. Endocrinology 142, 4047-4054

12. McClelland, P., Onyia, J. E., Miles, R. R., Tu, Y., Liang, J., Harvey, A. K., Chandrasekhar, S., Hock, J. M., and Bidwell, J. P. (1998) Intermittent administration of parathyroid hormone (1-34) stimulates matrix metalloproteinase-9 (MMP-9) expression in rat long bone. J Cell Biochem 70, 391-401

13. Miles, R. R., Crockett, D. K., Lim, M. S., and Elenitoba-Johnson, K. S. (2005) Analysis of BCL6-interacting proteins by tandem mass spectrometry. Mol Cell Proteomics 4, 1898-1909

14. Miles, R. R., Perry, W., Haas, J. V., Mosior, M. K., N'Cho, M., Wang, J. W., Yu, P., Calley, J., Yue, Y., Carter, Q., Han, B., Foxworthy, P., Kowala, M. C., Ryan, T. P., Solenberg, P. J., and Michael, L. F. (2013) Genome-wide screen for modulation of hepatic apolipoprotein A-I (ApoA-I) secretion. J Biol Chem 288, 6386-6396

15. Miles, R. R., Roberts, R. F., Putnam, A. R., and Roberts, W. L. (2004) Comparison of serum and heparinized plasma samples for measurement of chemistry analytes. Clin Chem 50, 1704-1706

16. Miles, R. R., Sluka, J. P., Halladay, D. L., Santerre, R. F., Hale, L. V., Bloem, L., Patanjali, S. R., Galvin, R. J., Ma, L., Hock, J. M., and Onyia, J. E. (2002) Parathyroid hormone (hPTH 1-38) stimulates the expression of UBP41, an ubiquitin-specific protease, in bone. J Cell Biochem 85, 229-242

17. Miles, R. R., Sluka, J. P., Halladay, D. L., Santerre, R. F., Hale, L. V., Bloem, L., Thirunavukkarasu, K., Galvin, R. J., Hock, J. M., and Onyia, J. E. (2000) ADAMTS-1: A cellular disintegrin and metalloprotease with thrombospondin motifs is a target for parathyroid hormone in bone. Endocrinology 141, 4533-4542

18. Miles, R. R., Sluka, J. P., Santerre, R. F., Hale, L. V., Bloem, L., Boguslawski, G., Thirunavukkarasu, K., Hock, J. M., and Onyia, J. E. (2000) Dynamic regulation of RGS2 in bone: potential new insights into parathyroid hormone signaling mechanisms. Endocrinology 141, 28-36

19. Miles, R. R., Turner, C. H., Santerre, R., Tu, Y., McClelland, P., Argot, J., DeHoff, B. S., Mundy, C. W., Rosteck, P. R., Jr., Bidwell, J., Sluka, J. P., Hock, J., and Onyia, J. E. (1998) Analysis of differential gene expression in rat tibia after an osteogenic stimulus in vivo: mechanical loading regulates osteopontin and myeloperoxidase. J Cell Biochem 68, 355-365

20. Onyia, J. E., Galvin, R. J., Ma, Y. L., Halladay, D. L., Miles, R. R., Yang, X., Fuson, T., Cain, R. L., Zeng, Q. Q., Chandrasekhar, S., Emkey, R., Xu, Y., Thirunavukkarasu, K., Bryant, H. U., and Martin, T. J. (2004) Novel and selective small molecule stimulators of osteoprotegerin expression inhibit bone resorption. J Pharmacol Exp Ther 309, 369-379

21. Onyia, J. E., Hale, L. V., Miles, R. R., Cain, R. L., Tu, Y., Hulman, J. F., Hock, J. M., and Santerre, R. F. (1999) Molecular characterization of gene expression changes in ROS 17/2.8 cells cultured in diffusion chambers in vivo. Calcif Tissue Int 65, 133-138

22. Onyia, J. E., Helvering, L. M., Gelbert, L., Wei, T., Huang, S., Chen, P., Dow, E. R., Maran, A., Zhang, M., Lotinun, S., Lin, X., Halladay, D. L., Miles, R. R., Kulkarni, N. H., Ambrose, E. M., Ma, Y. L., Frolik, C. A., Sato, M., Bryant, H. U., and Turner, R. T. (2005) Molecular profile of catabolic versus anabolic treatment regimens of parathyroid hormone (PTH) in rat bone: an analysis by DNA microarray. J Cell Biochem 95, 403-418

23. Onyia, J. E., Miles, R. R., Yang, X., Halladay, D. L., Hale, J., Glasebrook, A., McClure, D., Seno, G., Churgay, L., Chandrasekhar, S., and Martin, T. J. (2000) In vivo demonstration that human parathyroid hormone 1-38 inhibits the expression of osteoprotegerin in bone with the kinetics of an immediate early gene. J Bone Miner Res 15, 863-871

24. Saha, M. S., Miles, R. R., and Grainger, R. M. (1997) Dorsal-ventral patterning during neural induction in Xenopus: assessment of spinal cord regionalization with xHB9, a marker for the motor neuron region. Dev Biol 187, 209-223

25. Thirunavukkarasu, K., Halladay, D. L., Miles, R. R., Geringer, C. D., and Onyia, J. E. (2002) Analysis of regulator of G-protein signaling-2 (RGS-2) expression and function in osteoblastic cells. J Cell Biochem 85, 837-850

26. Thirunavukkarasu, K., Halladay, D. L., Miles, R. R., Yang, X., Galvin, R. J., Chandrasekhar, S., Martin, T. J., and Onyia, J. E. (2000) The osteoblast-specific transcription factor Cbfa1 contributes to the expression of osteoprotegerin, a potent inhibitor of osteoclast differentiation and function. J Biol Chem 275, 25163-25172

27. Thirunavukkarasu, K., Miles, R. R., Halladay, D. L., and Onyia, J. E. (2000) Cryptic enhancer elements in luciferase reporter vectors respond to the osteoblast-specific transcription factor Osf2/Cbfa1. Biotechniques 28, 506-510

28. Thirunavukkarasu, K., Miles, R. R., Halladay, D. L., Yang, X., Galvin, R. J., Chandrasekhar, S., Martin, T. J., and Onyia, J. E. (2001) Stimulation of osteoprotegerin (OPG) gene expression by transforming growth factor-beta (TGF-beta). Mapping of the OPG promoter region that mediates TGF-beta effects. J Biol Chem 276, 36241-36250

29. Fuchs-Young, R., Howe, S., Hale, L., Miles, R., and Walker, C. (1996) Inhibition of estrogen-stimulated growth of uterine leiomyomas by selective estrogen receptor modulators. Mol Carcinog 17, 151-159

30. Miles, Rebecca R. The Isolation and Characterization of a Novel G-protein-coupled receptor involved in Angiogenesis. College of William and Mary Master's Thesis, July 1994.

PLATFORM PRESENTATIONS

1. Sarmah B, Wooden C, Baker H, Yang D, Elia M, Truhlar S, Stokell D, Miles RR, Millican R, Feng Y, Qi Z, Heuer JG, and Breyer MD (2016) Genetic ablation or pharmacologic inhibition of the natriuretic peptide clearance receptor NPR-C delays chronic kidney disease progression in mouse models. American Society of Nephrology (ASN), Kidney Week Annual Meeting

2. Miles RR, Sluka JP, Hale LV, Travis K, Tu Y, Bloem L, Boguslawski G, Argot J, Hock JM, Santerre RF and Onyia JE (1998) Comparative Genomics of 3-5% of mRNA Expressed in Osteoblast-Enriched Femoral Metaphyseal Bone. International Conference on Progress in Bone and Mineral Research in Vienna, Austria.

3. Onyia JE, Hale LV, Miles RR, Cain RL, Tu Y, Hulman JF, Hock JM and Santerre RF. (1998) Molecular Characterization of Gene Expression Changes in ROS 17/2.8 Cells Cultured in Diffusion Chamber in vivo. International Conference on Progress in Bone and Mineral Research

4. Thirunavukkarasu K, Miles RR, Halladay DL, Galvin R, Chandrasekhar S, Martin TJ and Onyia JE. (1999) The osteoblast-specific transcription factor OSF2 regulates the expression of osteoclast inhibitory factor OPG: Implications for the potential role of OSF2 in bone resorption. Platform presentation: American Society for Bone and Mineral Research Meeting.

5. Onyia JE, Miles RR, Yang X, Halladay DL, Hale J, Glasebrook A, McClure D, Seno G, Churgay L, Chandrasekhar S, and Martin TJ. (1999) In vivo demonstration that parathyroid hormone (hPTH1-38) inhibits the expression of osteoprotegerin (OPG) in bone with the kinetics of an immediate early gene. Platform presentation: American Society for Bone and Mineral Research Meeting.

6. Thirunavukkarasu K, Halladay DL, Miles RR, Santerre RF, and Onyia JE. (2000) Regulator of G-Protein Signaling 2 (RGS2) Down Regulates PTH Signaling in Osteoblasts Via the $G_s\alpha$-Adenylate Cyclase-Protein Kinase A Pathway. American Society for Bone and Mineral Research Meeting

7. Onyia JE, Ma L, Galbreath E, Zhang Q, Zeng QQ, Cain RL, Hoover J, Miles RR, Halladay RR, Hale LV, Santerre RF, Harvey AK, Chandrasekhar S, Fox N, and Yang DD. (2001) ADAMTS-1: A Cellular Disintegrin and Metalloprotease with Thrombospondin Motifs is Essential for Normal Bone Growth and PTH Regulated Bone Metabolism. American Society for Bone and Mineral Research Meeting

8. Adams CS, Bemis KG, Bryant HU, Chandrasekhar S, Chen P, Dow E, Frolik CA, Gelbert L, Halladay DL, Huang S, Ma L, Miles RR, Onyia JE, and Sato S. (2002) Gene Array Analysis of the Bone Effects of Raloxifene and Alendronate Show that Alendronate Strongly Inhibits the Expression of bone formation marker genes. American Society for Bone and Mineral Research Meeting

9. Chandrasekhar S, Halladay DL, Miles RR, Onyia JE, Galvin RGS, Thirunavukkarasu K, Yang X. (2002) Regulation of osteoprotegerin (OPG) expression by Cbfa1 and TGF-beta Martin TJ. Midwest Connective Tissue Workshop

10. Galvin RJS, Onyia JE, Ma L, Halladay DL, Miles RR, Yang X, Fuson TR, Cain RL, Zeng QQ, Chandrasekhar S, Emkey R, Xu Y, Thirunavukkarasu K, Bryant HU, and Martin TJ. (2003) Novel and Selective Small Molecule Stimulators of Osteoprotegerin Expression Inhibit Bone Resorption. American Society for Bone and Mineral Research Meeting

11. Helvering LM, Onyia JE, Dow E, Wei T, Gelbert L, Adams C, Lawrence F, Bemis KG, Halladay DL**,** Miles RR, Kulkarni NH, Huang S, Chen P, Chandrasekhar S, Frolik CA, Sato M, Ma L, and Bryant HU. (2004) RNA profiling of antiresorptives reveal Alendronate and estrogen decrease bone formation genes while Raloxifene maintains their increase in the ovariectomized rat. World Congress on Osteoporosis, Rio De Janeiro, Brazil.

ABSTRACTS

1. Perkins DP, Williams GD, Briskey AS, Buquer SH, Antonellis P, Adams AC, Gonciarz M, Wang J, Miles RR (2021**)** Identification of SARS-COV2 siRNAs that inhibit viral replication. Oligonucleotide Therapeutic Society Meeting.

2. Miles RR, Amin P, Misra J, Spandau DF, Wek RC (2020) The Integrated Stress Response Facilitates Cutaneous Wound Healing. Cold Spring Harbor Translation Control Meeting

3. Miles RR, Amin P, Misra J, Spandau DF, Wek RC (2019) The Integrated Stress Response Facilitates Cutaneous Wound Healing Society of Investigative Dermatology Annual Meeting

4. Miles RR, Amin P, Misra J, Spandau DF, Wek RC (2018) The Integrated Stress Response and Cutaneous Wound Healing. IU School of Medicine Department of Biochemistry Research Day

5. Kulkarni NH, Gelbert L, Zhang M, Bemis KG, Maran A, Lin X, Li Q, Mishra S, Halladay DL, Wei T, Chandrasekhar S, Frolik CA, Sato M, Helvering LM, Turner R, Dow E, Adams C, Lawrence F, Miles RR, Huang S, Chen P, Ma L, Bryant HU, and Onyia JE. (2004) Gene expression profile identifies different classes of bone therapies: PTH, Alendronate and SERMs. European Calcified Tissue Society; European Symposium on Calcified Tissue (ECTS)

6. Kulkarni NH, Halladay DL, Miles RR, Frolik CA, Galvin RJS, Fuson TR, Martin TJ, and Onyia JE. (2003) Wnt signaling pathway: A target for PTH action in bone and bone cells. Plenary Poster: American Society for Bone and Mineral Research Meeting

7. Thirunavukkarasu K, Miles RR, Halladay DL, Yang X, Galvin RJS, Chandrasekhar S, Martin TJ, and Onyia JE. (2001) Cbfa- and Smad-binding Elements Mediate TGFβ Stimulation of Osteoprotegerin (OPG) Gene Expression. American Society for Bone and Mineral Research Meeting

8. Halladay DL, Miles RR, Thirunavukkarasu K, Chandrasekhar S, Martin TJ and Onyia JE. (2000) Identification of Signal Transduction Pathways and Promoter Sequences that Mediate Parathyroid Hormone 1-38 Inhibition of Osteoprotegerin Gene Expression. American Society for Bone and Mineral Research Meeting.

9. Feister HA, Yang X, Onyia JE, Miles RR, Hock JM, Bidwell J. (1998) Parathyroid Hormone Regulates the Expression of NuMA and Topoisomerase II-a in Bone. American Society for Bone and Mineral Research

10. R. Miles, C.H. Turner, R.H. Santerre, Y. Tu, P. McClelland, J. Argot, J.M. Hock, J. Onyia (1997) Analysis of Differential Gene Expression after an Osteogenic Stimulus in vivo: Mechanical Loading Regulates Osteopontin and Myeloperoxidase. American Society for Bone and Mineral Research

11. Hale L., Miles R., Howe S., Walker C., Fuchs-Young R. (1996) Raloxifene, a Selective Estrogen Receptor Modulator, Inhibits Estrogen Stimulated Proliferation of Leiomyoma Cells in Culture. Society for Gynecological Investigation

12. Fuchs-Young R., Hale L., Howe S., Miles R. Walker, C. (1995) Modulation of Fibroid Cells by Steroids and Their Antagonists. Barton Creek Symposium

13. Miles R., Fuchs-Young R. (1995) Development of a Non-radioactive Quantitative PCR Technique Used to Detect Progesterone Receptor Levels in Bone. American Society for Bone and Mineral Research Annual Meeting

14. R. Galvin, R. Miles, P. Bryan, R. Fuchs-Young (1995) Raloxifene Analogue LY139478 Up-regulates the B form of the Progesterone Receptor in Porcine Bone Marrow-derived Stromal Cells but not Osteoblast-like cells. American Society for Bone and Mineral Research Annual Meeting

15. M. Saha, K. Joubin, R. Miles, C. Sinor (1994) Vertebrate Brain Development in *Xenopus.* International *Xenopus* Conference

16. R. Fuchs-Young, A. Betuzzi, M. Radigan, R. Miles, G. Greene. (1992) Regulation of the 5' Flanking Region of the Progesterone Receptor Gene by Estrogen and Progesterone Receptors National Endocrine Society Meeting.

PATENTS

1. **US8802921 B2:** Engineered landing pads for gene targeting in plants. William M. Ainley, Ryan C. Blue, Michael G. Murray, David Corbin, Rebecca R. Miles, Steven R. Webb

2. **WO0123562 A2:** Osteoprotegerin Regulatory Region. Chandrasekhar S, Halladay DL, Martin TJ, Miles R, Onyia JE, and Thirunavukkarasu K.

AWARDS

1997 Lilly Endocrine Award for Leadership

2006 Lilly Integrative Biology Elite Award for Teamwork

2007 Lilly Integrative Biology Elite Award for Scientific Achievement

2008 Lilly Integrative Biology Elite Award for Teamwork

2017 Lilly Innovator Award Top 100

2018 IU School of Medicine Department of Biochemistry and Molecular Biology Research Day Outstanding Abstract

2021 Lilly Innovator Award